PhD Degree in Molecular Medicine

European School of Molecular Medicine (SEMM),

University of Milan and University of Naples “Federico II”

Faculty of Medicine

Settore disciplinare: BIO/10

The role of PRC1 in B cell development and adaptive immune responses

Federica Alberghini, MSc

IFOM, Istituto FIRC di Oncologia Molecolare

IFOM-IEO Campus, Milan, Italy

Matricola n. R08893

Supervisor: Dott. Stefano Casola, Ph.D., M.D.
IFOM-IEO Campus, Milan, Italy

Co-supervisor: Dott. Gioacchino Natoli, Ph.D., M.D.
IFOM-IEO Campus, Milan, Italy

Co-supervisor: Prof. Dott. Matthias Merkenschlager, Ph.D.
MRC Clinical Sciences Center, London, United Kindgom.

Anno Accademico 2012-2013

Table of Contents

List of Abbreviations

AID	Activation Induced Deaminase
Arf	Alternative Reading Frame
Atm	ataxia telangiectasia mutated
Atr	ataxia telangiectasia and Rad3 related protein
BAFF	B-cell activating factor
BAFF-R	BAFF receptor
Bcl2	B cell CLL/lymphoma 2
Bcl6	B cell CLL/lymphoma 6
Bcor	Bcl6 corepressor
BCR	B cell receptor
BER	base excision repair
BM	bone marrow
Bmi1	Bmi1 polycomb ring finger oncogene
bp	base pair
BrdU	Bromodeoxyuridine
C-term	Carboxy terminus
Casp-glow	FITC-conjugated VAD-FMK, a general caspase inhibitor
CB	centroblast
Cbx	chromobox homolog
CC	centrocyte
Ccng1	CyclinG1
CD	Cluster of differentiation
CDKNA	cyclin dependent kinase inhibitor A
cDNA	complementary DNA
CDR3	Complementarity Determining Region 3
ChIP	chromatin immunoprecipitation
CHK	checkpoint homolog (S. pombe)
cKit	v-kit Hardy-Zuckerman 4 feline sarcoma viral oncogene homolog; CD117
CLP	common lymphoid progenitor
Cr2	complement component (3d/Epstein Barr virus) receptor 2
CSR	Class Switch Recombination

DDR	DNA damage response
DLBCL	Diffuse Large B cell Lymphoma
Dll-1	Delta-like 1
DMEM	Dulbecco's Modified Eagle Medium
DNA	Deoxyribonucleic acid
dNTP	deoxynucleoside triphosphate
DSB	Double Strand Break
E2a	E2a immunoglobulin enhancer binding factors E12/E47
E2f	E2f transcription factor
Ebf1	early B-cell factor 1
Eed	embryonic ectoderm development
ELISA	Enzyme-linked immunosorbent assay
ER	Endoplasmic reticulum
ESC	Embryonic Stem Cell
EYFP	Enhanced Yellow Fluorescent Protein
Ezh2	enhancer of zeste homolog 2 (Drosophila)
DAPI	4',6-diamidino-2-phenylindole
FACS	Fluorescence Activated Cell Sorting
Fbxl10/Kdm2b	lysine (K)-specific demethylase 2B
FDC	Follicular Dendritic Cell
Flt3	fms-related tyrosine kinase 3
FO	Follicular
g	relative centrifugal force expressed in units of gravity
GC	Germinal center
H	histone
Hi	High
H2Ak119Ub	mono-ubiquitinated Histone H2A at Lysine 119
H3K27me2	di-methylated Histone H3 at Lysine 27
H3K27me3	tri-methylated Histone H3 at Lysine 27
H3K4me3	tri-methylated Histone H3 at Lysine 4
HSC	Hematopoietic Stem Cell
Ig	Immunoglobulin
IgV	Variable gene
IgH	Immunoglobulin heavy chain
IL	interleukin

Ink	inhibitor of cyclin-dependent kinase
Irf4	interferon regulatory factor 4
kDa	Kilodalton
LMPP	lymphoid-primed multipotent progenitor
LN	lymph node
Lo	Low
loxP	locus of X-over of P1
LPS	lipopolysaccharide
mAb	monoclonal antibody
MACS	Magnetic-activated cell sorting
Mb-1	CD79a molecule, immunoglobulin-associated alpha
Mcl1	myeloid cell leukemia sequence 1 (BCL2-related)
MHC	Major Histocompatibility Complex
MITF	Microphthalmia-associated transcription factor
MLN	mesentheric lymph nodes
MMR	mismatch repair
MPP	multipotent progenitor
MRN	protein complex consisting of Mre11, Rad50 and Nbs1
mRNA	Messenger RNA
MZ	Marginal zone
N-term	Amino terminus
NCOR	Nuclear receptor co-repressor
NCOR2/SMRT	Nuclear receptor co-repressor 2
ncRNA	Non-coding RNA
NFAT	Nuclear factor of activated T-cells
NHEJ	non-homologous end joining
NP	Nitrophenyl
NP-CGG	Nitrophenyl coupled to chicken gamma globulin
Pax5	paired box 5
PBS	Phosphate buffered saline
PC	plasma cell
PcG	Polycomb group
PCGF	polycomb group ring finger
Pcl	Polycomblike
PCR	Polymerase Chain Reaction

PFA	Paraformaldehyde
Pho	Pleiohomeotic
Pmaip1	phorbol-12-myristate-13-acetate-induced protein (Noxa)
PP	Peyer's Patches
PRC	Polycomb reppresive complex
Prdm1	PR domain containing 1, with ZNF domain (Blimp1)
PRE	Polycomb response element
R26	Rosa26
RAG	Recombination activation genes
Ring1	Ring finger protein 1, Ring1a, R1a
RNA	Ribonucleic acid
Rnf2	ring finger protein 2, Ring1b, R1b
RSS	Recombination Signal sequence
RT	room temperature
RT-PCR	Reverse Transcriptase PCR
RT-QPCR	quantitative real time-PCR
RYBP	Ring1 and Yy1 binding protein
Runx1	Runt related transcription factor 1
Sca1	stem cell antigen-1; Ly-6A/E
SEM	Standard Error of the Mean
SET	Su(var)3-9, Enhancer-of-zeste, Trithorax
SHM	Somatic Hypermutation
SPL	Spleen
SRBC	Sheep Red Blood Cell
ssDNA	single stranded DNA
Suz12	suppressor of zeste 12 homolog (Drosophila)
SWI/SNF	SWItch/Sucrose NonFermentable
TGF-β	Transforming growth factor beta
TF	transcription factor
T_{FH}	T follicular helper cell
TLR	Toll-like receptor
Tp53	Tumor protein 53
UPR	Unfolded protein response
Wnt	Wingless-related MMTV integration site 1
WT	Wild-type

Xbp1	X-box binding protein 1
Xist	X inactive specific transcript

Index of Figures

Index of Tables

Abstract

Polycomb (PcG) proteins are epigenetic modifiers that modulate accessibility of genomic loci by covalent modification of N-terminal histone tails. In mammals, PcG proteins act within at least two functionally and biochemically distinct complexes, named Polycomb repressive complex 1 and 2 (PRC1 and PRC2). Within PRC2, the Ezh2 methyltransferase is able to di- and tri-methylate lysine 27 of histone H3. This mark is recognized by chromodomain-containing PRC1 subunits. Once bound, PRC1 catalyzes monoubiquitination of lysine 119 of histone H2A, which results in permanent, yet reversible, and heritable locus silencing. PcG proteins modulate expression of genes involved in development, lineage specification and cell identity, and their deregulation leads to aberrant differentiation of a number of cellular lineages, including the hematopoietic subsets. Recently, independent studies on a number of PcG mutants have highlighted an essential contribution of the Polycomb system to homeostasis of the lymphoid lineage.

Expression of *Ring1a* and *Ring1b*, the catalytic subunits of PRC1, is maintained throughout B cell development. Using a conditional gene targeting approach *in vivo*, we addressed their function in resting naïve B lymphocytes and in B cells participating in a T cell-dependent immune response. Removal of a single subunit did not affect B cell development nor immune responses in mice. Instead, complete ablation of PRC1 function in B cells at early developmental stages resulted in a nearly complete block at the pro- to pre-B cell stage. Moreover, selective PRC1 inactivation in transitional B cells led to aberrant differentiation, with B cells acquiring features of mature cells while simultaneously retaining markers of earlier developmental stages. At the molecular level, loss of PRC1 in resting B cells read out in extensive transcriptional deregulation involving aberrant expression of several lineage determinants. Selective loss of *Ring1a* and *Ring1b*

in GC B cells caused a significant reduction in numbers and frequency of GC B cells. As a result of the impaired GC reaction, serum titers of antigen-specific, class-switched antibodies were significantly decreased and formation of memory B cells significantly impaired in mutant mice. Instead, mutant GC B cells showed premature onset of terminal differentiation, as assessed by the induction of genes coding for the master regulators of plasma cell differentiation *Prdm1*, *Irf4* and *Xbp1*. This result was confirmed by performing *in vitro* LPS stimulation assays, which showed an accelerated appearance of plasmablasts co-expressing Syndecan-1/CD138 and high levels of the Irf4 transcription factor in Ezh2 mutant B cell cultures. Increased apoptosis of PRC1 mutant cells as compared to control was also observed in the context of *in vitro* B cell activation. Importantly, activation of B cells with the RP105 Toll-Like Receptor agonist, which does not induce expression of Activation Induced Deaminase (AID) normalized the apoptotic rate of PRC1 deficient cells to wild-type levels. Moreover, several target genes of the germinal center master regulator Bcl6 were found up-regulated in PRC1 mutant cells. Together, this suggests that PRC1 may support GC function through at least two mechanisms. On the one hand, it may co-operate in establishing Bcl6 transcriptional program, thereby preventing premature terminal differentiation. On the other, it may participate in the repair of DNA damage caused by AID activity, thereby allowing tolerance of AID genotoxic activity by GC B cells.

Introduction

1.1. Chromatin and epigenetics

1.1.1. Chromatin compaction and nucleosomes

In each mammalian cell, DNA is wound up in the nuclear compartment, which is about 6 µm in size. Packaging of the DNA in such a restricted physical space is achieved thanks to the activity of specific proteins, named Histones (H), which bind to DNA and help its folding. Histones are a family of positively charged proteins that form a heptamer complex, each consisting of two subunits of Histones H2A, H2B, H3 and H4 around which 146 base pairs (bp) of negatively charged DNA are wrapped up. The complex of Histones and DNA is called nucleosome and represents the basic unit of chromatin. Nucleosomes interconnected by stretches of linker DNA form the so-called “beads-on-a-string” structure. Addition of Histone H1 leads to a higher degree of chromatin compaction, as the beads are pulled together on the string and coil into a helical structure known as the 30 nm fiber, or chromatosome. This packaging shortens the DNA molecule about 6-fold. Upon cell division, chromatin is further condensed and becomes visible under the microscope as chromosomes. This compaction level is achieved through mechanisms that are yet not fully understood (Kornberg and Lorch, 1999). Chromatin structure determines local chromatin accessibility, thereby affecting gene expression. Chromatin compaction is regulated in several ways, one of which is represented by post-translational modifications targeting the N-terminal region of Histones, which protrudes from nucleosomes. Such modifications include acetylation, phosphorylation, methylation, and ubiquitination, which do not only change the proteins’ biochemical properties, but also constitute

a “Histone code”, which is read by functional domains of chromatin-bound factors, including transcription factors (TFs). Because of their role in the modulation of gene expression, histone modifiers have received increasing attention over the last two decades (Strahl and Allis, 2000).

1.1.2. Epigenetics

In multicellular organisms, tissue and organ homeostasis rely on the correct functioning of a variety of differentiated cell types, each of which carries specific blueprints consisting of a specific set of genes that is turned on and off. Differential gene expression arising from a shared genome distinguishes for example fibroblasts from stem cells, determines signal responsiveness, secretory functions and defines cell identity. Research carried out over the last decade has highlighted the importance of epigenetic regulation in the establishment and maintenance of gene expression patterns. Epigenetic changes are defined as heritable, functionally relevant, modifications in the genome that do not alter the primary DNA sequence. Epigenetic changes may influence chromatin structure, determining whether genomic loci are comprised within the less compacted euchromatin (transcriptionally active conformation) or belong to the tighter heterochromatin (transcriptionally inactive). Furthermore, the heterochromatic state can be constitutive (stably repressed) or facultative (de-repressed upon certain conditions).

In the present work, we focused our attention on dissecting *in vivo* the role of Polycomb group (PcG) protein family members and epigenetic regulators *Rnf2/Ring1b* and *Ring1a* in B-cell lymphopoiesis.

1.2. Polycomb group proteins

1.2.1. Polycomb group proteins in life

PcG proteins are evolutionarily conserved epigenetic silencers first identified in *Drosophila melanogaster*, where they were shown to be crucial for the specification of anterior/posterior body segmentation and axial patterning. Across evolution, genes encoding PcG proteins have diversified, with vertebrates exhibiting several homologs for each PcG protein encoded by the *Drosophila* genome (Sparmann and van Lohuizen, 2006). PcG proteins play crucial roles during development and in a wide variety of biological processes including cell cycle progression, apoptosis, response to DNA damage, DNA replication, X-chromosome inactivation, genomic imprinting, regulation of stem cell function, establishment and restriction of cell identity and tissue homeostasis (Sparmann and van Lohuizen, 2006). The importance of the Polycomb axis in mammalian development is best underscored by the embryonic/perinatal lethality exhibited by several mouse PcG mutants including Eed (embryonic ectoderm development), Ezh2 (enhancer of zeste 2), Suz12 (Suppressor of Zeste 12 homolog), Rnf2 (Ring finger protein 2; *Ring1b*) and Bmi-1 (Bmi1 polycomb ring finger oncogene) (Voncken et al., 2003) (O'Carroll et al., 2001) (Pasini et al., 2004) (van der Lugt et al., 1994). PcG proteins exert their function in the context of functionally and biochemically distinct multimeric complexes, of which the best characterized and most extensively studied are Polycomb Repressive Complex 1 and 2 (PRC1 and PRC2).

1.2.2. Polycomb- mediated gene silencing

In mammals, the currently accepted model for Polycomb function involves the concerted action of PRC1 ad PRC2 to achieve silencing of targeted genomic loci. According to this model, PRC2 acts first and modifies chromatin through the catalytic activity of the Ezh2 methyltransferase, which catalyzes di- and tri-methylation of lysine-27 of Histone H3 (H3K27me2 and H3K27me3, respectively). Trimethylated Histone H3 serves then as a docking site for the chromodomain-containing proteins family, whose components can function as PRC1 subunits. CBX-mediated recognition of H3K27me3 brings along PRC1, which catalyzes the monoubiquitination of lysine-119 of Histone H2A (H2AK119Ub) through the enzymatic action of its E3 ubiquitin ligases Ring1b and, to a lesser extent, *Ring1a* (Sparmann and van Lohuizen, 2006) (Figure 1). However, recent studies have challenged this model. For instance, the existence of a subset of PRC2 target genes that lack H2AK119Ub was reported (Ku et al., 2008). Conversely, it has been shown that PRC1 can function independently of PRC2 (Schoeftner et al., 2006), (Sing et al., 2009). Furthermore, PRC1 has been reported to have chromatin-compacting activities that are independent of its catalytic function (Eskeland et al., 2010). Nevertheless, the majority of PcG target genes require activity of both PRC1 and PRC2 for stable gene repression (Ku et al., 2008).

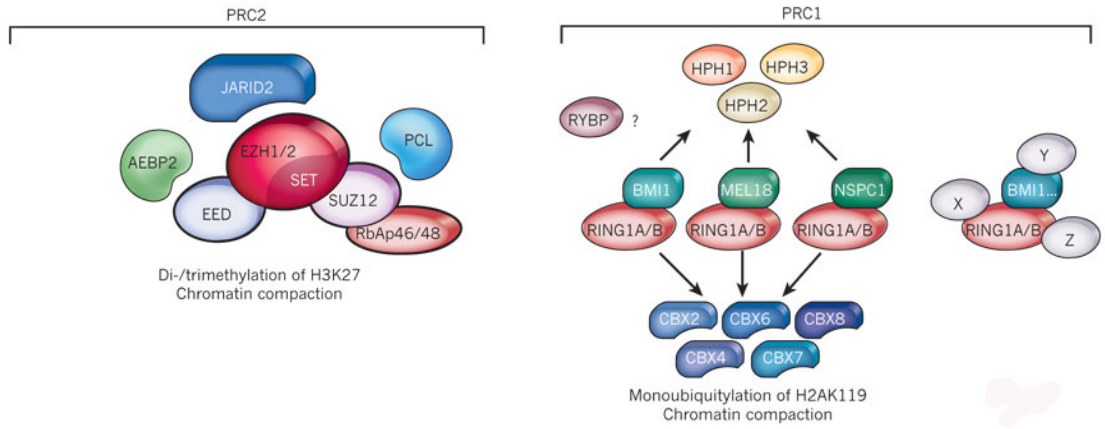

Figure 1. Polycomb repressive complexes and their components.

PcG proteins assemble into two main complexes: PRC1 and 2. Originally, PcG proteins were discovered in *Drosophila*, and several homologs have been found in mammals. Combinatorial heterogeneity of PRC1 is depicted by the availability of multiple Cbx subunits and the ability of Ring1a/b and Bmi-1 to assemble with other cellular components, too. Adapted from Margueron and Reinberg, *Nature*. 2011 Jan 20;469.

1.2.3. Diversity of PRC1 complexes

PRC1 is evolutionary more recent and biochemically and functionally more diverse than PRC2. The mammalian PRC1 is defined as a multi-subunit complex consisting of five core protein families, each of which consists of several members, namely chromobox proteins (*Cbx2/4/6/7/8*), *Ring1* (*Ring1A/B*), Polyhomeotic-like (PHC 1/2/3), polycomb group ring finger 1 to 6 (PCGF 1-6) and *Rybp/Yaf2* (Gao et al., 2012). Different combinations of these subunits can generate a diverse array of PRC1 sub-complexes, which are believed to exert their function in a tissue- and cell-specific manner. The catalytic activity of PRC1 resides in its Ring1 subunit and can be enhanced through binding to one of the PCGF orthologs (Gao et al., 2012) (Figure 2). Recent reports have described the existence of at least two PRC1 sub-

complexes in embryonic stem cells (ESCs), which are distinguished based on the presence of either *Rybp* or one of the *Cbx* family members. Using a combination of high-throughput analyses, authors were able to show that PRC1/*Rybp*-bound genes tend to be more expressed than PRC1/*Cbx7*-bound ones. Additionally, it was shown that the PRC1/*Rybp* complex can bind chromatin in an H3K27me3-independent fashion and Gene Ontology analyses revealed segregation of biological functions between the two complexes. *Rybp*-bound genes were mainly involved in cell cycle progression and metabolism regulation, whereas *Cbx*-bound ones primarily controlled developmental pathways (Tavares et al., 2012) (Yu et al., 2012) (Morey et al., 2013).

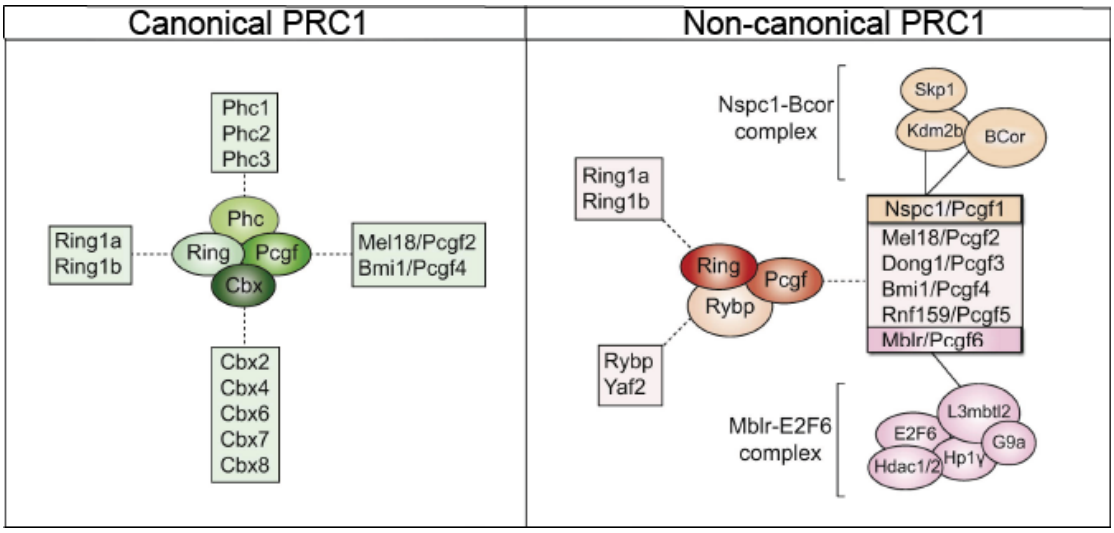

Figure 2. Diversity of PRC1 compexes.

PRC1 is more heterogeneous than PRC2 due to the availability of several orthologs for each component (listed within light green squares in a), which can give rise to multiple PRC1 sub-complexes. In addition, PRC1 subunits can form non-canonical PRC1 complexes with several cellular components as shown in b). Adapted from Turner and Bracken, *Cell Stem Cell*. 2013 Feb 7;12(2):145-6.

Adding to PRC1 complexity, recent studies have reported the association between PRC1 components and cell type-specific DNA-binding TFs. For instance, one of the PCGF homologs, *Bmi-1*, has been shown to associate with the Runx1/CBFβ TF on a subset of genomic targets in primary human thymocytes (Yu et al., 2012). Additionally, *Ring1b* was shown to participate in a complex with the B-cell CLL/lymphoma 6 (Bcl6) co-repressor *Bcor*, and to bind *bona fide* Bcl6 target genes in B lymphoma cells (Gearhart et al., 2006) (Sanchez et al., 2007). More evidence suggesting association between members of the PRC1 and cell-specific TFs has come from studies reporting association between the E2F family member E2F6 and PcG subunits (Attwooll et al., 2005) (Ogawa et al., 2002) (Trimarchi et al., 2001). Taken together, this supports a view of the PRC1 as a dynamic and plastic complex, whose subunit composition and association to specialized DNA binding proteins change in a cell-type- and stage-specific manner.

1.2.4. PRC1, H2AK119Ub and chromatin silencing

Histone modification and/or chromatin binding by PcGs correlate with repression of gene expression from targeted loci. Recent reports have started to shed light on the mechanisms through which epigenetic modifications imposed by PcG proteins read out into transcriptional repression. For PRC1, two separate classes of targets have been identified, namely those for which efficient silencing requires H2AK119Ub and those that are independent on E3 ligase activity for transcriptional repression.

1.2.4.1. H2AK119Ub and the transcriptional machinery.

H2AK119Ub is catalyzed by the Ring1 subunits of PRC1. In embryonic stem cells (ESCs) and in the mouse embryos, PRC1 catalytic activity is largely carried out by Ring1b, as its depletion leads to genome-wide loss of H2AK119Ub and, in the case of the mouse embryo, in embryonic lethality (Voncken et al., 2003). This suggests that in these biological systems, Ring1a is not able to compensate for Ring1b loss of function (van der Stoop et al., 2008). Efficient ubiquitination also requires association of the Ring subunits with one of the 6 mammalian PCGF orthologs and with the Kdm2/Fbxl10 subunit (Wu et al., 2013). How deposition of H2AK119Ub is able to prevent gene transcription and whether this modification alone is sufficient to ensure silencing is unknown. A recent study suggests that H2AK119Ub may hamper transcriptional elongation rather than initiation by preventing switches in RNA polymerase II (RNA pol II) phosphorylation status. Upon *Ring1b* inactivation and subsequent H2AK119Ub depletion, RNA pol II switches from the paused phosphorylation status (phosphorylated serine-5 of the C-terminal domain, CTD) to the one associated with active transcription (serine-2 phosphorylation on the CTD) on transcribed targets (Stock et al., 2007) (Dellino et al., 2004).

1.2.4.2. Chromatin compaction.

Evidence for PRC1-mediated chromatin compaction has come from studies showing decreased filament size when naked DNA was incubated with Pho-PRC1 (Francis et al., 2004). PRC1-compacted chromatin was shown to be resistant to remodeling activity mediated by the SWI/SNF complex (Francis et al., 2004). Importantly, chromatin compaction imposed by PRC1 was independent of its catalytic activity, as it was not affected in ESCs expressing a catalytically mutant

form of Ring1b (Eskeland et al., 2010). So far, the only PRC1 subunit able to compact chromatin was shown to be CBX (Grau et al., 2011). This observation may provide a link between H3K27me3 and chromatin compaction, as CBX contains chromodomains responsible for recognition of the H3K27me3 histone mark.

Together, this shows that Polycomb-mediated gene silencing is achieved through several, in part redundant, mechanisms. Recent evidence by our lab (Caganova et al., 2013) showed the existence of bivalent domains, namely loci simultaneously displaying activating and repressing chromatin marks, in differentiated somatic cells (see paragraph 1.2.6. for a more detailed description of bivalent domains). Bivalent domains were found on genes whose activation status critically defined the cell's fate.

Such evidence allows to speculate that Polycomb silencing may differ depending on the nature of the targeted locus. In case of loci in the need of stable repression (i.e. lineage-inappropriate genes), Polycomb may compact chromatin leading to formation of constitutive heterochromatin, thereby locking genes in highly condensed regions. Instead, if loci contain genes that need to be kept poised for future activation (i.e. genes likely to be activated following exposure to environmental stimuli), Polycomb may limit its activity to transcriptional silencing through inhibition of the activity of RNA pol II. However, more studies on local chromatin architecture and its changes during development are needed to clarify this issue.

1.2.5. Targeting Polycomb activity to the appropriate genomic loci.

PcG proteins are crucial in both the establishment and maintenance of cell-type-specific gene expression profiles. How PcG proteins are dynamically targeted to their respective target sites in a cell- and stage-specific fashion has been long studied and definitive answers are still missing. In *Drosophila*, Polycomb targeting is accomplished thanks to the presence of DNA sequences known as Polycomb Response Elements (PREs), which map many kilobases away from promoters they control and which bind several sequence-specific binding proteins, among which the Polycomb member Pleiohomeotic (PHO). Binding of PHO to *Drosophila* PREs is necessary for PcG complex recruitment and effective gene silencing(Bloyer et al., 2003; Ringrose et al., 2003). In mammals, multiple modes of Polycomb targeting have been proposed.

1.2.5.1. PcG proteins bind specific DNA elements

In ESCs, genome-wide mapping of PRC2 occupancy has led to the identification of GC-rich regions within CpG islands as preferred binding sites for PRC2. DNA methylation and presence of binding sites for transcriptional activators prevented PRC2 binding, suggesting a role for DNA methylation in regulating PRC2-chromatin interactions (Hunkapiller et al., 2012; Ku et al., 2008) (Dietrich et al., 2012). Further evidence for a role for CpG islands in PcG recruitment was recently provided by studies showing their involvement in recruitment of PRC1 in a PRC2-independent fashion. Work carried out in Klose's group has shown that Kdm2b/Fbxl10 subunit co-localizes with Ring1b on CpG-rich DNA regions in ESCs and mediates PRC1 recruitment. Recent studies in Helin's group have confirmed

and extended work by Klose and colleagues showing that Kdm2b/Fbxl10 interacts with a PRC1 complex including Ring1b and NSPc1 and binds DNA through its CXXC domain (Wu et al., 2013). Genome-wide analysis of Kdm2b/Fbxl10 occupancy in ESCs confirmed enrichment at un-methylated CpG islands. Interestingly, Kdm2b/Fbxl10 was shown to bind both active and silenced gene loci, but co-localization with Ring1b was observed only on the latter class of targets. Additionally, it was shown that Kdm2b/Fbxl10 is required for efficient ubiquitination of H2A, which was necessary to sustain ESC pluripotency (Farcas et al., 2012; Wu et al., 2013). Together, these studies support a model whereby Kdm2b/Fbxl10 favors PRC1 recruitment and hence H2A ubiquitination at CpG-containing target genes in ESCs.

1.2.5.2. PcG proteins interact with DNA-binding proteins

It is becoming increasingly evident that PcG targeting to genomic sites is contributed by the direct interaction between PRCs and ubiquitous or cell-type-specific transcriptional regulators. Recent studies have revealed an association between the transcriptional repressor Jarid2 and PRC2 in ESCs. Jarid2 is a catalytic- dead member of the Jumonji (Jmj) domain-containing family of lysine demethylases with DNA-binding activity. Jarid2 was reported to co-localize with PRC2 at 90% of PcG targets in ESCs and its loss correlated with decreased recruitment of PRC2 to chromatin and impaired differentiation (Landeira et al., 2010) (Pasini et al., 2010) (Shen et al., 2009). However, Jarid2 inactivation did neither result in substantial changes in the genome-wide distribution of H3K27me3 nor did it lead to a significant up-regulation of PRC2 silenced genes, which is instead a common feature of PcG mutants (Landeira et al., 2010). While Jarid2 was reported to modulate Ezh2 methyltransferase activity, the effects of such

regulation on Ezh2 silencing function remain unclear (Herz and Shilatifard, 2010). The current model based on experimental data supports the idea that Jarid2 is instrumental for the fine-tuning of PRC2 activity rather than for its recruitment to chromatin. A marginal role for the recruitment of PRC2 to target sites has been proposed for the accessory Polycomb-like (PCL) subunits, which in mammals are represented by Pcl1, Pcl2 and Pcl3. PCLs were first defined as factors able to boost Ezh2 catalytic activity. The finding that PRC2 occupancy on the inactive X-chromosome decreases following PCL2 depletion provided the first indication of the involvement of PCL subunits in PRC2 recruitment (Casanova et al., 2011). Further evidence came from studies in ESCs, where depletion of PCL3 resulted in loss of PRC2 binding at most genomic targets and in genome-wide H3K27me3 loss. Interestingly, PCL2 inactivation had minor effects in ESCs (Hunkapiller et al., 2012) (Walker et al., 2011). Together, these results point to non-redundant functions exerted by the two PCLs in ESCs. Both PRC2 and PRC1 have been also shown to interact with E2F6, YY1 and SNAIL1, which may provide sequence specificity to PcG recruitment (Trimarchi et al., 2001) (Ogawa et al., 2002) (Brown et al., 1998) (Caretti et al., 2004) (Herranz et al., 2008). Accumulating evidence indicates the existence of PRC1-like complexes recruited to target sites in the absence of H3K27me3 (Gearhart et al., 2006) (Yu et al., 2012) (Sanchez et al., 2007).

Finally, the interaction of PcG proteins with cell-type-specific TFs provides insights into the relatively unexplored mechanism of TF-mediated chromatin remodeling.

1.2.5.3. PcG proteins associate with non-coding RNAs

Non-coding RNAs (ncRNAs) have been shown to play an important role in Polycomb recruitment both in *cis* and *trans*. One of the first ncRNAs for which

interaction with PcG proteins was reported is X-inactive specific transcript (*Xist*). *Xist* binds to Ezh2, and this binding is required for the deposition of H3K27me3 on the inactive X-chromosome (Plath et al., 2003). Following *Xist*, other ncRNAs have been shown to bind PcG components and affect PcG-mediated gene silencing (Zhao et al., 2010). *HOTAIR*, a ncRNA transcribed from the *HOXC* locus binds to and targets PRC2 to the *HOXD* locus and few other genomic loci to achieve transcriptional silencing. Additionally, *HOTAIR* deregulation in epithelial cancer cells leads to PRC2 re-localization and changes in H3K27me3 levels, which ultimately influence cancer invasiveness and metastasis (Rinn et al., 2007) (Gupta et al., 2010). An example of ncRNA-mediated control of PcG function in *cis* is provided by *ANRIL*, which is transcribed from the *Cdkn2a* locus. Two independent studies showed that *ANRIL* binds to Cbx7 and Suz12, and *ANRIL* depletion leads to defective H3K27me3 deposition and *Cdkn2a* de-repression (Yap et al., 2010) (Kotake et al., 2011). Taken together, multiple mechanisms account for PcG targeting to specific genomic loci. The contribution of each of these mechanisms is likely to vary depending on the cellular context.

1.2.6. Polycomb in development and lineage commitment

ESCs are derived from the mammalian embryo inner cell mass at the blastocyst stage. ESCs can be kept in culture in an undifferentiated state and have been widely used to unravel molecular mechanisms underlying cell fate transitions occurring during early stages of mammalian development. ESCs are endowed with the opposing abilities to self-renew, thereby guaranteeing the maintenance of an undifferentiated state, and to undergo multi-lineage differentiation upon appropriate stimulation. Therefore, the genome of ESCs needs on the one hand to preserve a pluripotency-specific gene expression pattern, while on the other it

requires the ability to respond quickly to a plethora of differentiation stimuli. A large body of evidence has pointed at seminal roles played by epigenetic modifiers, including PcG proteins, in the regulation of these processes. In ESCs, PcG proteins share target occupancy with *Sox2*, *Nanog* and *Oct4*, whose activity is essential for the maintenance of pluripotency (Boyer et al., 2005; Lee et al., 2006) (Boyer et al., 2006). Evidence showing that deprivation of *Oct4* from ESCs results in Suz12 loss at specific promoters suggests a possible role for these transcription factors in PcG recruitment (Squazzo et al., 2006). Genome-wide studies in ESCs have reported the existence of "bivalent domains", namely genomic loci, often encoding for critical lineage determinants, that display simultaneous presence of activating (H3K4me3) and repressing (H3K27me3) chromatin marks in proximity of the transcriptional start site (TSS). Bivalent promoters are characterized by RNA pol II binding and minimal transcriptional activity. It has been suggested that bivalency poises genes for activation and is resolved once ESCs receive a differentiation signal into two alternative ways: i) H3K27me3 is removed and the target gene marked now only by H3K4me3 is transcriptionally activated, or ii) H3K4me3 is removed while H3K27me3 is retained, which leads to stable gene repression. However, this model has been challenged by recent studies on ESCs lacking H3K4me3 (Hu et al., 2013). PcG inactivation in ESCs causes bivalent genes, including lineage determinants, to be aberrantly expressed, which contributes to abnormal differentiation and, in some instances, to impaired proliferation (Bernstein et al., 2006; Roman-Trufero et al., 2009).

Polycomb targets often control early developmental steps involved in axial patterning and organogenesis. The PcG axis modulates also critical signal transduction pathways (TGFβ, Wnt), which are active during gastrulation and lineage commitment (Boyer et al., 2006).

1.2.7. Polycomb function in post-natal life

In addition to their role in embryonic development, a growing body of evidence implicates PcG proteins in the homeostasis of adult stem cells and in the differentiation of lineage-committed precursors. PcG proteins exert their function through the regulation of essential cellular processes including cell proliferation, survival and differentiation.

1.2.7.1. PcG proteins regulate cell cycle progression and survival

A growing body of evidence implicates PcG proteins in the control of cell cycle progression. PcG proteins exert their function regulating the checkpoint that enables cells to transit from G_1 to S. The latter transition is under the control of the retinoblastoma tumor suppressor protein 1 (Rb1), which regulates the E2F transcription factor and thereby initiation of DNA replication. In its hypo-phosphorylated form, Rb1 prevents S phase entry by interacting with E2F. Upon mitogenic stimulation, Rb is phosphorylated by cyclin-dependent kinase 4 (Cdk4), causing E2F factors to be released. The latter event leads to E2F-dependent activation of a substantial number of target genes, including several necessary for DNA replication (Nevins, 2001). Polycomb genes *Ezh2* and *Eed* are directly targeted by E2F transcriptional activation and facilitate proliferation of both normal and cancer cells (Bracken et al., 2003). Both PRC1 and PRC2 regulate the transcription of several cyclin-dependent kinase inhibitors (*Cdkn*), including *Cdkn1a*/ $p21^{CIP1}$, *Cdkn2a,* which encodes for $p16^{INK4A}$ and $p19^{ARF}$ and *Cdkn2b/*$p15^{INK4B}$ (Jacobs et al., 1999). $p21^{CIP1}$ and $p16^{INK4A}$ exert their roles by binding to Cdk4 and inhibiting its activity. Instead, $p19^{ARF}$ binds to and antagonizes the activity of MDM2, thereby stabilizing p53 expression that can ultimately induce

cell cycle-arrest or apoptosis (Sherr, 2001). By modulating the functions of cell cycle inhibitors, PcG proteins also regulate cellular senescence. Senescence is defined as a permanent arrest at the G_0 phase of the cell cycle, usually resulting from excessive telomere shortening and/or irreparable DNA damage (Campisi and d'Adda di Fagagna, 2007). Entry into senescence was shown to coincide with dissociation of PRC complexes from the *Cdkn2a* locus. Accordingly, deprivation of PcG members accelerates cellular senescence, while their overexpression inhibits its bypass (Agherbi et al., 2009).

The role of PcG proteins in the regulation of apoptosis is not fully understood. Genes coding for the pro-apoptotic factors Phorbol-12-myristate-13-acetate-induced protein *(Pmaip1/Noxa*) and BCL2-like 11 (Bcl2l11) are direct targets of Polycomb (Yamashita et al., 2008) (Wu et al., 2010). Additionally, both PcG complexes repress the locus encoding the p19Arf tumor suppressor, which induces p53-dependent apoptosis (Kamijo et al., 1998) (Zhang et al., 1998). The involvement of PRC1 in the regulation of p53-dependent apoptosis came from studies in hematopoietic stem cells, where loss of the PRC1 component *Bmi1* results in proliferative arrest and p53-dependent cell death (Park et al., 2003). Moreover, two independent studies have recently reported a role for *Ring1b* in the regulation of p53-dependent apoptosis in germ cell tumors. Specifically, it was shown that Ring1b interacted directly with Mdm2 and p53 to induce Mdm2-dependent p53 ubiquitination and degradation. Conversely, loss of Ring1b resulted in p53 stabilization and induction of apoptosis (Su et al., 2013) (Wen et al., 2013). Of note, *Bmi1*$^{-/-}$ memory T cells undergo apoptosis in a *Cdkn2a*-independent manner, primarily as a result of *Pmaip1*/Noxa up-regulation (Yamashita et al., 2008).

Chromatin accessibility influences the cellular response to genotoxic damage (Sulli et al., 2012). The DNA damage response (DDR) features DNA lesion sensing, checkpoint activation, cell cycle arrest, transduction of the damage signal and ultimately assembly of the repair machinery. Successful DDR allows cell cycle resumption, while failure to repair DNA damage leads to senescence or apoptosis. The DDR relies on the sequential recruitment of several proteins to sites of DNA damage, whose activity is regulated by post-translational modifications (d'Adda di Fagagna, 2008; Sulli et al., 2012) (Figure 3). Mounting evidence implicates PcG proteins as regulators of the DDR in mammalian cells.

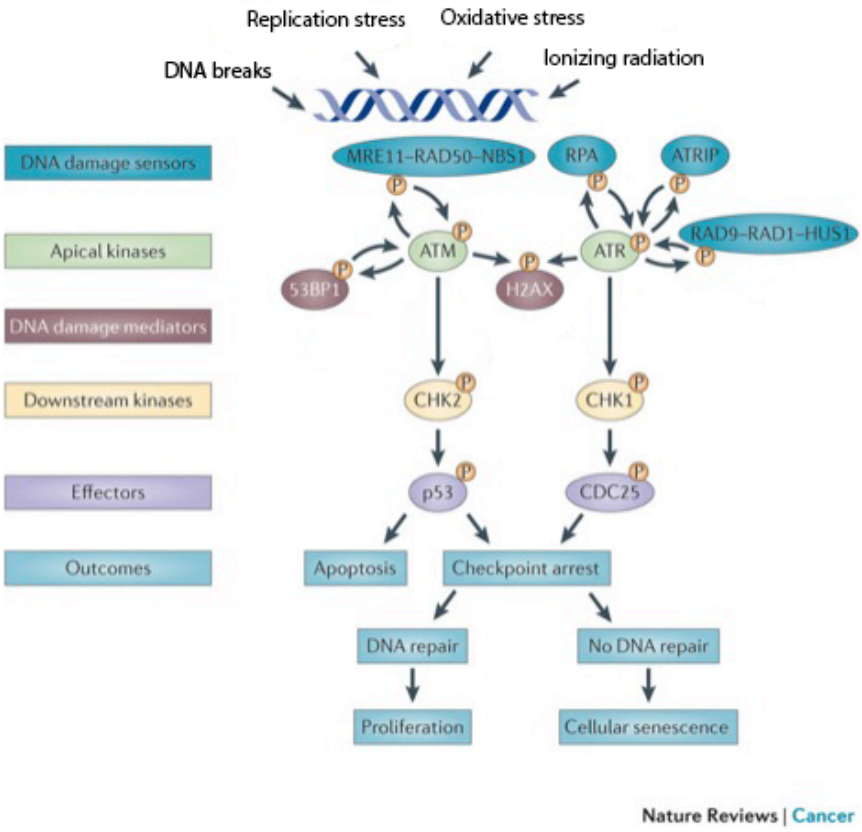

Figure 3. Simplified view of the DNA damage repair pathways.

Following DNA damage induction from various agents, DNA damage sensing is thought to be mediated by the MRN complex, the Rad complex and ssDNA (single stranded DNA) binding protein protein Rpa and its partner Atrip. Sensing of DNA damage results in phosphorylation and activation of the crucial ATM and ATR kinases, which in turn activate Chek1 and Chek2. This leads to the recruitment of effector molecules that mediate DNA repair, transcriptional regulation, chromatin remodeling, DNA replication, cell cycle control and apoptosis, among which CDC25 and p53. Adapted from Sulli, G. *et al.*, *Nat Rev Cancer*. 2012 Oct;12(10):709-20.

Upon DNA damage induction, PRC1 components Ring1b, Bmi-1 and Cbx subunits are rapidly recruited to sites of DNA damage (Ginjala et al., 2011), (Ismail et al., 2010). The mechanism mediating recruitment of PRC1 components to chromatin is not fully understood. Once recruited to sites of damage, Ring1b and Bmi-1

mediate ubiqutination of Histone H2AX, which is required for DDR activation. In accordance with this, cells devoid of Bmi-1 display increased sensitivity to ionizing radiation and genotoxic insults (Facchino et al., 2010; Ginjala et al., 2011; Ismail et al., 2010). In addition to PRC1 members, Ezh2 and H3K27me3 binding at sites of DNA damage has been documented, and removal of PRC2 components increases cells sensitivity to ionizing radiation (Facchino et al., 2010) (Chou et al., 2010) (Caganova et al., 2013). Ezh2 was shown to be required to mediate phosphorylation of Chek1 and suppress p21 degradation, which is necessary to maintain cell cycle arrest rather than apoptosis (Wu et al., 2011). Therefore, current evidence suggests that PcG proteins favor DDR by distinct mechanisms, which include suppression of transcription at sites of DNA damage, DDR factor recruitment and contribution to the repair process.

1.2.7.3. Polycomb proteins in hematopoiesis

Hematopoietic stem cells (HSCs) are multipotent cells endowed with the ability to self-renew and differentiate into all blood cell types. Similarly to ESCs, HSCs carry bivalent domains at promoters of lineage-specific TFs poised for expression (or stable repression) once HSCs differentiate into a particular type of blood cell (Cui et al., 2009). The essential role of the Polycomb axis in hematopoiesis is underscored by several studies reporting hematologic dysfunctions in mouse PcG mutants (Cales et al., 2008; Su et al., 2003; van der Lugt et al., 1994). Expression of the PRC1 component *Bmi-1* is high in HSCs, while it decreases upon differentiation, suggesting a role in HSCs. Indeed, *Bmi-1*$^{-/-}$ mice, while displaying unaffected fetal hematopoiesis, experience severe progressive post-natal anemia due to progressive HSC exhaustion (van der Lugt et al., 1994). *Bmi-1*$^{-/-}$ HSCs are

unable to support long-term hematopoietic reconstitution due to a failure to self-renew. Bmi-1-dependent control of HSCs self-renewal is mainly achieved through repression of the *Cdkn2a* locus (Park et al., 2003). Indeed, *Bmi-1* deficient HSCs display increased levels of both $p16^{INK4A}$ and $p19^{ARF}$, which results in cell-cycle arrest and p53-dependent apoptosis (Park et al., 2003). Bmi-1 has also been implicated in the control of mitochondrial function, as it was observed that *Bmi-1*$^{-/-}$ cells display increased levels of reactive oxygen species (ROS) and sustained activation of the DDR pathway. Notably, Chk2 deletion was able to rescue many of the defects observed in *Bmi-1*-deficient mice, and, hence, to improve their survival. In particular, the rescue was primarily beneficial to very early hematopoietic progenitors (Liu et al., 2009). This suggests that, in addition to de-repression of the *Cdkn2a* locus, also hyper-activation of the DDR pathway plays a role in HSC dysfunction following *Bmi-1* inactivation. In addition to loss of self-renewal ability, *Bmi-1*$^{-/-}$ HSCs display premature expression of the B cell lineage developmental regulators *Ebf1* and *Pax5* and their downstream target genes (Oguro et al., 2010). Taken together, *Bmi-1* activity is crucial to ensure HSC maintenance by restricting proliferation and lineage differentiation, thereby supporting self-renewal. The function of other PRC1 components in the hematopoietic system has also been addressed. Inactivation of *Mel-18* in mice resulted in decreased bone marrow (BM) cellularity, with the lymphoid compartment being predominantly affected. This was due to impaired proliferation of lymphocyte progenitors in response to interleukin 7 (IL-7), suggesting a role for Mel-18 in cell cycle progression (Akasaka et al., 1997). Another study reported that loss of *Mel-18* results in increased HSC self-renewal (Kajiume et al., 2004). This suggests that *Mel-18* deficiency may have different functions depending on the state of differentiation. Analogously, selective *Ring1b* inactivation in mouse HSCs resulted in overall BM hypoplasia, with a concomitant enlargement of the fraction of lineage-negative (Lin^-) cells. Ring1b was shown to

restrict progenitor's cell proliferation by inhibiting cyclin D2 (*Ccnd2*) expression and to support expansion of lymphoid and myeloid-committed progeny through repression of the *Cdkn2a* locus (Cales et al., 2008).

The function of PRC2 components in the regulation of the early stages of hematopoiesis remains controversial. *Ezh2* loss-of-function studies did not reveal alteration in HSC homeostasis nor myeloid development. Instead, these studies revealed that loss of *Ezh2* resulted primarily in impaired B- and T-cell development, as a result of inefficient VDJ recombination (Su et al., 2003). On the other hand, over-expression of *Ezh2* prevents HSC exhaustion during serial transplantation. Similarly, loss of *Eed* and *Suz12* enhances the proliferative capacity of HSCs (Majewski et al., 2008; Neff et al., 2012; Tanaka et al., 2012). Overall, this shows that removal of PcG activity affects HSC homeostasis, with different, and sometimes opposing, outcomes depending on the stage of differentiation where PcG function is lost and the specific PcG component that is inactivated.

1.2.7.4. Polycomb proteins and lymphocyte development

Accumulating evidence implicates several members of the Polycomb family in the regulation of lymphocyte development. Indeed, as previously mentioned, conditional ablation of *Ezh2* results in impaired rearrangement of immunoglobulin (Ig) genes, resulting in B cell lymphopenia and severe immunodeficiency (Su et al., 2003). Members of the PRC1 have also been implicated in early steps of B cell development, with Mel-18 dictating mitotic response to IL-7 stimulation (Akasaka et al., 1997). *Mel-18* was also reported to prevent proliferation of mature B cells following B cell receptor (BCR) stimulation through the failure to induce c-MYC expression (Tetsu et al., 1998). This suggests that Mel-18 fulfills different functions

depending on the differentiation state of the B cell. Additionally, it has been long known that Polycomb proteins are expressed in mature B cells, in particular upon recruitment into an immune response (Raaphorst et al., 2000b). Moreover, deregulated expression of PRC1 and PRC2 members is commonly detected in human Hodgkin and Non-Hodgkin B cell lymphomas arising from mature B cells (Raaphorst et al., 2000a; van Kemenade et al., 2001). Recently, our group has shown that *Ezh2* function is crucial to prevent premature terminal differentiation of mature B cells. This regulation is manly exerted through the direct repression of the PC determinants *Blimp1* and *Irf4 (Caganova et al., 2013)*. In agreement with data from our lab showing a critical role for Ezh2 in mature B cells recruited into the germinal center reaction (Caganova et al., 2013), recent studies have reported relevant frequencies of *Ezh2* gain-of-function mutations in human follicular and large B cell lymphoma that originate from GC B cells (FL and DLBCL, respectively) (Morin et al., 2010). Importantly, inhibition of Ezh2 by recently identified small molecule inhibitors has been proposed as a novel therapeutic target for the treatment of Non-Hodgkin lymphomas featuring *Ezh2*-activating mutations (McCabe et al., 2012). While evidence is available concerning the role of PRC2 in early and late B lymphocyte development, fewer studies have addressed the role of PRC1 in the same processes. In particular, to our knowledge there has been yet no functional dissection of the role of PRC1 in peripheral B cell maturation and B-cell responses. Therefore, the present study has primarily focused on the understanding of PRC1 function in resting mature B cells and in terminal differentiation.

1.3. B cell development

B cell development is a tightly controlled process whereby HSCs undergo stepwise proliferation and differentiation to ultimately generate functional, non-autoreactive cells (Figure 4). Research carried out over the past decades has dissected the main molecular events underlying B lineage specification, which now allow high-resolution investigations of processes that instruct each differentiation step.

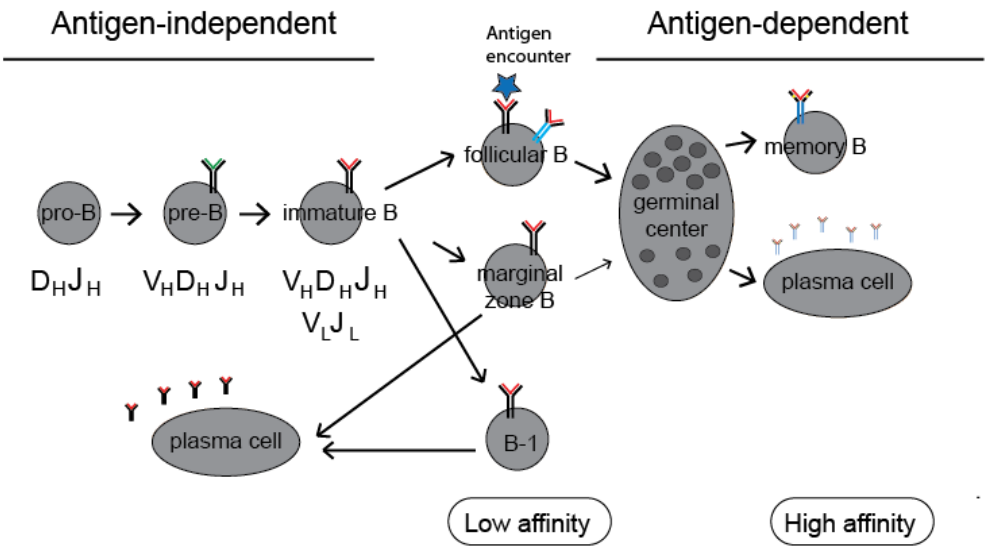

Figure 4. Schematic view of B cell development.

Post-natal B cell development starts in the BM, where CLPs give rise to pro-B cells that start VDJ recombination. Upon expression of a functional surface Ig, they leave the BM and transit to secondary lymphoid organs. The three major mature B cell subsets are follicular (FO), marginal zone (MZ) and B-1 B cells. MZ and B-1 B cells are mainly devoted to the production of low-affinity antibodies by differentiating into antibody-secreting plasma cells following pathogen encounter. FO B cells are instead mainly recruited in T cell-dependent antigen responses. Following antigen encounter and

supported by T cell help, they form germinal centers (GC), which feature robust B cell proliferation, Ig gene mutations, selection of high-affinity Ig mutants and eventually their terminal differentiation. The GC reaction aims at producing high-affinity Ig-expressing memory B cells and plasma cells secreting high-affinity antibodies for the cognate antigen.

1.3.1. Early B cell development

In mice and humans, the early steps of B cell development take place in the BM, where HSCs start a stepwise developmental path featuring progressive loss of multilineage differentiation potential. In order to give rise to lymphocytes, HSCs first differentiate into multipotent progenitors (MPP), which are characterized by loss of self-renewal ability. Together, the pool of HSCs and MPP are characterized by lack of lineage determinants, high expression of stem cell antigen-1 (Sca-1)^{hi} and the protein tyrosine-kinase receptor Kit. They are commonly referred to as the LSK subset (Ikuta and Weissman, 1992; Li and Johnson, 1995). Loss of self-renewal ability coincides with expression of FMS-related tyrosine kinase 3 (FLT3), which is dependent on the Ikaros (IKZF1) and PU.1 TFs. FLT3 expression is believed to mark the first commitment of progenitors towards the lymphoid lineage, as its overexpression decreases the differentiation of MPP into megakaryocytes and erythrocytes (Adolfsson et al., 2001; Adolfsson et al., 2005; Forsberg et al., 2006; Yoshida et al., 2006). In response to Flt-3 ligand and IL-7 stimulation, MPPs start expressing early B cell factor 1 (Ebf1) and the TF E2a, which mark the entry into the common lymphoid progenitor (CLP) pool (Medina et al., 2004; Nutt and Kee, 2007). Further exposure of CLPs to IL-7 yields up-regulation of Paired box protein 5 (Pax5), which marks the definitive commitment towards the B cell lineage (Hagman and Lukin, 2006; Lin and Grosschedl, 1995; Sun, 2004).

1.3.1.1. V(D)J recombination.

The ability of lymphocytes to exert their protective functions relies on the expression of diversified immunoglobulin (Ig) molecules on the surface of B and T cells, namely the B and T cell receptor (TCR) respectively, which mediate pathogen recognition. The BCR consists of two identical Ig heavy (H) and light chains (L) assembled together via disulfide bonds. Each Ig chain consists of a variable region responsible for the recognition of antigen and a constant region, which mediates the effector function of the receptor. The variable region of the receptor is generated via a gene rearrangement process termed VDJ recombination, whereby starting from an array of gene segments, a unique variable (V), diversity (D) and joining (J) gene segments are joined together (only V and J segments are joined to yield the IgL chain) (Tonegawa, 1983). VDJ is dependent on the activity of the gene products of the Recombination Activating Genes 1 and 2 (RAG1 and RAG2) (McBlane et al., 1995; Melek et al., 1998; van Gent et al., 1995). RAG proteins bind to and cleave DNA at specific recombination signal sequences (RSSs) flanking each V, D and J gene segment (Eastman et al., 1996). Through the action of RAG proteins V, D and J gene segments are brought in close proximity and ultimately joined by components of the classical non-homologous end joining (NHEJ) repair pathway (Difilippantonio et al., 2000; Li et al., 1995) (Figure 5).

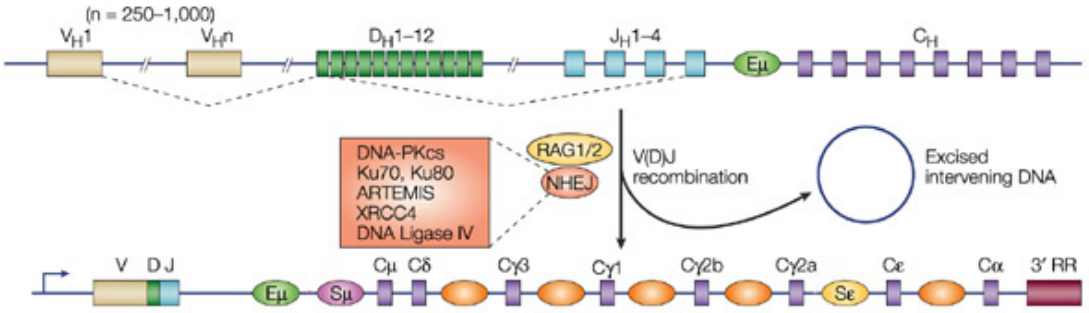

Figure 5. V(D)J recombination at Ig heavy chain locus.

The variable region of the IgH chain is assembled from variable (V_H), diversity (D_H), and joining (J_H) gene segments by V(D)J recombination. The process of rearrangement involves cleavage of the recombination signal sequences (RSS) in the DNA, which flank the rearranging gene segments, by the RAG1 and RAG2 enzymes. Joining of the DNA ends requires non-homologous end-joining (NHEJ) proteins, including Ku70, Ku80, ARTEMIS, X-ray repair cross-complementing protein 4 (XRCC4), DNA ligase IV and the catalytic subunit of DNA-dependent protein kinase (DNA-PKcs). Transcription of the rearranged locus is driven by an upstream promoter (blue arrow). Adapted from Chauduri and Alt, *Nat Rev Immunol*. 2004 Jul;4(7):541-52.

V(D)J is a highly regulated process, which involves introduction of DNA DSBs and deletion of large genomic segments. Chromatin accessibility and regulation of RAG expression are central mechanisms that modulate V(D)J recombination (Johnson et al., 2004; Morshead et al., 2003; Osipovich et al., 2004). Upon successful VDJ recombination, a pre-BCR complex is assembled on the cell surface, which consists of the newly rearranged IgH chain and a surrogate IgL chain. Signaling through the pre-BCR inhibits further rearrangement at the IgH locus, a process which is called allelic exclusion, whereas it stimulates clonal expansion of pre-B cells (Gorman and Alt, 1998). Following clonal expansion, pre-

B cells exit cell cycle and rearrange their IgL chain genes. Successful pairing of IgH and IgL chains to form a functional BCR marks the transition from pre-B to immature B cells. Should these cell fail to express an auto-reactive BCR, they are allowed to leave the BM and migrate to secondary lymphoid organs to complete their maturation (Rajewsky, 1996).

1.3.2. Peripheral B cell development.

1.3.2.1. Transitional B cells.

Once released from the BM, B cells migrate to the spleen as “so-called” transitional B cells (Allman et al., 1992) (Allman et al., 1993). While uniformly retaining expression of the early differentiation markers AA4.1/CD93 and the Heat Stable Antigen (HSA)/CD24, transitional B cells are divided into two main subsets based on expression of additional surface molecules. T1 B cells are defined as IgM^{hi},IgD^{-},$CD21^{-}$,$CD23^{-}$, while T2 B cells, the direct precursors of the long-lived mature B cell pool, acquire expression of IgD, CD21 and CD23 (Norvell and Monroe, 1996) (Loder et al., 1999) (Figure 6). An additional subset named T3, resembling T2 cells except for lower surface IgM expression, has been described, but its origin function remain poorly understood (Allman et al., 2001a). Within the spleen, T1 cells localize to the outer zone of the periarteriolar lymphoid sheath (PALS) (Liu, 1997). Here, they are in close proximity to macrophages, which engulf self-reactive, negatively selected lymphocytes. T2 cells, on the contrary, reside in B cell follicles (Loder et al., 1999) (Liu, 1997). Besides residing in different splenic areas, T1 and T2 cells are also functionally distinct. T1 B cells retain sensitivity to negative selection and are driven into apoptosis upon BCR engagement due to failure to up-regulate pro-survival molecules and progress in

the cell cycle (Chung et al., 2002; Norvell et al., 1995). T2 B cells, on the contrary, acquire sensitivity to T helper cell-derived survival signals and respond to BCR engagement with proliferation and survival rather than apoptosis (Chung et al., 2002)(Figure 6). *In vivo* bromodeoxyuridine (BrdU) labeling studies revealed rapid turnover of transitional B cells, including T2 cells, as compared with the mature B cell compartment. This reflects a shorter life-span of transitional B cells (1-4 days) in comparison with mature B cells (80-120 days) (Allman et al., 1993). At the molecular level, the B cell activating factor (BAFF/TNFSF13B/BLyS/TALL1) plays a major role in sustaining the transition from the transitional to the mature B cell compartment. Indeed, B cell-specific ablation of BAFF or its receptor, BAFF-R, resulted in impaired development beyond the T1 stage (Sasaki et al., 2004; Schiemann et al., 2001).

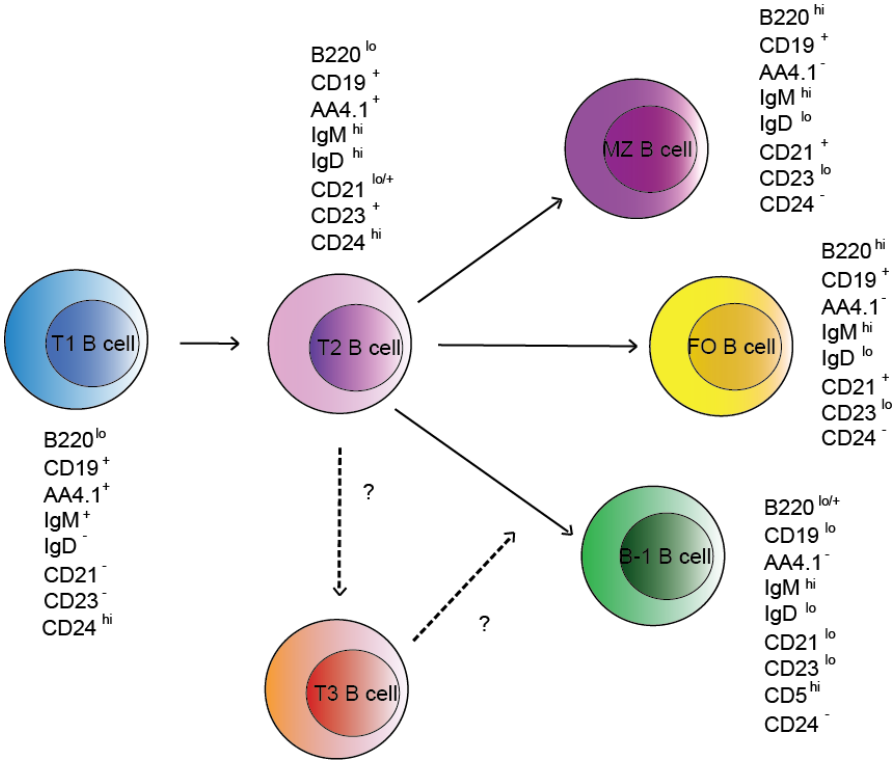

Figure 6. Schematic view of peripheral B cell development.

Upon exit from the BM, newly formed T1 B cells undergo negative selection aimed at purging the system from auto-reactive B cells. Non-autoreactive T2 B cells are then driven towards the FO, MZ or B-1 fate depending on expression of specific TFs. Markers used for immunophenotipic characterization of each developmental stage are listed.

1.3.2.2. Mature B cell subsets

In the mouse, mature B cells comprise three major phenotypically and functionally distinct subsets represented by Follicular (FO), Marginal Zone (MZ) and B1 B cells (Casola, 2007).

FO B cells

Also called B2 B cells, they are the most abundant mature B cell subset present in secondary lymphoid organs. Identified as $IgM^{hi}IgD^{hi}CD21^{lo}CD23^{+}$, FO B cells are endowed with the ability to recirculate through B cell areas of the spleen, lymph nodes (LNs) and mucosa-associated lymphoid tissues. FO B cells are the main mediators of T cell-dependent immune responses, although they can also take part to T cell-independent responses (Casola, 2007).

MZ B cells

MZ B cells are identified as $IgM^{hi}IgD^{-}CD21^{hi}CD23^{lo}$. They consist of a self-replenishing subset residing in the spleen in close proximity to the marginal sinus. MZ B cells capture and transport antigens in the form of immune complexes to FO B cells residing in the nearby splenic follicle. MZ B cells respond to BCR-mediated recognition of blood-borne pathogens by rapidly proliferating and differentiating into plasma cells (PC) secreting low-affinity antibodies in a T-cell independent manner (Cinamon et al., 2008; Martin and Kearney, 2002; Song and Cerny, 2003).

B-1 B cells

This mature B cell subset, identified as $IgM^{hi}IgD^{-}B220^{lo}CD19^{hi}CD23^{lo}$, mainly resides in body cavity sierosa. Based on surface expression of CD5, B-1 B cells can be further divided into the B-1a ($CD5^{+}$) and B-1b ($CD5^{-}$) B cell subsets (Stall et al., 1992). While B-1a B cells originate predominantly from fetal liver progenitors, B1-b B cells derive from BM progenitors (Montecino-Rodriguez et al., 2006). B-1 B cells are capable of self-renewing and can respond to bacterial antigens by rapidly differentiating into short-lived PCs (Alugupalli et al., 2004; Fagarasan and Honjo, 2003; Hardy, 2006) (Haas et al., 2005). They represent the main source of so-called natural antibodies that represent our first protection against invading pathogens.

1.3.2.3 Determinants of peripheral B cell development

1.3.2.3.1. BAFF

Receptors for BAFF include B cell maturation antigen (BCMA), transmembrane activator and calcium modulator and cyclophilin ligand interactor (TACI) and BAFF receptor (BAFF-R). They are expressed on the surface of B lymphocytes (Bossen and Schneider, 2006; Li et al., 2008), activated T cells and regulatory T cells (BAFF-R) (Mackay and Leung, 2006) and monocytes (Chang et al., 2006) and dendritic cells (Chang et al., 2008) (TACI). In humans, the BAFF-R is expressed at low levels on the surface of early BM B cell emigrants and its expression increases upon cell maturation (Darce et al., 2007; Sasaki et al., 2004). BAFF-R is crucial for the survival of late transitional B cells, as mice lacking either BAFF or its receptor display a prominent block in the transition from the T1 to the T2 stage (Schiemann et al., 2001). In addition, BAFF is required for survival of FO and MZ B cells, while it is dispensable for B-1 B cell persistence (Crowley et al., 2008; Scholz et al., 2008). BAFF induces survival of B cells via activation of the Nuclear Factor Kappa-light-chain-enhancer of activated B cells (NF-kB) pathway (Sasaki et al., 2006) and promotes cell growth, protein synthesis and glycolysis through activation of the protein kinase mammalian target of rapamycin (mTOR) pathway (Matsuzawa et al., 2008; Patke et al., 2006; Vallabhapurapu et al., 2008; Woodland et al., 2008). Central to the pro-survival activity of BAFF is the up-regulation of the anti-apoptotic B cell lymphoma 2 (*Bcl-2*) family member myeloid cell leukaemia sequence 1 (*Mcl1*) (Bouillet et al., 1999; Cariappa et al., 2007; Mills et al., 2008; Opferman et al., 2003; Wang et al., 1999).

1.3.2.3.2. The BCR

Surface expression of a functional BCR is critical for survival of mature B cells. Indeed, acute ablation of the BCR signaling complex in peripheral resting B cells results in rapid disappearance of the cells (Kraus et al., 2004; Lam et al., 1997). Additionally, antigen specificity, BCR surface density and strength of intracellular signaling have all been implicated in transitional B cell fate decisions (Casola, 2007). Cells receiving strong signaling through the BCR are thought to differentiate towards the B1 B cell compartment. Weaker signaling coupled to additional cues will instead favor the development of FO and MZ B cells (Casola et al., 2004).

1.3.2.3.3. Pax5

Pax5 is the major determinant of B cell identity. Pax5 is expressed starting from the pro-B cell stage, where it regulates antigen receptor assembly and establishes the transcriptome profile that enables further B cell maturation and function, at the same time preventing the expression of lineage-inappropriate genes (Cobaleda et al., 2007b; Nutt et al., 1999; Revilla et al., 2012; Souabni et al., 2002). In peripheral B cells, while preserving the B cell-specific gene expression program and thereby cell identity, Pax5 promotes the survival of B lymphocytes, in part through the regulation of BCR signaling (Cobaleda et al., 2007b; Delogu et al., 2006). In addition, Pax5 is also responsible for preventing premature onset of terminal differentiation (Delogu et al., 2006).

1.3.2.3.4. Notch2

Notch2 belongs to the Notch family of receptors, which play important functions in the development of hematopoietic lineages (Maillard et al., 2005). Notch2 is expressed on all mature B cells, and its natural ligand is Delta-like 1 (Dll-1), which is produced by splenic dendritic cells (DCs). B cell-specific deletion of Notch2 impairs development of MZ B cells, while the FO B cell compartment remains untouched (Saito et al., 2003). Similarly, inducible inactivation of Dll-1 leads to selective loss of MZ B cells (Hozumi et al., 2004). The role of Notch2 in MZ B cell development is further supported by the fact that animals carrying B cell-specific inactivation of the RBP-Jκ (Igκ-J region recombination-signal-binding protein 1) TF, which mediates the effects of Notch2 on gene expression, lack MZ B cells (Tanigaki et al., 2002). Conversely, B cells lacking the Notch2 transcriptional repressor, MINT (MSH homeobox homologue 2 (MSX2)-interacting nuclear target), display preferential commitment towards the MZ B cell compartment, with a concomitant decrease in FO B cells (Kuroda et al., 2003). Together, this indicates that Notch2 plays a pivotal role in MZ B cell development.

1.3.2.3.5. Aiolos

Aiolos is a zinc-finger transcription factor of the *Ikaros* gene family expressed throughout B cell development (Morgan et al., 1997). Aiolos expression levels are low during early B cell developmental stages and rise in peripheral B cells. Indeed, in *Aiolos*-deficient animals early B cell development is unaffected (Wang et al., 1998). Instead, development of the MZ and B-1 subsets is impaired, while FO B cells are normal, but display reduced activation thresholds following BCR engagement (Wang et al., 1998). In accordance with this, *Aiolos* mutant mice

display spontaneous GC development. Moreover, lack of Aiolos leads to the production of autoantibodies and development of autoimmune disease in aged animals (Sun et al., 2003).

1.3.2.3.6. NFAT

Nuclear factor of activated T cells (NFAT) was originally identified as a calcium-inducible TF necessary for expression of inteleukin (IL)-2 in T cells (Shaw et al., 1988). NFAT proteins are a family of four related TFs that can bind to regulatory elements of several different genes in different cell types (Crabtree and Olson, 2002; Kiani et al., 2000). The NFAT family members NFATc1, NFATc2 and NFATc3 are expressed in B cells and can be activated by BCR cross-linking or CD40 signaling (Ho et al., 1995; Timmerman et al., 1997; Venkataraman et al., 1994; Verweij et al., 1990). Lack of NFATc1, but not NFATc2, in B cells leads to selective loss of the B1-a compartment through a cell intrinsic mechanism. This indicates that NFATc1 function is necessary to sustain development/survival of B1-a cells and that its function cannot be compensated by the presence of NFATc2, which is also expressed in B-1a cells (Berland and Wortis, 2003).

1.3.3. B cell-mediated immunity

1.3.3.1. The germinal center response

During T cell-dependent immune responses, antigens are presented to naïve FO B cells in the form of immune complexes often exposed on the surface of follicular dendritic cells (FDCs). Antigens are recognized and internalized by B cells via their BCR. Once internalized, protein antigens are cleaved and the resulting peptides loaded on MHC-class II (MHCII) molecules, which are eventually exposed on the

cell's surface. Antigen-primed B cells migrate towards the edge of the follicular T cell zone, where they present the antigen to follicular helper T cells (T_{FH}). Concomitant MHCII/TCR pairing and co-stimulatory signals delivered following CD40/CD40L and CD80/CTLA4 interactions result in full B cell activation, which triggers the GC response. GCs consist of a densely packed dark zone, where antigen-specific B cell centroblasts proliferate at high rate, and a light zone, where resting B cell centrocytes, T_{FH} cells, FDCs and macrophages reside in close proximity (Klein and Dalla-Favera, 2008a). Within the dark zone, centroblasts undergo clonal expansion and diversify their V genes through a process called Ig somatic hypermutation (SHM), which leads to non-templated single nucleotide substitutions/deletions preferentially within the portion of the V gene coding for the hypervariable regions (also called complementarity determining regions or CDRs) of the BCR. SHM depends on the activity of the Activation-Induced cytidine Deaminase (AID) enzyme, whose expression is induced in GC B cells (Muramatsu et al., 2000). GC Centroblasts up-regulate a substantial number of genes associated with cell proliferation, while limiting the expression of negative regulators of the cell cycle. GC B cells also prevent full activation of the DDR pathway in order to undergo Ig SHM and class switch recombination (CSR) (Ranuncolo et al., 2007; Ranuncolo et al., 2008a; Ranuncolo et al., 2008b). Centroblasts are highly prone to undergo apoptosis as a result of the up-regulation of pro-apoptotic factors including CD95/Fas and down-regulation of anti-apoptotic proteins including members of the BCL2 protein family (Martinez-Valdez et al., 1996) (Klein et al., 2003) (Basso et al., 2010). Rapid execution of programmed cell death is instrumental for the clearance of B cells displaying non-functional or low affinity BCRs as a result of Ig SHM (Figure 7) (Basso and Dalla-Favera, 2010).

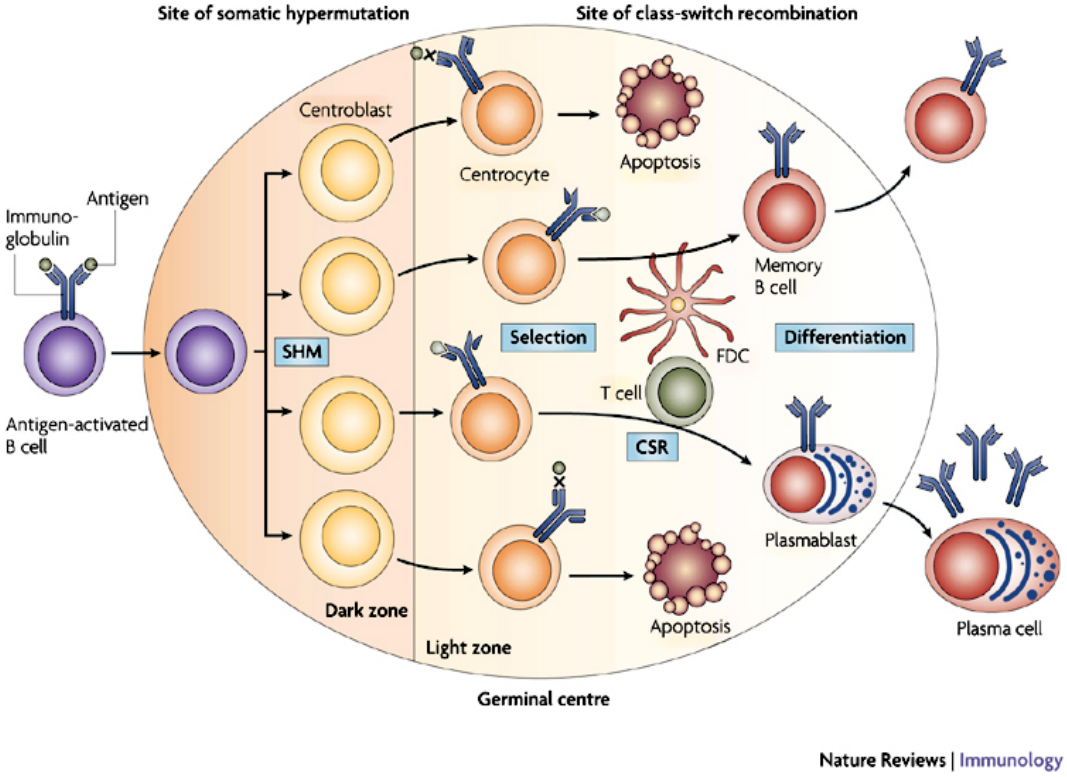

Figure 7. Schematic view of the GC reaction.

In T cell-dependent immune responses, following antigen encounter, FO B cells enter the GC reaction. The GC is characterized by the presence of a dark zone, where large centroblasts undergo massive proliferation and SHM of their Ig gene loci, and a light zone. In the light zone, smaller resting centrocytes are tested for improved antigen binding, undergo CSR and differentiate into high-affinity B or memory B cells. From Klein and Dalla Favera, *Nat Rev Immunol*. 2008 Jan;8(1):22-33.

B cells expressing mutated BCRs migrate to the light zone of the GC, where they turn into resting centrocytes. In the light zone, centrocytes are selected on the basis of improved antigen binding via their BCR (Rajewsky, 1996). Only B cells expressing BCRs with the best affinity for the cognate antigen will succeed in capturing the antigen presented on FDCs and present it T_{FH} cells. Co-stimulatory signals provided by TF_H cells represent the key event for positive selection of GC B cells (Vinuesa et al., 2005). This stringent selection process leads the majority of

GC B cells to succumb by apoptosis and to be rapidly cleared by local macrophages (Klein and Dalla-Favera, 2008b). T_{FH} cells residing in the GC also provide signals that promote Ig CSR, whereby B cells exchange their IgH constant region through a recombination process dependent on AID, to improve the effector function of their BCR (Kawabe et al., 1994; Vinuesa et al., 2005). *In vivo* imaging experiments have provided evidence that GC trafficking is not limited to a unidirectional movement of B cells from the dark to the light zone, but is contributed by a substantial migration in the opposite direction. This observations support a model whereby B cells undergo iterative rounds of proliferation, Ig mutation and antigen-based selection, with the goal to express antibodies with increasing affinity for cognate antigen (Victora et al., 2010). Eventually, through mechanisms that remain poorly understood, antigen-selected GC B cells activate differentiation programs that lead to their exit form the GC as long-lived, terminally differentiated, antibody-secreting plasma cells (PCs) of memory B cells.

1.3.3.2. Bcl6: an essential transcription factor for GC B cells

The transcription factor BCL6 is a master regulator of the GC response (Cattoretti et al., 2005; Fukuda et al., 1997). *Bcl6* encodes a zinc finger transcription factor, which acts primarily as a sequence-specific transcriptional repressor. Bcl6 exerts its repressive function primarily via interaction with co-repressors including BCOR, SMRT and NCOR (Dhordain et al., 1998; Huynh and Bardwell, 1998; Wong and Privalsky, 1998). Through the latter complexes, Bcl6 is thought to silence genes involved in cell growth inhibition and apoptosis (Hatzi et al., 2013). Instead, Bcl6 influences B cell development through the interaction with the Mi-2-NuRD complex (Dent et al., 1997; Fujita et al., 2004; Parekh et al., 2007; Ye et al., 1997). Bcl6 renders GC B cells tolerant to DNA damage through direct suppression of the

DNA damage sensor ATR and other DDR factors such as Tp53 and Chek1 (Phan and Dalla-Favera, 2004; Ranuncolo et al., 2008a; Ranuncolo et al., 2008b). On the other hand, excessive accumulation of DNA damage is prevented by a signaling pathway that, in response to high levels of genotoxic stress, promotes ATM-dependent phosphorylation and degradation of Bcl6 (Phan et al., 2007b; Ranuncolo et al., 2007). Bcl6 supports GC B cell proliferation by inhibiting CDK inhibitors such as *Cdkn1a* and *Cdkn2a* (Basso et al., 2010) (Klein et al., 2003). In GC B cells, Bcl6 also inhibits premature onset of the plasma cell (PC) transcriptional program via direct repression of the *Prmd1/Blimp1* locus, which is required for PC development (Vasanwala et al., 2002) (Figure 8A). Reduction of Bcl6 expression is needed to allow the differentiation of GC B cells into antibody-secreting PCs. In centrocytes, down-regulation of Bcl6 is mediated by: 1) CD40 signaling, which leads to *Bcl6* transcriptional silencing (Niu et al., 1998; Polo et al., 2008) and 2) BCR signaling, which leads to phosphorylation and hence degradation of Bcl6 protein (Phan et al., 2007a) (Figure 8B).

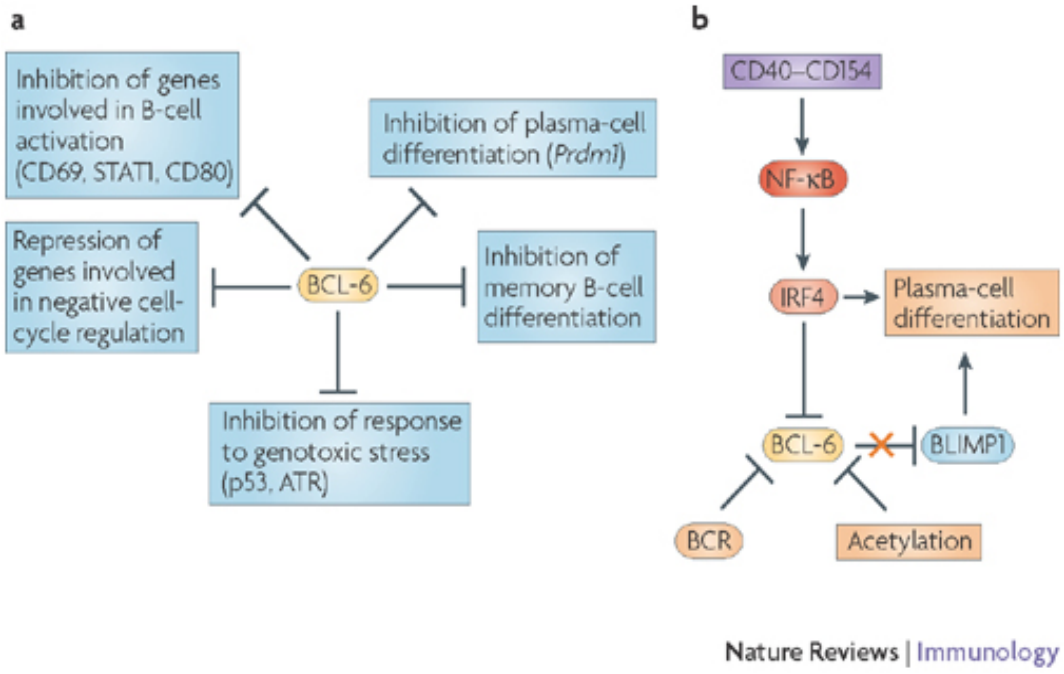

Figure 8. Biological functions and pathways regulated by Bcl-6.

a) In centroblasts, Bcl6 supports the function of Aid and SHM by inhibiting the DDR pathway and stimulating cell cycle progression. In addition, Bcl-6 prevents premature differentiation towards the plasma cell or memory B cell fate by repressing key TFs.

b) In centrocytes, interaction of B cells with T_{FH} cells through CD40 activates NF-kB signaling, which stimulates expression of the *Bcl6* repressor *Irf4*. In addition, signals delivered trough the BCR induce proteasomal degradation of Bcl6. Down-modulation of Bcl6 releases the break on the *Prmd1* gene, allowing terminal differentiation towards the PC fate. From Klein and Dalla Favera, *Nat Rev Immunol*. 2008 Jan;8(1):22-33.

Interestingly, Ring1b forms a protein complex with BCOR and thus has been suggested to regulate Bcl6-mediated gene silencing (Sanchez et al., 2007). The functional relationship between Polycomb- and Bcl6-mediated gene silencing has been recently confirmed by our lab. Indeed, we could show that a substantial

number of Bcl6 targets were up-regulated upon conditional inactivation of Ezh2 in GC B cells (Caganova et al., 2013). This suggests that Polycomb and Bcl6 may co-operate in silencing at least a subset of common targets (Velichutina et al., 2010).

1.3.4. Terminal B cell differentiation.

1.3.4.1. Plasma cell development.

Following a T cell-dependent immune response, high-affinity B cells enter one of two possible differentiation routes and either become terminally differentiated PCs or memory B cells. Differentiation into functional antibody-secreting PCs is a step-wise process that requires the combined expression of TFs Blimp1, Irf4 and Xbp1 (Figure 9). The activation of Blimp1 is critical in PC precursors to extinguish the (GC) B cell transcriptional programs through the direct repression of Pax5 and Bcl6 (Lin et al., 2002; Shaffer et al., 2002). In line with this, PC differentiation is phenotypically characterized by loss of B-cell specific markers including CD19, CD23 and surface Ig, and the acquisition of PC-specific ones such as CD138/Syndecan 1.

1.3.4.2. Regulation of PC development.

1.3.4.2.1. Blimp1.

The transcription factor Blimp1 is encoded by the *Prdm1* (positive-regulatory-domain-containing 1) gene. Blimp1 is required for the formation of both short-lived and long-lived PCs (Angelin-Duclos et al., 2000; Kallies et al., 2004) (Shapiro-

Shelef et al., 2003). In GC B cells, *Prmd1* is repressed by the concerted actions of Bcl6 and Metastasis-associated 1 family, member 3 (MTA3), which bind to intron 5 of the gene (Fujita et al., 2004; Tunyaplin et al., 2004). In late GC B cells, induction of Blimp1 depends on: i) signaling through the IL-21 receptor, which induces the activation of the TF STAT3 and ii) CD40 signaling, which leads to NF-kB dependent up-regulation of Interferon Regulatory Factor 4 (IRF4) (Kwon et al., 2009). Together, STAT3 and IRF4 bind to an IL-21 responsive element downstream the *Prmd1* gene and mediate its full expression (Kwon et al., 2009). Recent evidence from our group has demonstrated a critical role for Ezh2 in the modulation of IL-21-dependent terminal differentiation. Indeed, we could show that Ezh2 limits, through H3K27me3, the induction of Blimp1 in response to IL-21 stimulation, thereby contributing to the persistence of B cells within the GC (Caganova et al., 2013). To induce PC differentiation Blimp1 acts both as a transcriptional inducer and repressor. It : i) inhibits cell proliferation induced by c-MYC and E2F1 (Lin et al., 1997; Shaffer et al., 2002), ii) induces Irf4 expression (Klein et al., 2006; Sciammas and Davis, 2004; Shaffer et al., 2002); iii) silences the (GC) B cell-specific transcriptional program via repression of *Pax5* and *Bcl6* (Lin et al., 2002; Shaffer et al., 2002) and iv) activates the TF X-box binding protein 1 (Xbp1) to allow sustained secretion of Ig molecules (Reimold et al., 1996; Shaffer et al., 2002) (Figure 9). Importantly, Blimp1 appears also to be critical for the maintenance of long-lived BM PCs (Shapiro-Shelef et al., 2005).

1.3.4.2.3. Interferon Regulatory Factor 4.

Interferon regulatory factor 4 (Irf4) is a TF essential for PC development (Klein et al., 2006; Sciammas et al., 2006). Its expression is not restricted to PCs, as *Irf4* is also required to support B cell function at early developmental stages (Lu et al.,

2003; Mittrucker et al., 1997). In GC B cells, *Irf4* levels are low in centroblasts, but rise in centrocytes as a result of CD40 signaling. In these cells, high levels of Irf4 together with IL-21 contribute to activate Blimp1 expression, promote CSR and hence drive PC development. Blimp1 can also induce *Irf4* expression (Sciammas et al., 2006) thereby generating a feed-forward positive loop that is needed to ensure repression of *Bcl6* (Sciammas and Davis, 2004). Recently, Sciammas and co-workers reported a dynamic control of Irf4 abundance, which contributes to the stepwise differentiation of B cells during a GC response. Specifically, low levels of Irf4 were required for the recruitment of B cells into the GC through the up-regulation of *Bcl6* and *Pou2af1*. Instead, high levels of the TF diverted cells into the PC developmental path. Differential expression of Irf4 in developing B cells was shown to determine shifts in genome-wide binding of the TF, ultimately resulting in distinct patterns of gene expression (Ochiai et al., 2013). Irf4 is also required to induce *Xbp-1* and thereby sustained Ig secretion in PCs (Sciammas et al., 2006; Skalet et al., 2005).

1.3.4.2.2. X-box binding protein 1 and the unfolded protein response

The TF Xbp1 activates a transcriptional program that sustains the high rate of Ig synthesis of PCs (Calfon et al., 2002; Reimold et al., 2001). Loss of Xbp1 leads to impaired Ig secretion, ultimately resulting in failure to control infections (Reimold et al., 2001). In PCs, transcription of Xbp1 is induced by *Blimp1* (Shaffer et al., 2004), Activating Transcription Factor 6 (ATF6) and IL-4 (Iwakoshi et al., 2003; Yoshida et al., 2000). *Xbp1* mRNA is then cleaved through the endoribonuclease function of the activated IRE1 dimers to yield a spliced form of the transcript. Spliced Xbp1 displays the same DNA binding region as its precursor, but yields a more stable and more efficient transcriptional activator (Calfon et al., 2002; Lee et al., 2002;

Yoshida et al., 2001). Xbp1 activates genes that elicit a PC-specific unfolded protein response (UPR) whereby, in contrast with stress-induced UPR, increase in size of the endoplasmic reticulum (ER) and enhanced protein synthesis co-exist and apoptosis is not induced (Gass et al., 2002). Xbp1 target genes encode factors that regulate protein targeting to the ER, protein folding, degradation of mis-folded proteins, protein glycosylation, trafficking between ER and Golgi and targeting of secretory vescicles to the plasma membrane. In addition, Xbp1 regulates cell and organelle size (Shaffer et al., 2004).

1.3.4.2. Memory B cell development.

Memory B cells represent a subset of resting long-lived, antigen-experienced lymphocytes. Memory B cells are predominantly, but not exclusively, generated during the GC reaction and provide life-long protection against foreign antigens (Kaji et al., 2012) (Rajewsky, 1996). Memory B cells can express either IgM or Ig-class switched antibodies. Recent work by the Weill/Reynaud group has assigned different functions to IgM and Ig-switched memory B cells. Whereas IgM^+ memory B cells are preferentially recruited into the GC during secondary immune responses, Ig-switched memory cells differentiate directly into PCs upon antigen re-encounter (Dogan et al., 2009). These results partition memory B cells into two groups, of which one (IgM^+ cells) is devoted to the generation of increasingly higher BCRs as a result of subsequent rounds of Ig SHM in GCs, whereas the other (Ig-switched cells) provides a ready source for high-affinity neutralizing antibodies (Weill et al., 2013). The different fate of IgM vs. IgG memory B cells may depend on the different signaling properties of the BCRs expressed by the two types of cells (Pierce and Liu, 2013) (Martin and Goodnow, 2002) (Kometani et al., 2013). The mechanisms leading to B cell memory formation remain poorly

understood. Activation of the TF STAT5 as a result of cytokine stimulation of late GC B cells has been proposed as a mechanism driving memory B cell formation (Scheeren et al., 2005). Also, sustained CD40 signaling during the GC response has been proposed to skew differentiation towards the memory B cell fate (Arpin et al., 1995). Finally, recent evidence has suggested that differentiation into memory B cells expressing different Ig isotypes relies on divergent genetic programs activated by different transcriptional regulators (Wang et al., 2012). Another yet open question is how memory B cells are maintained. Whereas work by Maruyama and Rajewsky has excluded a role for antigen in memory B cell maintenance, recent work has challenged this conclusion (Dogan et al., 2009) (Maruyama et al., 2000).

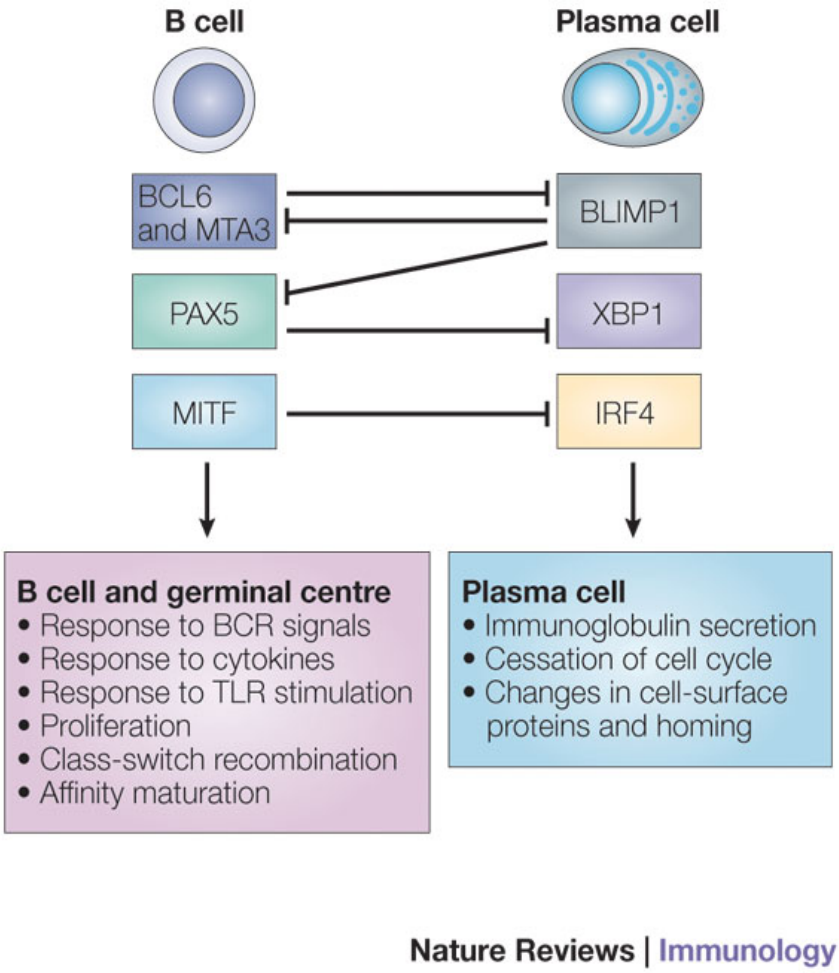

Figure 9. Opposing transcriptional networks in GC and PC development.

Several TFs, including Bcl6, Mta3, Mitf (microphthalmia-associated transcription factor) and Pax5 prevent PC development by repressing *Blimp1*, *Xbp1* and *Irf4*. In PCs, Blimp1 represses B cell gene expression programs. This mutual repression system prevents premature terminal differentiation and the reversion of plasma cells to a B cell stage. In addition to PC determinants, Bcl6, Mta3, Pax5 and Mitf also regulate the expression of genes required for B cell and GC functions, which are outlined in the pink box. Blimp1, Xbp1 and Irf4 induce the expression of genes that are required for plasma cells, whose categories are outlined in the blue box. From Shapiro-Shelef and Calame, *Nat Rev Immunol*. 2005 March;5(3):230-42.

2. Materials and Methods

2.1. Mice

Mice were housed and bred in animal facility at the IFOM-IEO Campus Institute, Milan, Italy. Animal handling followed European Community recommendations.

Wt.

C57BL/6J mice were purchased from Charles River

Mutants (genetic background).

Ring1a$^{-/-}$ (del Mar Lorente et al., 2000)(BL/6)

Ringb^{fl} (Cales et al., 2008) (BL/6)

R26-EYFP$^{fl\text{-}STOP}$ (Srinivas et al., 2001) (BL/6)

Cre lines (genetic background).

Mb1-cre (Hobeika et al., 2006) (BL/6)

Cd23-cre (Kwon et al., 2008) (BL/6)

Cγ1-cre(Casola et al., 2006) (BL/6)

Aicda-cre (Crouch et al., 2007) (BL/6)

2.1.2. Genomic DNA extraction from tail biopsy

Tail lysis buffer	100 mM Tris-HCl pH 8.5
	5 mM EDTA
	200 mM NaCl
	0.2 % SDS

1 cm of a tail biopsy was incubated in 400 µl of lysis buffer with Proteinase K (100 µg/ml) at 56˚C, shaking at 850 rpm, overnight in Thermomixer compact. 350 µl of lysate were transferred into a new tube and 1 ml of isopropanol was added, mixed by inverting and centrifuged at maximum speed for 1 min. DNA pellet was dissolved in 200 µl of miliQ water by incubation at 60˚C for 20 min.

2.1.3. Genotyping strategy

The genotypes of all mice offsprings were analyzed by polymerase chain reaction (PCR) performed on genomic DNA extracted from tail. For amplification, primers summarized in **Table 1** and PCR reagents listed in **Table 2** were used. PCR conditions are summarized in **Table 3**. PCRs were run in automatic thermocycler GeneAmp PCR System9700 (Applied Biosystems).

Table 1. Primers used for genotyping, annealing temperatures and amplicon sizes.

Gene	Primer ID	Sequence	T_A (°C)	Product (bp)
Ring1b WT vs Fl	Ring1b Fl Rv	GTTCCATTTGTCTGCACAGCCTGAG	58	Ring1b WT 250 bp
	Ring1b Del Fw	TAATTCCATGAAAGCATCAAAGT		Ring1b^{fl} 270 bp
	Ring1b Del Rv	AGCACTGTGCTCCTTTTTGAT		Ring1b$^{\Delta}$ 500 bp
Ring1a WT vs KO	Ring1a WT Fw	CTTCCGCAGACCTCTCTCAG	60	Ring1a WT 221 bp
	Ring1a WT Rv	TTGCGCTCATCTTAGGCTTT		
	Ring1a KO Fw	TGCTCGAGATGTCATGAAGG		Ring1a KO

	Ring1a KO Rv	TATGTCCCCCGTTGACTGAT		196 bp
Mb1-cre	Mb1cre_Fw	CCCTGTGGATGCCACCTC	58	Mb1-cre
	Mb1cre_Rv	GTCCTGGCATCTGTCAGAG		430 bp
Cγ1-cre	IgG1 Fw	TGTTGGGACAAACGAGCAATC	58	Cγ1-cre 450
	IgG1 Rv	GTCATGGCAATGCCAAGGTCGCTAG		bp
	Cγ1-creF	GGTGGCTGGACCAATGTAAATA		Cγ1 WT 240 bp
Cd23-	Cd23-cre Fw	GATGTGAGGGACTACCTCCTGTACC	60	Cd23-cre
cre	Cd23-cre Rv	CCAGCATCCACATTCTCCTT		348 bp
Aicda-	UCre F	ACGAACCAAGGTGACAGCAATG	60	Cre
cre	UCre R	CTCGACCAGTTTAGTTACCC		350 bp

Table 2. PCR Reagents

PCR master mix	**µl**
H2O	14.4
5x flexi buffer	5
MgCl2 25 mM	2
dNTPs 2.5 mM	2
primer Fw 50 µM	0.2
primer Rv 50 µM	0.2
GO Taq	0.2
DNA	1
total	25

Table 3. Genotyping PCR conditions.

PCR cycle		
Temperature(°C)	Time (min)	
94	2:30	
94	0:30	
T_A	0:30	33x
72	0:30	
72	5:00	
4	hold	

2.1.4. Mice immunization

6 to 8 weeks old mice were immunized with Alum (Imject ® Alum, aqueous solution of aluminium hydroxide (40 mg/ml) and magnesium hydroxide (40 mg/ml), Pierce) precipitated NP_{25}CGG (100µg per mouse, 4-Hydroxy-3-nitrophenylacetyl

hapten conjugated to Chicken gamma globulin, Biosearch Tech.) intraperitoneally. For recall responses, secondary immunizations with 50 µg of Alum precipitated $NP_{25}CGG$ were performed 60 days after primary immunization. For immunohistochemical visualization of $BCL6^+$ GCs, mice were immunized with 10^8 sheep red blood cells (Thermo Scientific) and analysis of GC formation was performed 8 days later.

2.1.5. In vivo proliferation assay

Mice immunized with $NP_{25}CGG$ were injected with 200 µg EdU (BrdU analog, Invitrogen) intraperitoneally on day 12 post-immunization, 1 h prior to analysis. For EdU detection, EdU detection kit (Click-iT™ EdU Alexa Fluor® 647, Invitrogen) was used following the manufacturer's instructions.

2.2. Cell culture techniques

2.2.1. B cell purification

Erythrocyte lysis buffer	
solution A	0.17 M Tris pH 7.65
solution B	0.83 % NH_4Cl
working solution	9 parts B + 1 part A

B cell medium	DMEM
	10 % FCS
	2 mM glutamine
	200 U/ml pen/strep
	NEAA
	50 µM b-ME
	1 mM Na Pyruvate

FACS buffer	1x PBS
	1 % BSA
	0.05 % NaN3

For B cell analysis, mice of 6-8 weeks of age were used.

BM cell suspension was obtained by flushing tibia with 5 ml B cell medium.

SPL and LN were collected and smashed for single cell suspensions. Erythrocyte lysis was performed on SPL and BM cell suspensions using 1 ml of erythrocyte lysis buffer with incubation of 3 min on ice. Reaction was stopped by adding 10 ml of B cell medium and cells were washed in Fluorescence-activated cell sorting (FACS) buffer. Live cells were counted using Erythrosin B dye to distinguish live and dead cells. All centrifugation steps were performed for 5 min at 280 g at 4°C.

2.2.2. In vitro B cell culture

MACS buffer	1x PBS
	0.5 % BSA
	2 mM EDTA

Splenic B cells were purified following the protocol of B cell purification with the exception of using magnetic cell sorting (MACS) buffer instead of FACS buffer. B cells were purified through LS columns (Miltenyi Biotec) following manufacturer's B Cell Isolation Kit depletion protocol (Miltenyi Biotec). Specifically, CD43-expressing B cells (activated B cells, PCs and B1a cells) T cells, NK cells, dendritic cells, macrophages, granulocytes, and erythroid cells were indirectly magnetically labeled by using a cocktail of biotin-conjugated antibodies against CD43 (Ly-48), CD4 (L3T4), and Ter-119, followed by Anti-Biotin MicroBeads incubation. This procedure allows the isolation of untouched resting B cells from single cell suspensions of lymphoid tissues.

Purified B cells were cultured in B cell medium and stimulated with 20 µg/ml LPS (Lipopolysacharide, Sigma) with or without 15 ng/ml IL-4 (Recombinant Murine Interleukin 4, GRF-10600, Immunological Sciences); or 1 µg/ml RP105 (Monoclonal rat-anti mouse CD180, functional grade purified RP/14, eBiosciences). Cells were cultured at a density of 0.5 - 1 x 10^6 cells/ml at 37°C at 6 % CO2.

For iGB cultures, purified B cells were seeded on a feeder layer of irradiated (120 Gy, 1 hour) 40 LB cells that had previously received 120 Gy irradiation over a 1 hour interval. Cells were seeded at a starting density of 2x10^4 cells/mL in 40 mL of B cell medium supplemented with 1 ng/ml IL-4. Cells were left at 37°C at 6 % CO2. Medium was changed at day 2 following activation. At day 4, iGB cells were harvested and counted. To induce plasma cell differentiation, iGB cells were seeded on a freshly irradiated 40LB feeder layer at a density of 2x10^4 cells/ml in 40 mL of B cell medium supplemented with 10 ng/ml IL-21 (Peprotech).

2.3. Imaging Techniques

2.3.1. Immunostaining for flow cytometry and cell sorting

Cells were stained in 10 µl / $1x10^6$ cells of FACS buffer containing antibodies of choice for 20 min at 4˚C in dark and subsequently washed twice with 200 µl of FACS buffer. List of antibodies as well as working dilutions are listed in Table 4.

Table 4. Antibodies used for flow cytometry.

Antibodies and antigen	Company	dilution
Monoclonal Rat-anti mouse CD5 (PE)	eBiosciences	1/200
Anti mouse CD95 (Fas)	eBiosciences	1/170
Anti mouse IgM clone R331.12 (Alexa 488)	home made	1/400
Anti mouse Kappa clone R331.18 (Alexa 488)	home made	1/800
Monoclonal Rat-anti mouse CD138 (PE)	BD Biosciences	1/200
Monoclonal Rat-anti mouse CD19 (Cy7 PE)	eBiosciences	1/400
Monoclonal Rat-anti mouse CD21/CD35 (PE)	eBiosciences	1/1000
Monoclonal Rat-anti mouse CD23 (FITC)	eBiosciences	1/100
Monoclonal Rat-anti mouse CD25 (APC)	eBiosciences	1/200
Monoclonal Rat-anti mouse CD38 (APC)	eBiosciences	1/600
Monoclonal Rat-anti mouse CD43 (PE)	eBiosciences	1/100
Monoclonal Rat-anti mouse IgD (PE)	eBiosciences	1/3000
Monoclonal Rat-anti mouse IgG1 (biotin)	BD Biosciences	35064
Monoclonal Rat-anti mouse/human CD45R(B220) (Cy7PE)	eBiosciences	1/400
Monoclonal Rat-anti mouse/human CD45R(B220) (FITC)	eBiosciences	1/200
Monoclonal Rat-anti mouse CD24/HSA (PE)	eBiosciences	1/400
Monoclonal Rat-anti mouse CD93/AA4.1 (APC)	eBiosciences	1/600
Monoclonal Rat-anti mouse CD268/BAFF-R (APC)	Biolegend	1/600
NIP (PE)	home made	1/4000
Antigen Fluorescein Peanut Agglutinin (PNA)	Vector Laboratories	1/800
Streptavidin (APC)	eBiosciences	1/800
Streptavidin (FITC)	eBiosciences	1/400

2.3.2. Intracellular immunostaining for flow cytometry

Cells were stained in 10 µl / $1x10^6$ of FACS buffer containing antibodies of choice (Table 4) for 20 min at 4˚C in dark and subsequently washed twice with 200 µl of

FACS buffer. Surface stained cells were fixed in BD Cytofix/Cytoperm™ buffer for 20 min on ice in U bottom 96 well microplate, washed by Perm/Wash™ Buffer (P/W) and refixed in BD Cytofix/Cytoperm™ buffer for 20 min on ice. Cell were then incubated in blocking buffer (10 % normal goat serum in P/W buffer) for 30 min at RT shaking and stained Alexa488-labeled Rat-anti mouse IRF4 (IRF4 3E4, BioLegend, working dilution 1/400) in staining solution for 60 min at RT, shaking. Cells were washed twice with P/W buffer and fixed in 1 % formaldehyde in PBS. Samples were acquired and analyzed using FACSCalibur (Becton Dickinson) and FlowJo software. All centrifugation steps were performed at 780 g for 10 sec at 4°C.

2.3.4. Immunostaining of SPL sections

2.3.4.1. Immunofluorescence

Fluorescent immunostaining was performed on frozen SPL sections obtained from immunized C57BL6/J mice (snap-frozen, OCT-embedded samples). Spleens were cut in 6 µm-thick slices and placed on Microscope Slides Superfrost ultra Plus® (Thermo Scientific). Samples were washed once in 1x PBS, hen fixed for 5’ at RT in 80% ethanol. Slides were then again washed 3x for 5’ with 1x PBS. Avidin solution from the Avidin/biotin Blocking System (Covance) was added and incubated 10’ at RT. Slides were then briefly washed 3x in 1x PBS and incubated 10’ at RT with Biotin solution from the Avidin/biotin Blocking System (Covance). Slides were then briefly washed 3x in 1x PBS and incubated for 45’ with pre-incubation solution (1x PBS, 0,005% FBS, 0,001% BSA). Following incubation, antibodies were added in sequence. The primary antibody used was a monoclonal rat anti-human MOMA-1 (Abcam, diluted 1:50 in pre-incubation solution). Incubation was performed at RT for 90’ in the dark. Slides were then washed 5’

each with 1x PBS and secondary Streptavidin coupled to Cy3 (SouthernBiotech) was added at a 1:250 dilution. Incubation was performed for 60’ at RT. Following 3 washes, of 5’ each, with 1x PBS, slides were incubated with Monoclonal Rat-anti mouse/human CD45R(B220) (eBioscience) at a 1:100 dilution for 60’ at RT, shielded from light. Slides were washed 3x in 1x PBS for 5’. DNA was stained with 4',6-diamidino-2-phenylindole (DAPI) for 5’ and washed with 1x PBS immediately after. Slides were then mounted in 50% Glycerol and stored in the dark at +4°C until acquisition. Images were acquired on a Widefield BX61 microscope (Olympus) using the MetaMorph (Molecular Devices) software. Image analysis was performed using ImageJ (NIH).

2.3.4.2. Immunohistochemistry.

Histochemical analysis was performed for GC scoring. Spleens were snap-frozen in liquid N_2 and isopentane, fixed in 4 % buffered formalin and embedded in paraffin. Tissue cross-sections were cut at 3 or 5 µm thickness for immunostaining, mounted Microscope Slides Superfrost ultra Plus® (Thermo Scientific) and stored at room temperature. Before immunostaining, the slides were passed through ethanol steps decreasing in concentration (100%, 95%, 80%), for 3’ each to remove paraffin. Slides were then re-hydrated 5’ in RT H_2O. Removal of bonds between paraffin and internal antigen was performed at 95°C for 1 hour in sodium citrate buffer (2.1% citric acid, 2.94% sodium citrate in 1 L distilled water) followed by air-drying for 40’ below a fume hood. Sections were used for routine stains (eosin and hematoxylin) or immunohistochemistry. Before immunohistochemistry, slides were incubated with Avidin/biotin Blocking System (Covance) as described in paragraph 2.3.4.1. Slides were then washed with 1x PBS and incubated for 2 hours at RT in pre-incubation solution (1x PBS, 0,005%

FBS, 0,001% BSA). Incubation with rabbit polyclonal anti-Bcl6 antibody (Cell Signaling, #4242) 1:200 in pre-incubation solution was performed overnight at +4°C. On the following day, slides were washed 3x, 5' in 1x PBS and incubated with secondary antibody (anti-rabbit IgG coupled to HRP, 1:200, Vector) for 45' at RT. Binding of secondary antibody was then revealed upon incubation with ABC kit (VECTASTAIN Elite ABC Kit) and eosin. Slides were rinsed in water and de-hydrated in alcohol series (80%, 95%, 100%) for 10'' each. Slides were then mounted in glycerol and stored at RT until acquisition. Images were acquired on a Full Manual BX51 (Olympus) Microscope using the MetaMorph (Molecular Devices) software. Image analysis was performed using ImageJ software (NIH).

2.3.5. Immunostaining for detection of apoptosis.

For detection of apoptotic cells CaspGLOW^{TM} Fluorescein Active Caspase Staining Kit was used with specific modifications in protocol. *Ex vivo* purified or *in vivo* cultured cells were incubated in 100 µl of B cell medium containing 1 µl of FITC-VAD-FMK (carbobenzoxy-valyl-alanyl-aspartyl-[O-methyl] fluoromethylketone), a cell-permeant pan caspase inhibitor that irreversibly binds to the catalytic site of caspase proteases, for 1 h at 37°C and 6 % CO_2. Cells were collected by centrifugation (280 g for 5 min) and washed with 200 µl of wash buffer. If required cells were stained following the protocol of chapter 2.3.1. (Immunostaining for flow cytometry), acquired by FACSCalibur (Becton Dickinson) and analyzed using FlowJo software.

2.3.6. Cell cycle analysis

2.3.6.1. *In vitro.*

One million of *in vitro* activated B cells was collected by centrifugation for 5 min at 280 g and washed in PBS. cells were fixed in 100 µl of BD Cytofix/Cytoperm buffer (BD Biosciences) for 30 min on ice and washed with P/W and incubated in BD Cytoperm Plus Buffer (BD Biosciences) for 10 min on ice. After washing in P/W buffer cells were re-fixed in 100 µl of BD Cytofix/Cytoperm buffer for 5 min on ice and washed by P/W buffer again. For DNA staining cells were resuspended in 1 ml of cold propidium iodide (50 µg/ml) + RNase (250 µg/ml) and incubated overnight at 4°C. Samples were acquired by FACSCalibur (Becton Dickinson) and analyzed using FlowJo software.

2.3.6.2. *Ex vivo*.

Purified splenic B cells were stained following the protocol of chapter 2.3.1. (Immunostaining for flow cytometry). Surface stained cells were fixed in 100 µl of BD Cytofix/Cytoperm buffer (BD Biosciences) for 30 min on ice and washed with P/W and incubated in BD Cytoperm Plus Buffer (BD Biosciences) for 10 min on ice. After washing in P/W buffer cells were re-fixed in 100 µl of BD Cytofix/Cytoperm buffer for 5 min on ice and washed by P/W buffer again. For DNA staining cells were resuspended in 1 ml of cold propidium iodide (50 µg/ml) + RNase (250 µg/ml) and incubated overnight at 4°C. Samples were acquired by FACSCalibur (Becton Dickinson) and analyzed using FlowJo software.

2.4. Biochemical techniques.

2.4.1. Enzyme-Linked Immunosorbent Assay (ELISA).

ELISA methods are immunoassay techniques that combine the specificity of immunological reaction with the sensitivity of enzyme assays and allow quantification of immunoglobulins or antigens. One of the most common ELISA applications is to measure the amount of immunoglobulins in blood serum. Coating was performed with 50 µl of capture antibodies (**Table 5**) or antigens (**Table 6**) diluted to working concentration in coating buffer (0.5 M Carbonate-bicarbonate buffer pH 9.6) overnight at 4˚C in NUNC Maxisorp white 96 well microplate. Coating solution was removed and plate washed 3 times with 450 µl of washing buffer (0.05 % Tween20 in PBS). Plate was blocked in blocking buffer (3 % BSA in PBS) for 1 h at 37°C. 50 µl of serum or standard. in Reagent Diluent (1 % BSA in PBS) was added to the plate and incubated 1 h at RT. Plate was washed 4 times with 450 µl of washing buffer. 50 µl of the Detection Antibody (**Table 5** and **Table 6**). was added and plate was incubated 1 h at RT. Plate was washed 5 times with 450 µl of washing buffer. 50 µl of the Streptavidin-Eu^{3+} (Perkin Elmer, 1/15000 dilution in reagent diluent) was added and plate was incubated for 30 min at RT in the dark. Plate was washed 6 times with 450 µl of washing buffer. 50 µl of room temperature DELFIA Enhancement Solution (4001-0010 Perkin Elmer) was added and incubated for 15 min at RT, shaking (50 - 100 rpm). Absorbance measurement was performed using Victor$^{3\ TM}$ 1420 Multilabeled Counter and Wallac 1420 Workstation Software (Perkin Elmer™). ELISA based quantification of antibody titers in blood serum of resting/immunized mice was performed according to the Bethyl ELISA Protocol supplied with Mouse ELISA Quantitation Set.

Table 5. ELISA reagents for total antibody titers detection of resting mice.

capture antibodies	clone	company	working conc.
Monoclonal rat anti-mouse IgM	L-OMM-3	AbD Serotec	1 µg/ml
Monoclonal rat anti-mouse IgG1	LO-MG-13	AbD Serotec	1 µg/ml
Monoclonal goat anti-mouse IgG3	LO-MG3-13	AbD Serotec	1 µg/ml
Monoclonal goat anti-mouse Ig2a	LO-MG2a-9	AbD Serotec	0.5 µg/ml
Monoclonal goat anti-mouse Ig2b	LO-MG2b-1	AbD Serotec	1 µg/ml
Monoclonal goat anti-mouse IgA	A90-130-A	Bethyl	1 µg/ml
standards			
mouse IgM	11E10	Southern Biotech	10 ng/ml
mouse IgG1	15H6	Southern Biotech	10 ng/ml
mouse IgG3	B10	Southern Biotech	100 ng/ml
mouse IgG2a	HOPC-1	Southern Biotech	100 ng/ml
mouse IgG2b	A-1	Southern Biotech	100 ng/ml
mouse IgA	S-107	Southern Biotech	400 ng/ml
detection antibodies			
anti-mouse IgM (biotin)	R33.24.12	home made	125 ng/ml
anti-mouse IgG1 (biotin)	A85-1	BD Pharmingen	125 ng/ml
anti-mouse IgG3 (biotin)	R40.81	BD Pharmingen	500 ng/ml
anti-mouse IgG2a (biotin)	LO-MG2a-7	AbD Serotec	500 ng/ml
anti-mouse kappa chain (biotin)	R331.18	home made	500 ng/ml
anti-mouse IgA (biotin)	11-44-2	Southern Biotech	500 ng/ml

Table 6. ELISA reagents for antigen specific antibody titers detection of immunized mice.

antigens	clone	company	working conc.
NP(4)-BSA	N505010	Biosearch Technologies	2 µg/ml
NP(23)-BSA	N505010	Biosearch Technologies	2 µg/ml
BSA			2 µg/ml
capture antibodies			
Monoclonal rat anti-mouse IgM	L-OMM-3	AbD Serotec	1µg/ml
Monoclonal rat anti-mouse IgG1	LO-MG-13	AbD Serotec	1µg/ml
standards			
mouse IgM	11E10	Southern Biotech	10 ng/ml
mouse IgG1	15H6	Southern Biotech	10 ng/ml
Detection antibody			
anti-mouse IgM (biotin)	R33.24.12	home made	125ng/ml
anti-mouse IgG1 (biotin)	A85-1	BD Pharmingen	125ng/ml

2.4.2. Immunoblot analysis.

Cells were harvested by centrifugation for 5 min at 280 g and washed in cold PBS. For protein extraction cell pellet was resuspended in 8 M Urea lysis buffer (8 M Urea, 0.1 M NaH_2PO_4, 0.01 M Tris pH 8.0) and incubated 30 min in rotation at RT. Sonication was performed in 2 cycles of 10 sec each. Lysates were centrifuged at maximum speed for 10 min to remove debris. Lysates were quantified with a protein assay reagent (Bio-Rad Laboratories). 20 - 50 µg of proteins, in Laemmli loading buffer (62.5 mM Tris-HCl pH 6.8, 2 % (w/v) SDS, 5 % (v/v) 2-mercaptoethanol and 10 % (v/v) glycerol) and 10 µl of NOVEX ® Sharp Pre Stained protein standard (Invitrogen) were loaded onto home-made 12% polyacrylamide minigels and transferred by dry iBlot® Dry Blotting Device (Invitrogen) to nitrocellulose membranes (iBlot® Transfer Stack, Invitrogen) in 7 min. After blotting, the membranes were stained with Ponceau S staining solution (0.1 % Ponceau S (w/v) and 5 % acetic Acid (w/v)) to verify equal loading and transfer. Membranes were briefly washed in water and blocked for 1 h at RT in blocking solution 5 % BSA in TBS-T (20 mM Tris HCl pH 7.4, 500 mM NaCl, 0,1 % Tween). After blocking, filters were incubated with primary antibodies (Table 7), diluted in blocking solution, for 1-2 hours at RT or overnight at 4°C. After three washes, of 5 min each in TBS-T, membranes were incubated with the appropriate horseradish peroxidase conjugated secondary antibody diluted in blocking solution for 30 min at room temperature. Membranes were washed three times for 5 min in TBS-T and the bound secondary antibody was revealed using the ECL Western Blotting Substrate (Pierce) and detected using the Chemidoc™ XRS+ imaging System (Biorad). Image analysis was perforfmed using the Image Lab™ software (Biorad).

2.4.3. Immunoprecipitation.

Cells belonging to the A20 mouse B lymphoma were harvested by centrifugation at 4°C for 5 min at 280 g and twice washed in cold PBS. For protein extraction, the cell pellet was resuspended in 200 µl S300 lysis buffer (25 mM Tris HCl pH 7.6, 300 mM NaCl, 10% Glycerol 0,25% NP-40)/107 cells. Chromatin was mechanically sheered via pipetting up and down with a p1000 tip. Lysates wer then kept on ice for 10 minutes and cellular debris was removed via centrifugation at 17.900 g for 15 minutes. Lysates were quantified with a protein assay reagent (Bio-Rad Laboratories). 50 µl of protein G agarose slurry/sample were washed 2x in ice-cold 1x PBS, centrifuged at 4390 g and equilibrated with 50 µl of S300 lysis buffer . 1 mg of lysate/ip was then added to protein G and left to rotate at +4°C for 1 hour. Following lysate pre-clearing, 10% of lysate from the isotype control was stored at -80°C to serve as input. 1 mg of lysate was precipitated using 5 µg of anti-Ring1b (Cell Signaling) and a corresponding amount was precipitated with 5 µg of an isotype-matched antibody (monoclonal mouse anti-FLAG M2, Clone M2, Sigma-Aldrich), overnight at 4°C. On the following day, 50 µl of equilibrated protein G slurry was added to each immunoprecipitation, and left to rotate for 1-2 hours at 4°C. Subsequently, beads were precipitated by centrifugation at 4390 g and washed three times, 5 minutes each, at 4°C and on rotation, with cold S300 buffer. Immunoprecipitated and input material were then resuspended in Laemmli loading buffer (see paragraph 2.4.2). Samples were run, loaded and interactions visualized as described in paragraph 2.4.2, using primary and secondary antibodies listed in Table 7.

Table 7. Antibodies used for immunoblot protein detection.

primary antibodies	clone	company	dilution
Rabbit anti-Ring1b	D22F2	Cell Signaling	1/1000
Rabbit anti-H2AK119Ub	D27C4	Cell Signaling	1/1000
Rabbit anti-Ring1a		Cell Signaling	1/1000
Rabbit anti-Bcl6		Cell Signaling	1/1000
Rabbit anti-H2A total	07-690	Millipore	1/1000
Rabbit anti-BCOR	12107-1-AP	Proteintech	1/1000
secondary antibodies			
Polyclonal Goat anti mouse	170-6516	BioRad	1/20000
Polyclonal Goat anti rabbit	170-6515	BioRad	1/20000
Polyclonal Goat anti rat	NA935	Amersham	1/5000

2.5. Molecular Biology Techniques

2.5.1. RNA and DNA extraction

From more than $1x10^5$ cells, total RNA was extracted using QIAGEN RNeasy minikit following the manufacturer's protocol. A DNAse (QIAGEN) digestion step was added before elution to ensure the complete elimination of contaminant DNA. For sorted cells with total cell numbers lower than $1x10^5$, RNeasy AllPrep MicroKit (QIAGEN) was used following the manufacturer's protocol. This kit enables separate elution of total RNA and genomic DNA from one cell pellet.

2.5.2. cDNA synthesis

Complementary DNA (cDNA) was produced using SuperScript® VILO™ cDNA Synthesis Kit (Invitrogen) following the manufacturer's protocol. Specifically, master mix (containing 5X VILO™ Reaction Mix, 10X SuperScript® Enzyme Mix,

water and RNA) was incubated for 10 min at RT. For increased yields of cDNA incubation time was prolonged to 120 min at 42°C. Reaction was terminated by 5 min incubation at 85°C. 1 - 5 ng of cDNA were used for real time PCR reaction. Eventually, cDNA was used for Microfuidic cards (AB).

2.5.3. Real-time quantitative PCR (RT-QPCR).

For gene expression analysis RT-QPCR was performed using 1 - 5 ng of DNA, 500 nM primers mix and 10 µl of LightCycler® 480 SYBR Green I Master containing Hot-start polymerase (Roche) in a final volume of 20 µl per reaction in 96-well format. Reaction conditions were: 95°C for 10 min, 45 cycles of 95°C for 1 sec, 60°C for 10 sec, 72°C for 1 sec. Accumulation of fluorescent products was monitored using a LightCycler® 480 Real-Time PCR System (Roche). Specificity of PCR reaction was controlled by the melting-temperature profiles of final products (dissociation curve). Ribosomal protein large p0 (Rplp0) gene gene was used as a control house-keeping gene for normalization.), primers are listed in Table 8. Transcript fold enrichment was calculated by DDct method.To measure the deletion efficiency (DE) of *Ring1b* lox-P flanked exon 2, QPCR analysis was performed on genomic DNA. Ring1bΔ primers were used to detect remaining *Ring1b* exon 2 and primers annealing to Gapdh gene used as a loading control (Table 13). DE was calculated as DE (%) = 100% - retained exon 2 (%) for Ring1b$^{fl/fl}$and DE (%) = 50% / retained exon 2 (%) x 100 for Ring1b$^{fl/+}$.

Table 8. Primer sequences for quantitative PCR analysis.

Rplp0 Fw	TTCATTGTGGGAGCAGAC	RNA
Rplp0 Rv	CAGCAGTTTCTCCAGAGC	RNA
Ring1b Δ Fw	GTTCCATTTGTCTGCACAGCCTGAGA	DNA
Ring1b Δ Rv	AGATGCTGAAGACTGGAGGGGTGT	DNA

p21Cdkn1a Fw	CCACAGCGATATCCAGACATTC	RNA
p21Cdkn1a Rv	CGGAACAGGTCGGACATCA	RNA
Ring1a Fw	AACTGAGTCTCTATGAGCTGCA	RNA
Ring1a Rv	CACTCCTTGTTCCCGCTCCCG	RNA
Prmd1 Fw	GACGGGGGTACTTCTGTTCA	RNA
Prmd1 Rv	GGCATTCTTGGGAACTGTGT	RNA
Irf4 Fw	CAATGTCCTGTGACGTTTGG	RNA
Irf4 Rv	GGCTTCAGCAGACCTTATGCT	RNA
Xbp1 Fw	TAGAAAGAAAGCCCGGATGA	RNA
Xbp1 Rv	CACCAGCCTTACTCCACTCC	RNA
Gapdh4d FW	AGCGCTGACCTTGAGGTCTCCTTG	DNA
Gapdh4d Rv	GTTGCCTACGCAGGTCTTGCTGAC	DNA

2.5.4. RT-QPCR using TaqMan® Micro Fluidic Cards.

For quantitative analysis of 95 gene transcript levels (Table 9), RT-QPCR using customed TaqMan® Array 384-well Micro Fluidic Cards (Applied Biosystems) was run on the ABI PRISM® 7900HT Real-Time PCR System and analyzed with Sequence Detection System software (SDS 2.1 software). Relative gene expression values were obtained from 7900HT system data using the Comparative CT Method for relative quantification.

Table 9. List of genes of the TaqMan® Microfluidic Cards.

Assay ID	Gene Symbol
Mm00545720_m1	Ada,mCG5441
Mm00507774_m1	Aicda,m32207
Mm01223702_m1	Apaf1,m0338
Mm00431867_m1	Atm,mCG5641
Mm01223652_m1	Atr,m0240
Mm00464379_m1	Bach2,m2764
Mm00432042_m1	Bad,m4907
Mm00432045_m1	Bak1,m24181
Mm00432050_m1	Bax,mCG23178
Mm00477631_m1	Bcl2,m28637
Mm01333921_m1	Bcl2l11,m1895
Mm00477633_m1	Bcl6,m25078

Mm00551516_m1	Bcor,m5540
Mm00432073_m1	Bid,m29741
Mm01197846_m1	Blnk,mCG2382
Mm03053308_g1	Bmi1
Mm00515386_m1	Brca1,mCG20241
Mm01218747_m1	Brca2,m45046
Mm00442712_m1	Btk,m15066
Mm00432322_m1	Casp7,m4266
Mm00483084_m1	Cbx2,m3903
Mm00520006_m1	Cbx7,m1514
Mm00438070_m1	Ccnd2,m29731
Mm01273583_m1	Ccnd3,m5576
Mm00438084_m1	Ccng1,mCG3474
Mm01301785_m1	Ccr7,m5362
Mm00515420_m1	Cd19,mCG22404
Mm00432423_m1	Cd79a,mCG7279
Mm00434143_m1	Cd79b,mCG3044
Mm00444543_m1	Cd86,m30169
Mm01303209_m1	Cdkn1a,m26433
Mm00438168_m1	Cdkn1b,mCG22259
Mm00494449_m1	Cdkn2a,m23699
Mm00483243_m1	Cdkn2c,mCG2421
Mm01255578_m1	Cflar,m17843
Mm01176757_m1	Chek1,mCG4138
Mm00501607_m1	Creb1,m13880
Mm01219960_m1	Crtc2,mCG22212
Mm01292123_m1	Cxcr4,mCG20049
Mm00445735_m1	Diablo,m1111
Mm00432939_m1	E2f1,mCG3689
Mm00395519_m1	Ebf1,m40647
Mm00469651_m1	Eed,m14758
Mm00468440_m1	Ezh1,mCG20227
Mm00468464_m1	Ezh2,mCG2028
Mm00487425_m1	Fos,mCG5518
Mm00514924_m1	Foxm1,m32524
Mm00490672_m1	Foxo1,m648
Mm01185722_m1	Foxo3,m8802
Mm01234672_m1	Gpr183,m42733
Mm01246322_m1	Grb2,mCG6612
Mm00442838_m1	Hoxc4,mCG15669
Mm00711781_m1	Id2,mCG3640
Mm00456421_m1	Ikzf1,mCG3994
Mm01306721_m1	Ikzf3,mCG21902
Mm00516431_m1	Irf4,mCG4922
Mm00492567_m1	Irf8,mCG21199
Mm00434561_m1	Jak2,mCG9104
Mm00802897_m1	Lck,mCG12243
Mm01217488_m1	Lyn,mCG3575
Mm00442479_m1	Mapk1,mCG131169
Mm00725832_s1	Mcl1,mCG16749
Mm01233136_m1	Mdm2,mCG3393
Mm00484944_m1	Mdm4,mCG12581
Mm01227378_m1	Msh6,mCG15886
Mm00504304_m1	Myb,mCG140750
Mm00435502_m1	Pax5,mCG2326
Mm00478032_m1	Pdcd6ip,mCG14774

Mm01282781_m1	Pik3r1,mCG115224
Mm00777269_mH	Pin1,mCG67927
Mm00549397_m1	Plcg2,mCG127079
Mm00451763_m1	Pmaip1,mCG12628
Mm00712819_m1	Polq,mCG128238
Mm00448326_m1	Pou2af1,mCG4163
Mm00476128_m1	Prdm1,mCG17867
Mm00440894_m1	Prkce,mCG20408
Mm00433209_m1	Ptk2,mCG18061
Mm00487905_m1	Rad51,mCG6194
Mm01270936_m1	Rag1,mCG12558
Mm00501300_m1	Rag2,mCG12559
Mm00441097_m1	Rasgrf1,mCG122247
Mm00803291_m1	Rev3l,mCG125811
Mm00501395_m1	Ring1,mCG23002
Mm00803321_m1	Rnf2,mCG8545
Mm01974474_gH	Rplp0,mCG17387
Mm01719550_s1	Spib,mCG147775
Mm01304152_m1	Suz12,mCG19060
Mm01333032_m1	Syk,mCG121753
Mm01175598_m1	Tcfe2a,mCG145500
Mm01731287_m1	Trp53,mCG20908
Mm00557629_m1	Trp53bp2,mCG4715
Mm00457357_m1	Xbp1,mCG14698
Mm00445118_m1	Xrcc2,mCG1077
Mm00459213_m1	Xrcc4,mCG116563
Mm00456392_m1	Yy1,mCG13054

2.6. Statistical Analysis

2.6.1 Student's t-test.

Statistical analysis of normally distributed values (Gaussian) was performed by two-tailed unpaired Student's t-test. Differences were considered significant at *p-value*<0.05.

2.6.2. 2-way ANOVA.

Statistical analysis to compare two independent variables in grouped samples was performed using 2-way ANOVA test. Differences were considered significant at $p<0.05$.

2.6.3. Microarray analysis.

Affymetrix GeneChip® Arrays were performed at GeneChip® Mouse Gene 1.0 ST Array platform. The GeneChip® Mouse Gene 1.0 ST Array with more than 750,000 unique 25-mer oligonucleotides covers the whole genome transcript. Each of the 28,853 covered genes is represented on the array by approximately 27 probes spread across the full length of the gene. Raw data (CEL files) were filtered and normalized with Affymetrix Power Tools (APT) Software Package, using the rma-sketch algorithm to generate Log2 transformed intensity values. Log2 transformed data were annotated and analyzed using the annotation "pd.mogene.1.1.st.v1" (Benilton Carvalho, Platform Design Info for Affymetrix MoGene-1_1-st-v1; R package version 3.6.0), "mogene11stprobeset.db" (Arthur Li, Affymetrix Mouse Gene 1.1 - ST Array Probeset Revision 4 annotation data (chip mogene11stprobeset); R package version 4.0.1.), "mogene11sttranscriptcluster.db" (Arthur Li, Affymetrix Mouse Gene 1.1-ST Array Transcriptcluster Revision 4 annotation data (chip mogene11sttranscriptcluster); R package version 4.0.1.) and the "affy" (Gautier et al., 2004) package of R software version 2.16.0 (http://www.r-project.org). In order to identify genes with significant changes in their expression, a t-test was applied. A false discovery rate (FDR) correction was also introduced when p values were calculated. Genes with a cut-off of 1.5-fold change and p value ≤ 0.05 were considered up- or down- regulated between different groups.

2.6.4. Gene Ontology Analysis.

Gene pathway enrichment was assessed using Ingenuity Pathway Analysis software Gene Set Enrichment analysis was performed accessing the Gene Set Analysis Tool

kit V2 (Zhang et al., 2005) (http://bioinfo.vanderbilt.edu/webgestalt/) in September 2013. A hypergeometric test was run to identify ten overrepresented Gene Ontology categories among Biological Process, Molecular Functions and Cellular Component. Adjusted p values were calculated applying Benjamini & Hochberg multiple test.

3. Results

3.1. Normal B cell development in *Ring1a* and *Ring1b* single mutants.

To address the roles of *Ring1a* and *Ring1b* in B cell development, we analyzed the effects of the deletion of single PRC1 components on lymphocyte homeostasis. Previous work in the lab had shown that transcripts for *Ring1a* and *Ring1b* are detected throughout B cell development (Figure 10).

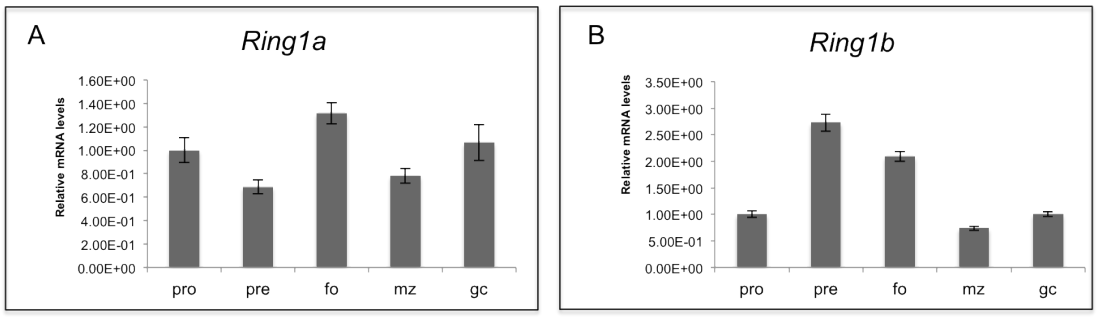

Figure 10. PRC1 catalytic subunits are expressed throughout B cell development.

(A) *Ring1a* mRNA levels in sorted B cell populations. (B) *Ring1b* mRNA levels in sorted B cell populations. mRNA levels were normalized to the housekeeping gene RPPLO and to levels measured in pro B cells. Pro=Pro B, Pre=Pre B, Fo= follicular B, MZ= marginal zone B, GC= germinal center B cells.

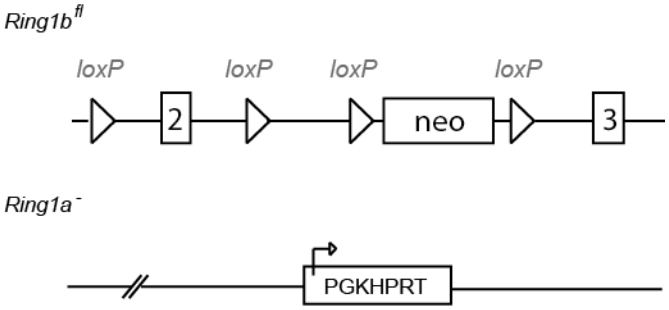

Figure 11. Structure of conditional *Ring1b* and *Ring1a* null alleles in PRC1 mutant mice.

Schematic depiction of the (A) floxed *Ring1b* locus (*Ring1b*^{fl}) and (B) the incativated *Ring1a (Ring1a*$^{-}$*)* allele.

Given the embryonic lethality of *Ring1b*-deficient mice, we employed conditional gene targeting (**Figure 11**) to achieve B cell-specific E3 ligase inactivation (Voncken et al., 2003). *Ring1b*$^{fl/fl}$ mice carry *loxP* sites flanking exon 2 of the *Ring1b* gene that contains the starting ATG codon (Cales et al., 2008) (Figure 11A). *Ring1a*$^{-/-}$ mice were generated by homologous recombination-mediated replacement of *Ring1a* coding exons with an HPRT minigene in embryonic stem cells (Figure 11B). *Ring1a*$^{-/-}$ animals are viable and fertile and show no overt phenotypes (del Mar Lorente et al., 2000). Work in our lab has shown that ablation of *Ring1b* at early stages of B cell development (*Ring1b*^{fl}*; Mb1-cre* mutants, Figure 12) or in peripheral B cells (*Ring1b*^{fl}*; Cr2-cre* mutants, Figure 12) did not affect B cell maturation. Furthermore, ability of *Ring1b*$^{-/-}$ cells to participate in T cell-dependent immune responses was unaffected (L. D'Artista, F. Mainoldi and S. Casola, unpublished data). In a similar fashion, analysis of mice devoid of *Ring1a* did not reveal major impairments in B cell development.

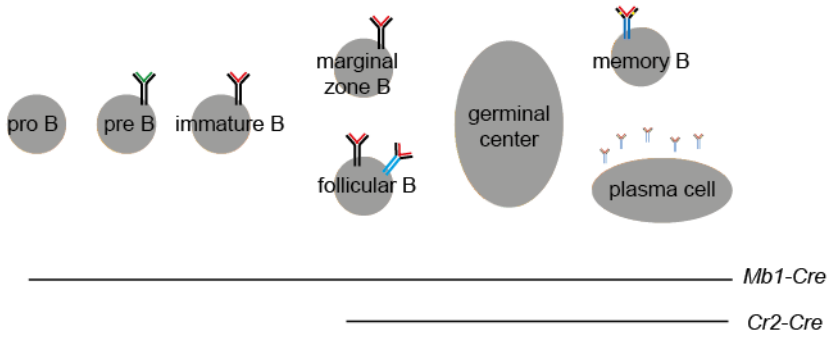

Figure 12. Schematic view of B cell development and timing of *Mb1-cre*- and *Cr2-cre*- mediated deletion.

Analysis of BM subsets of *Ring1a*-deficient animals revealed normal distribution among B cell subsets (Figure 13).

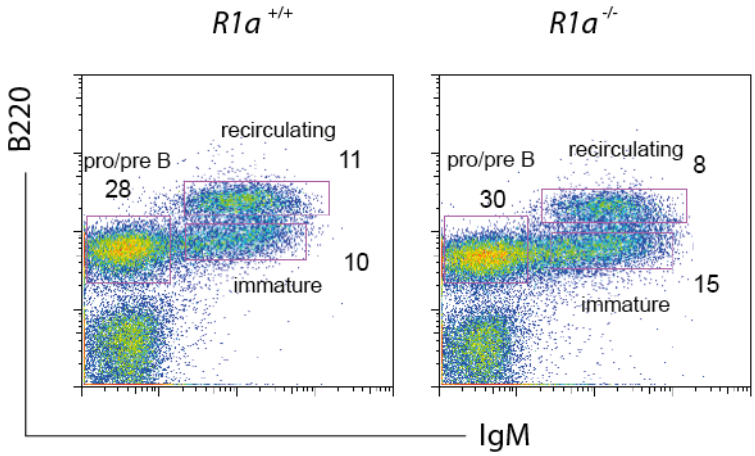

Figure 13. *Ring1a*$^{-/-}$ cells are able to proceed through early B cell developmental stages.

Flow cytometric analysis of control (left) and mutant (right) BM B cell subsets. Numbers indicate frequency of corresponding gated populations and are representative of 3 independent experiments. *R1a*=*Ring1a*.

In the periphery, B cell numbers were comparable to those of wild-type animals, and so was the distribution of B cells between the follicular (FO) and marginal zone (MZ) B cell subsets (Figure 14 and Figure 15).

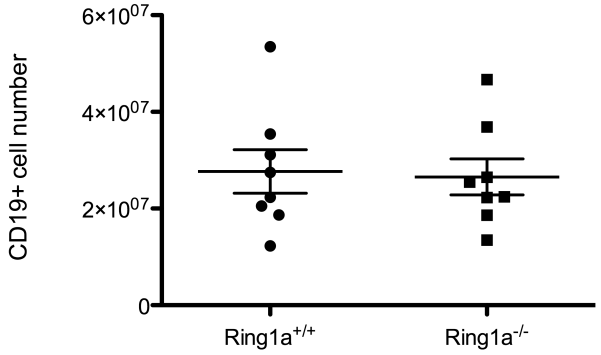

Figure 14. Absolute numbers of CD19$^+$ cells in spleens of control and mutant animals.

We then asked whether lack of *Ring1a* would influence the ability of mature B cells to participate in T-dependent immune responses. To test this, experimental and control animals were immunized with alum-precipitated 4-nytrohenyl-acetyl (NP) coupled to chicken gamma globulin (CGG) and germinal center (GC) formation was analyzed 14 days later. Flow cytometric analysis of cell frequencies within the CD19$^+$CD38^{lo}FAS^{hi} GC subset indicated no substantial differences between wild-type and mutant animals (Figure 16).

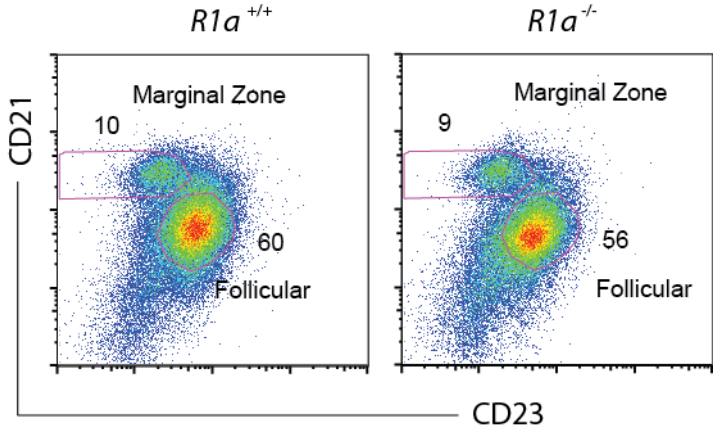

Figure 15. *Ring1a* is dispensable for peripheral B cell development.

Flow cytometric analysis of the main control (left) and mutant (right) splenic B cell subsets. Numbers indicate frequency of corresponding gated populations and are representative of 7 independent experiments.

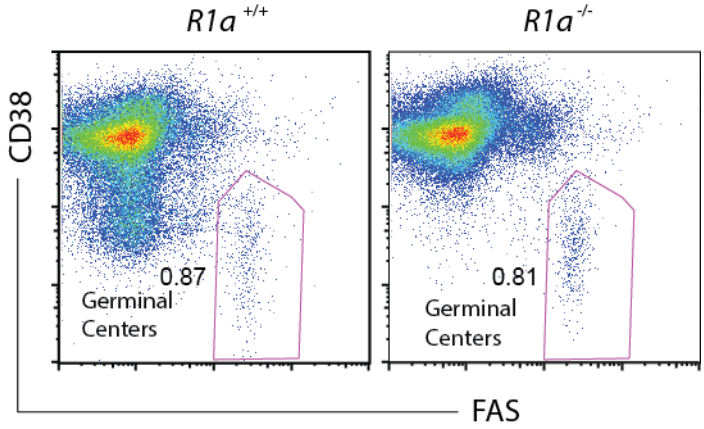

Figure 16. *Ring1a*$^{-/-}$ cells can give rise to germinal centers.

Flow cytometric analysis of the control (left) and mutant (right) splenic GC formation at day 14 following immunization with NP-CGG. Numbers indicate frequency of corresponding gated populations and are representative of 3 independent experiments.

Given early embryonic lethality of *Ring1b* mutant animals, we wondered whether failure to detect any defect in *Ring1b*-deficient B cells may reflect strong counter-

selection of mutant B cells in the periphery. To address this, we purified naïve B cells from spleens of *Ring1b^{fl}; Cr2-cre* and control animals and estimated protein levels of *Ring1a* and *Ring1b.* Immunoblotting revealed efficient deletion of *Ring1b* in peripheral B cells and levels of monoubiquitinated H2A (H2AK119Ub) similar to those of control animals. This may reflect the fact that the mark is not diluted in the absence of cell proliferation and active ubiquitin removal, or may reflect compensatory mechanisms employed by the cell to avoid the loss of the H2AK119Ub mark. Up-regulation of Ring1a in *Ring1b*-deficient B cells argues in favor of the latter hypothesis (Figure 17).

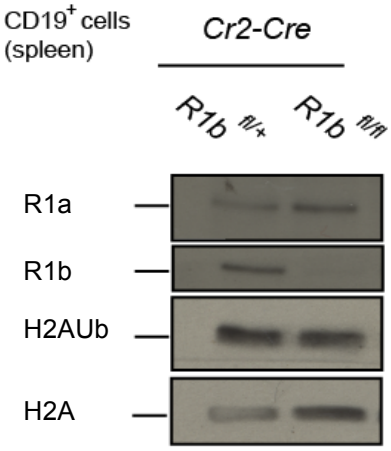

Figure 17. Up-regulation of Ring1a following Cre-mediated deletion of Ring1b in peripheral B cells.

Immunoblot analysis of levels of Ring1a, Ring1b and H2AK119Ub (H2AUb) in CD19^{+} cells isolated from spleens of control (*R1b $^{fl/+}$*, left column) and mutant (*R1b $^{fl/fl}$*, right column) animals. Results shown are representative of 3 independent experiments.

Taken together, this suggests that PRC1 activity is important in B cell development, and that lack of the major E3 ubiquitin ligase, Ring1b, activates a compensatory mechanism that involves up-regulation of its paralog, Ring1a.

3.2. PRC1 in early B cell development.

To overcome possible compensatory mechanisms activated by loss of only one of the PRC1 ubiquitin ligases, we generated compound *Ring1a*$^{-/-}$*Ring1b*$^{fl/fl}$ mutant mice and bred them to *Mb1-cre* knock-in animals to address the role of PRC1 in early B cell development. In *Mb1-cre* mice, Cre-mediated recombination starts in pro-B cells and continues throughout B-cell development (Hobeika et al., 2006) (Figure 12). Flow cytometric analysis of bone marrow (BM) cell suspensions revealed a significant block in B cell development in PRC1 conditional mutant mice. In the latter animals, most B cells represented B220^{+}IgM^{-}CD43^{+} pro B cells (Figure 18A and B).

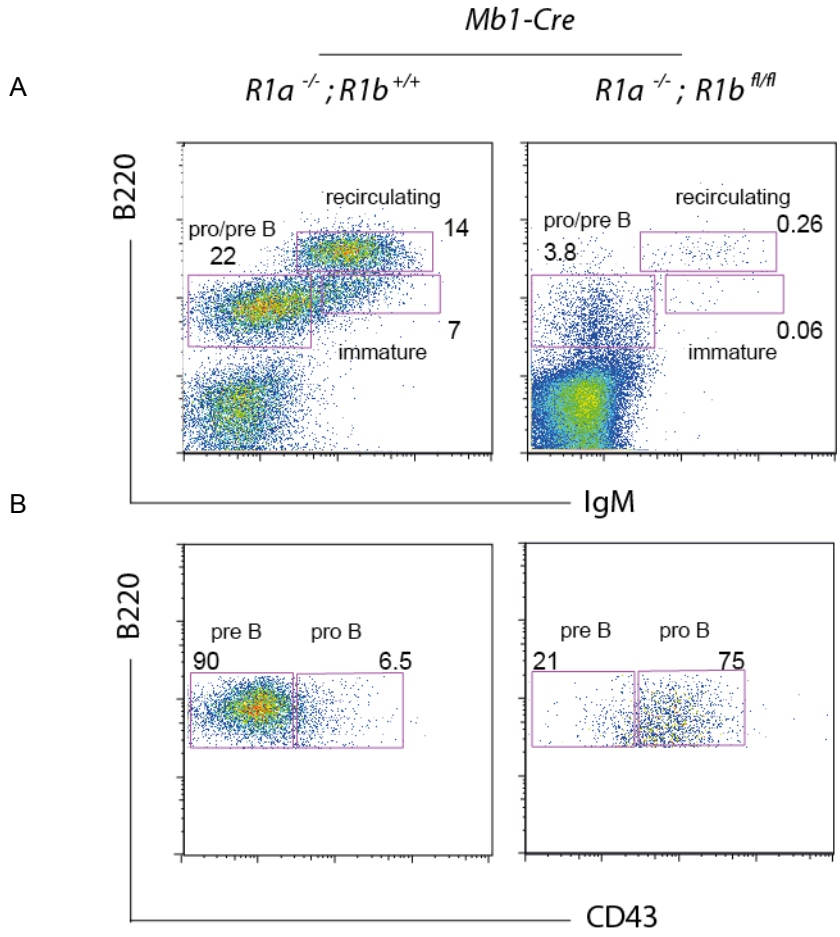

Figure 18. B cells devoid of PRC1 are blocked at the pro B cell stage. Flow cytometric analysis of control (left) and mutant (right) BM (a) and $B220^{+}IgM^{-}$ (b) pro/pre B cells. Numbers indicate frequency of corresponding gated populations and are representative of 3 independent experiments. *R1b=Ring1b*.

Such increase in the proportion of pro B cells was not mirrored by absolute B cell numbers, which remained unchanged (Figure 19).

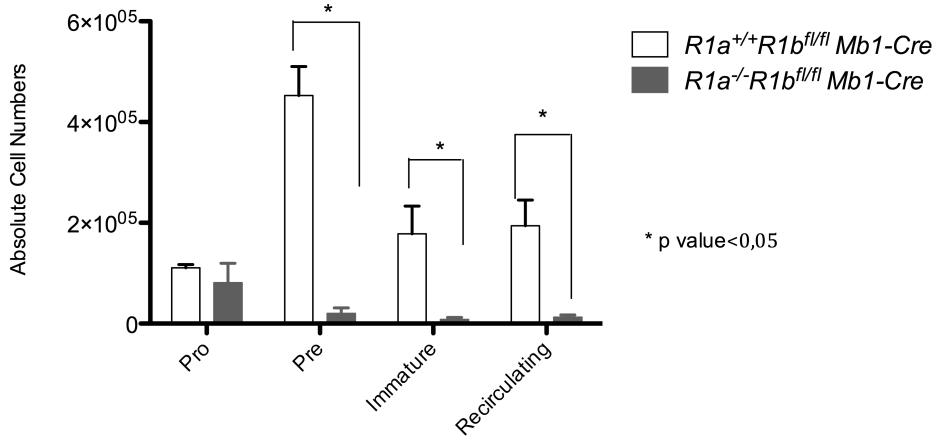

Figure 19. Absolute numbers of progenitor (pro and pre) and IgM$^+$ (immature and recirculating) B cells upon conditional PRC1 ablation in pro-B cells.

Bars represent absolute cell numbers within each compartment. Pro= Pro-B cells (B220$^+$IgM$^-$CD43$^+$). Pre=Pre B cells (B220$^+$IgM$^-$CD43$^+$), immature (B220$^+$IgM^{lo}CD43$^-$) and recirculating (B220$^+$IgM^{hi}CD43$^+$). Results are shown as average +/- SEM of 3 independent animals/genotype.

Instead, the pre B cell compartment of mutant animals was more than 4-fold decreased in both frequency and absolute numbers. As a consequence of the observed block in transition from the pro- to the pre- B cell stage, frequency and numbers of immature (B220^{lo}IgM$^+$) and recirculating (B220$^+$IgM$^+$) B cells were significantly reduced (Figure 18A and Figure 19). Additionally, the few CD19$^+$ B cells retrieved in the spleen of *Ring1a$^{-/-}$; Ring1b$^{fl/fl}$;Mb1-cre* mice retained Ring1b expression (Figure 20), suggesting that only escapers of Cre-mediated recombination could give rise to mature peripheral B cells.

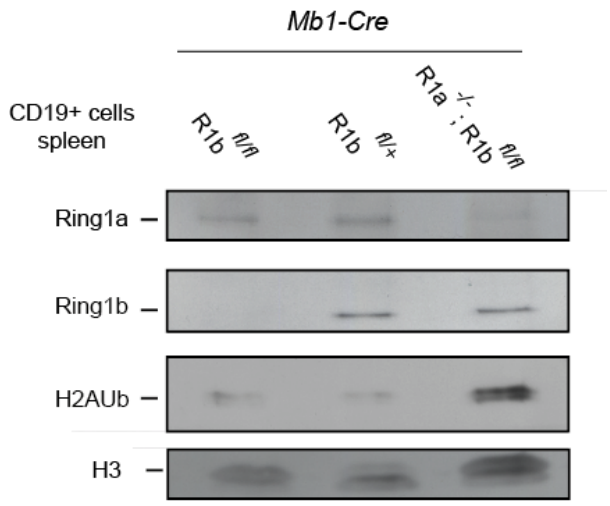

Figure 20. Counter-selection of *Ring1a*$^{-/-}$*Ring1b*$^{-/-}$ B cells.

Western blot analysis of MACS-sorted CD19^{+} splenic B cell suspensions from animals of the indicated genotypes. H3= histone H3.

Together, the block in transition from the pro-B to the pre-B cell stage and the counter-selection of PRC1 mutant B cells in peripheral lymphoid organs highlight an essential contribution of PRC1 in early B cell development.

3.3. PRC1 in peripheral B cell development

3.3.1. PRC1 is critical for peripheral B cell maturation

To address the role of *Ring1a* and *Ring1b* in peripheral B cell development, we bred *Ring1a*$^{-/-}$*Ring1b*$^{fl/fl}$ mice to *Cd23-cre* transgenic animals. In compound mutants, the deletion of the PRC1 is induced in the majority of B cells expressing the FcεRII low affinity IgE receptor (Kwon et al., 2008). Such receptor starts being expressed in B cells at the late transitional stage, which then develop into mature B lymphocytes. PRC1 inactivation in peripheral B cells marginally affected the

number of CD19^{+} B cells in the spleen, mesenteryc lymph nodes and Peyer's patches (Figure 21).

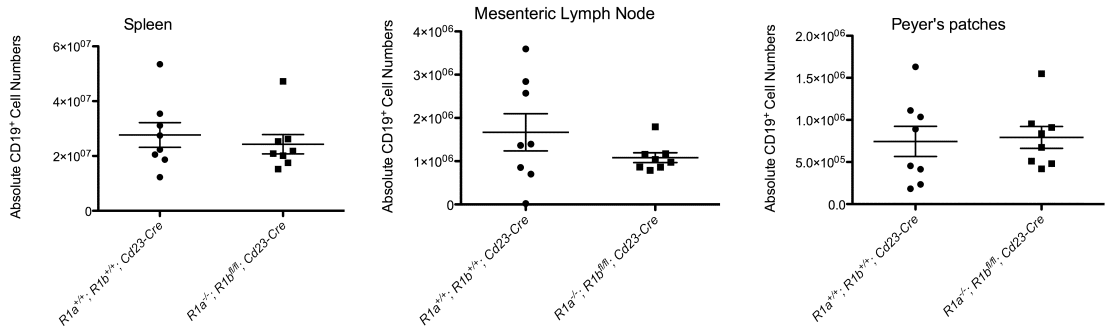

Figure 21. Absolute numbers of Cd19^{+} cells in secondary lymphoid organs are not affected by loss of *Ring1a* and *Ring1b*.

PRC1-deficient peripheral B cells were then subjected to a comprehensive immunophenotypic analysis. This revealed aberrant expression of several surface markers in mutant B cells when compared to controls. The most striking alteration in PRC1 conditional mutant mice was the overepresentation of B cells expressing the CD93/AA4.1 marker, which typically identifies transitional and immature B cells (Allman et al., 2001b) (Figure 22 and Figure 23).

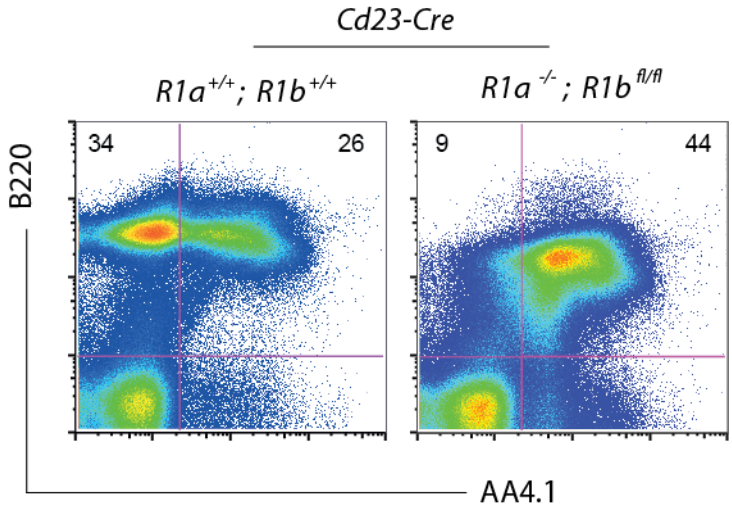

Figure 22. The majority of CD19^{+} cells in the periphery of mutant animals are AA4.1^{+}.

Flow cytometric analysis of control (left) and mutant (right) spleens. Numbers indicate frequency of corresponding gated populations and are representative of at least 9 independent experiments.

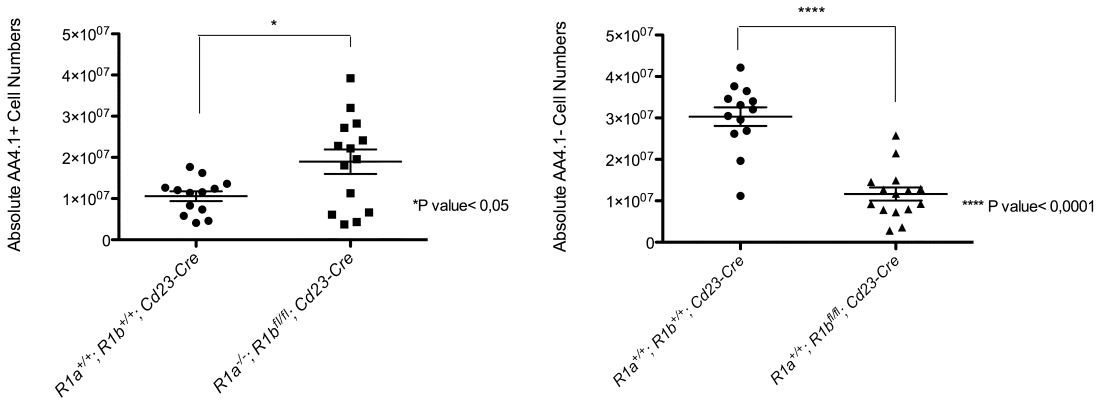

Figure 23. Absolute numbers of AA4.1^{+} and AA4.1^{-} cells in spleens of control and mutant animals.

In mutant splenic B cells, expression of AA4.1 was associated with that of the immature marker CD24/HSA and the pro-apoptotic receptor CD95/FAS to levels comparable to those detected in *bona fide* $B220^{+}AA4.1^{+}$ immature transitional B cells in control animals (Figure 24).

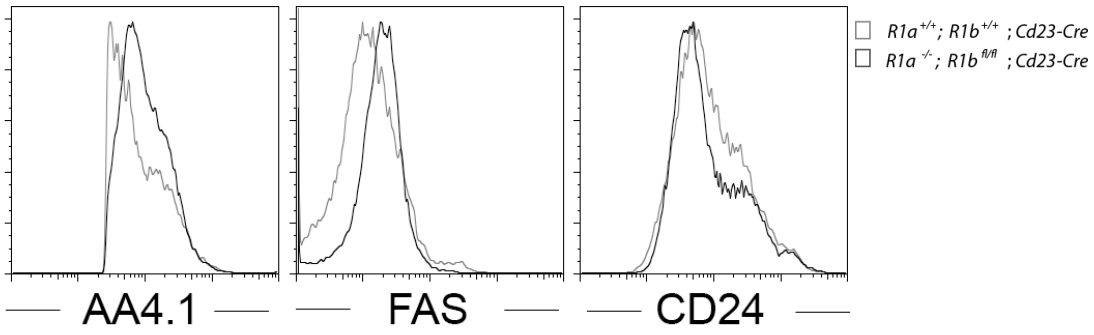

Figure 24. Levels of surface markers within $AA4.1^{+}$ cells in *Ring1a/Ring1b* mutants is comparable to those of wild-type transitional B cells.

Flow cytometric analysis of surface marker expression comparing levels of AA4.1, FAS and CD24 between immature transitional $B220^{+}AA4.1^{+}$ cells from controls (light grey line) and the over-grown $B220^{+}AA4.1^{+}$ found in mutant *Ring1a*$^{-/-}$;*Ring1b*$^{ff/fl}$;*Cd23-cre* animals (dark grey line). Data are representative of 6 independent experiments.

These results highlighted the possibility that PRC1 inactivation in late transitional B cells (when *Cd23-cre* expression is induced) impairs their differentiation into mature follicular (FO) and marzinal zone (MZ) B cells. Quite surprisingly, the majority of $AA4.1^{+}$ B cells in the spleen of *Ring1a*$^{-/-}$;*Ring1b*$^{fl/fl}$;*Cd23-cre* mice also expressed high levels of the complement receptor Cr2/Cd21, which marks mature B cells. Moreover, levels of the pro-survival receptor BAFF-R, which increases during B cell maturation, were comparable between PRC1 mutant $B220^{+}AA4.1^{+}$ B cells and control *bona fide* mature B cells ($B220^{+}AA4.1^{-}$) (Figure 25). Next, we

addressed whether expression of the BCR, which mediates tonic signaling required for survival of peripheral B cells, was retained on B cells of *Ring1a*$^{-/-}$*;Ring1b*$^{fl/fl}$*;Cd23-cre.* Mutant B cells expressed IgM and IgD similar to their WT counterparts, suggesting that surface BCR expression is retained in B cells devoid of PRC1 (Figure 26). Of note, IgM expression was higher in PRC1 deficient B cells, which is in agreeement with higher abundance of immature cells in mutant animals (Figure 26B).

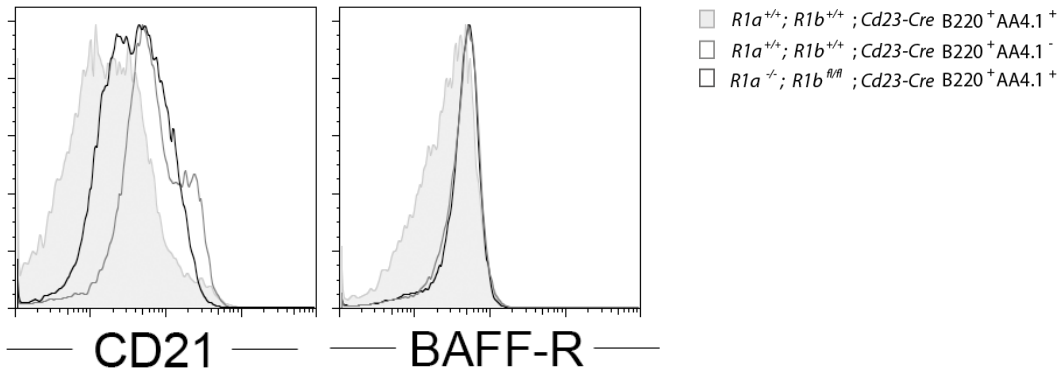

Figure 25. Levels of Cr2/CD21 and BAFF-R are similar between AA4.1^{+} PRC1 mutant cells and AA4.1^{-} wild-type cells.

Flow cytometric analysis of surface expression the B cell maturation-associated marker Cr2/CD21 and BAFF-R comparing *bona fide* mature B cells (B220^{+}AA4.1^{-}) from spleens of control animals (light grey line) and B220^{+}AA4.1^{+} cells constituting most of the B cells retrieved in the periphery of *Ring1a/Ring1b* mutants (dark grey line). The wild-type B220^{+}AA4.1^{+}(full ivory histogram) population displaying lower levels of both Cr2/CD21 and BAFF-R is shown. Data are representative of 6 independent experiments.

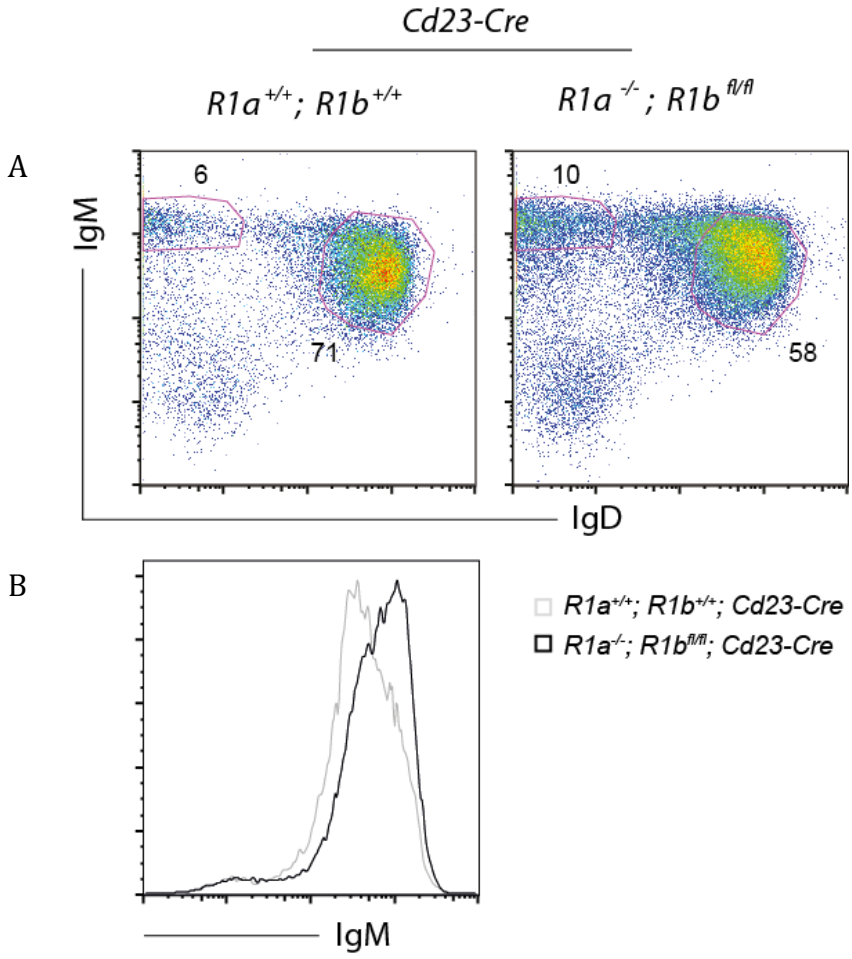

Figure 26. *Ring1a/Ring1b* mutant cells express surface IgM and IgD.

(A) Flow cytometric analysis of IgM and IgD expression on $B220^+$ cells in the spleens of mutant (right) and control animals (left). (B) Comparison of IgM expression on B cells from spleens of control (light grey line) and mutant animals (black line). Data are representative of 3 independent experiments.

To assess the degree of PRC1 inactivation, $AA4.1^+B220^+$ B cells were purified from the spleens of *Ring1a*$^{-/-}$;*Ring1b*$^{fl/fl}$;*Cd23-cre* mice and tested by immunoblotting analysis for Ring1a and Ring1b expression. Lack of Ring1a was coupled to reduced levels of the Ring1b protein. A similar analysis was also performed on a minor fraction of $B220^+AA4.1^-$ mature B cells detected in compound mutants. In those cells, levels of Ring1b and H2AK119Ub were more reduced than in their $AA4.1^+$ counterparts, in accordance with their longer

exposure to Cre activity. These results suggest that PRC1 is required for correct maturation of transitional B cells (Figure 27).

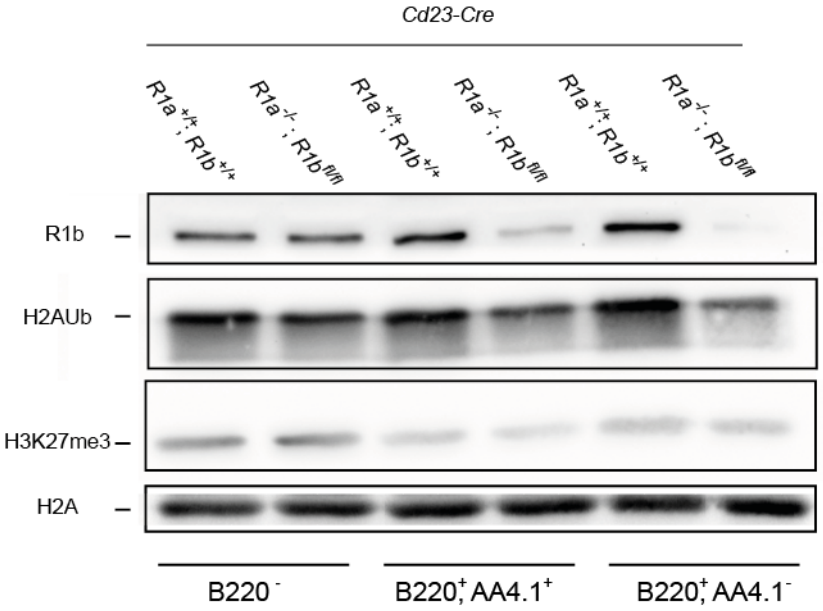

Figure 27. Loss of Ring1a and Ring1b is compatible with peripheral B cell maturation.

Western blot analysis of sorted splenic B cell populations from animals of the indicated genotypes. Results are representative of 2 independent experiments.

3.3.2. PRC1 mutant B cells migrate into follicles and the marginal zone

B cell maturation is associated with the ability of cells to home to B cell follicles in secondary lymphoid organs. Also, a fraction of mature B cells in the spleen resides in the MZ, in close proximity with the blood stream where it is involved in the recognition and response to blood-borne pathogens (Lopes-Carvalho and Kearney, 2004). To address whether expression of the Cr2/CD21 and the BAFF-R

markers reflected the acquisition of FO and MZ properties by PRC1 mutant cells, we performed both immunophenotypic and histological analyses. By flow cytometric analysis, we identified both bona fide FO ($CD19^{+}CD21^{+}CD23^{+}CD38^{+}$) and MZ ($CD21^{hi}CD23^{lo}CD38^{hi}$) B cells in the spleens of PRC1 mutant mice (Figure 28 and Figure 29), which resembled peripheral B cells retrieved in spleens of control animals. Further analysis of relative frequencies and absolute numbers of FO and MZ B cells revealed that loss of PRC1 mainly affects the former subset, leaving the latter relatively untouched (Figure 29).

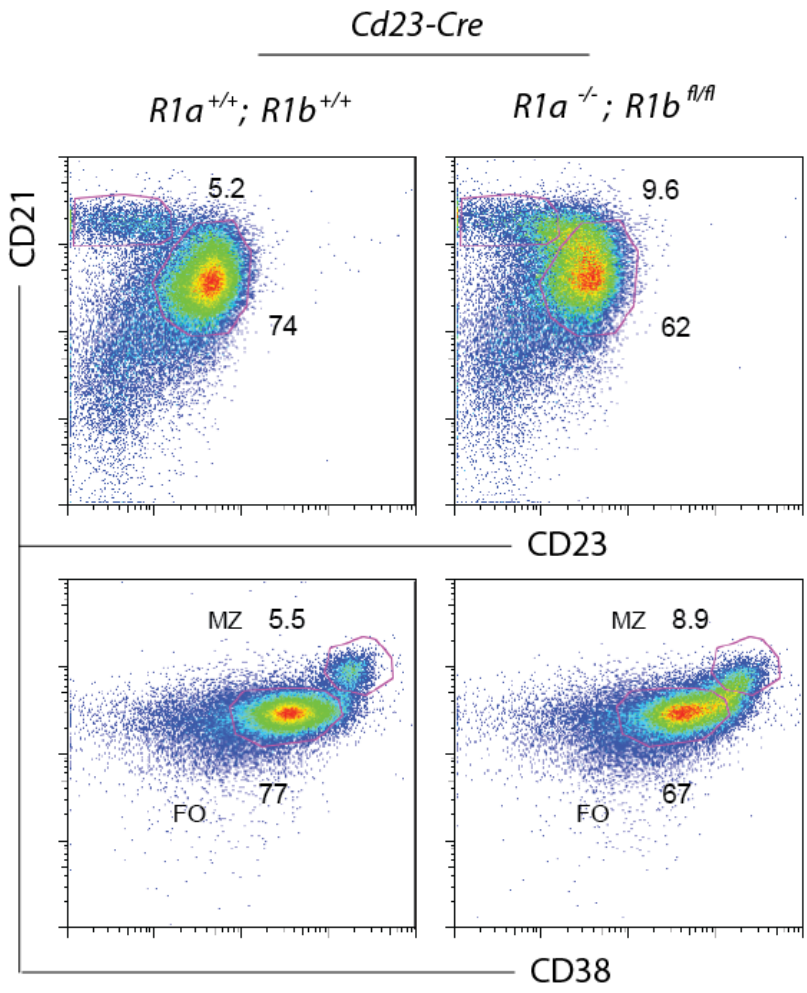

Figure 28. *Ring1a/Ring1b* mutant cells display markers of mature cells and segregate into mature B cell subsets.

Flow cytometric analysis of the FO ($CD19^+CD21^+CD23^+CD38^+$) and MZ ($CD21^{hi}CD23^{lo}CD38^{hi}$) B cell subsets in spleens of control (left) and mutant (right) animals. Data are representative of 6 independent experiments.

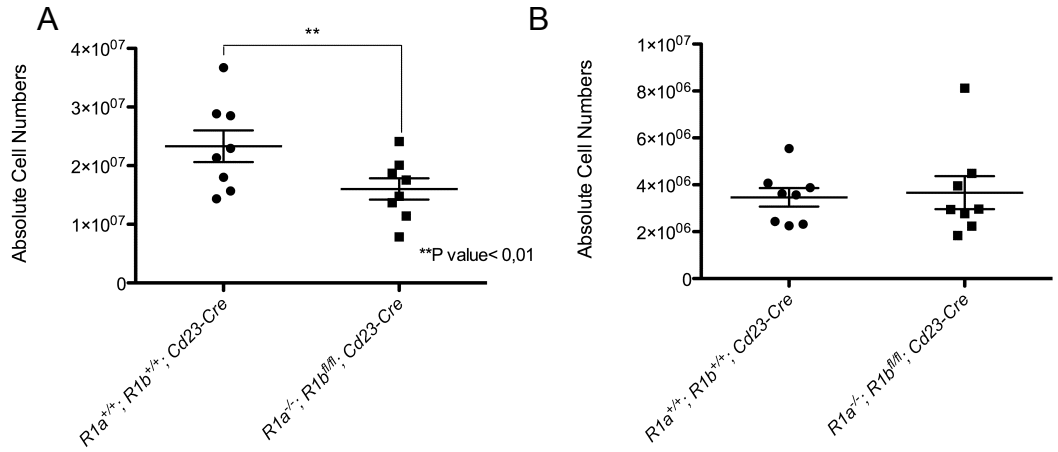

Figure 29. Loss of PRC1 impairs maturation in the follicular B cell subset.

Absolute numbers of (A) splenic FO ($CD19^+CD21^+CD23^+CD38^+$) B cells in and (B) MZ ($CD21^{hi}CD23^{lo}CD38^{hi}$) wild-type and mutant animals.

The concomitant presence of surface markers typical of immature (Cd24/HSA, Cd95/FAS and Cd93/AA4.1) and mature (Cr2/Cd21, Cd38) B cells suggests that the loss of *Ring1a* and *Ring1b* in resting peripheral B lymphocytes leads to a defect in maturation whereby cells undergo aberrant maturation towards the mature B cell compartment. The identity of FO and MZ B cells was further assessed performing immunofluorescence analysis of splenic sections of PRC1 control and mutant mice. This analysis showed proper distribution of PRC1 mutant B cells within $B220^+$ folicular B cell areas. Moreover, lack of PRC1 did not preclude the ability of a subset of mutant B cells to reside in the marginal zone delimited by $MOMA1^+$ macrophages (Figure 30 and Figure 31A and B). Additionally, in spite of

reduced frequency and absolute numbers of FO B cells revealed by immunophenotypic analysis, no difference between the size of mutant and control follicles was highlighted by immunofluorescence analysis (Figure 31A).

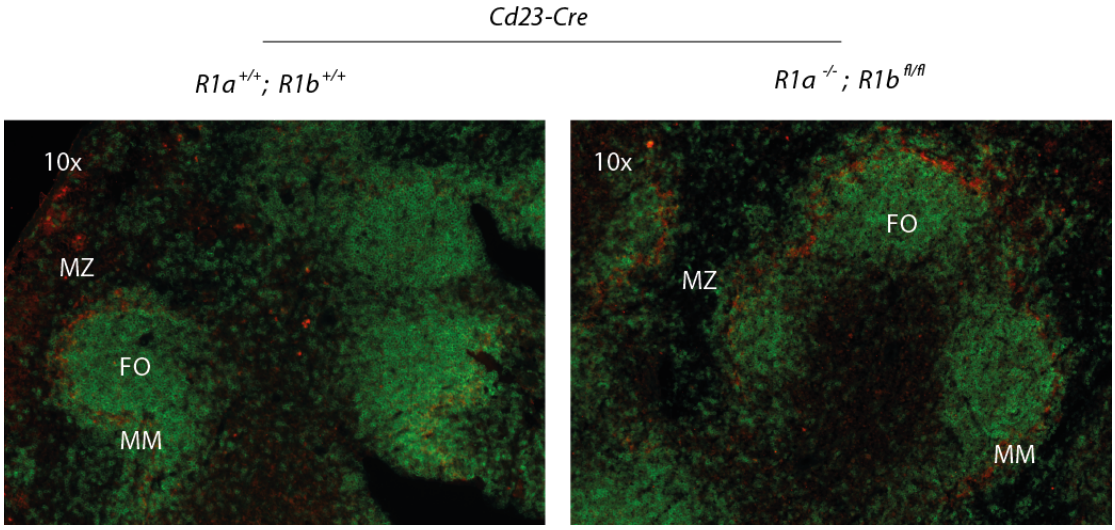

Figure 30. *Ring1a*$^{-/-}$*Ring1b*$^{-/-}$ B cells home to spleen follicles and form the marginal zone layer.

Immunufluorescence analsysis of control (left) and mutant (right) spleen sections for B220 (green) and MOMA-1 (red). Indicated are the B220^{+} marginal zone (MZ) B cell layer, the follicle (FO) and the MOMA1^{+} metallophilic macrophages (MM).

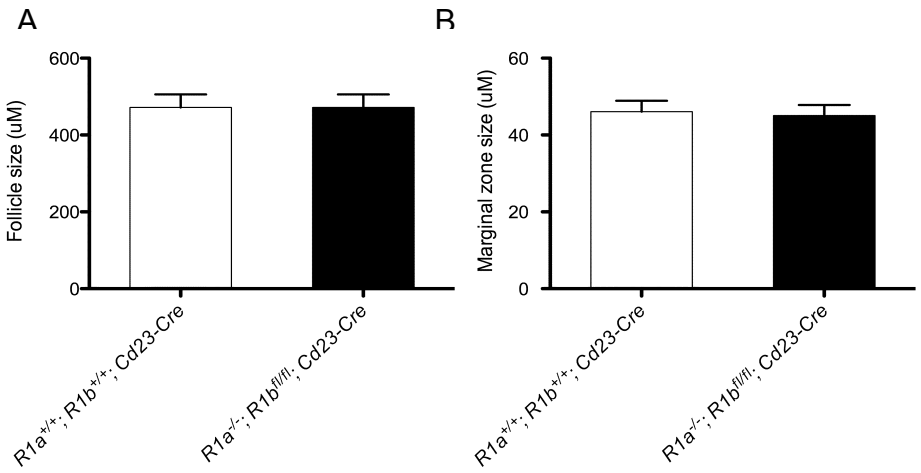

Figure 31. Marginal zone and B cell follicles are formed upon knock-out of *Ring1a* and *Ring1b*.

Quantification of (A) marginal zone thickness and (B) of B cell follicles diameter in control and mutant animals. Results are shown as mean +/- SEM of a total of 30 measurements (A) per sample from two independent animals and 22 measurements for (B).

3.3.3. PRC1 inactivation in mature B cells delays bone marrow exhaustion

The recruitment of B cells into the mature B cell pool is marked by their ability to recirculate through secondary lymphoid organs and to the BM. Presence of adequate numbers of mature B cells in peripheral lymphoid organs is sensed by the BM, which slows down progenitor B cell production. Conversely, lack of adequate B cell peripheral maturation results in homeostatic compensatory mechanisms leading to more sustained and prolonged B cell production (Keren et al., 2011).

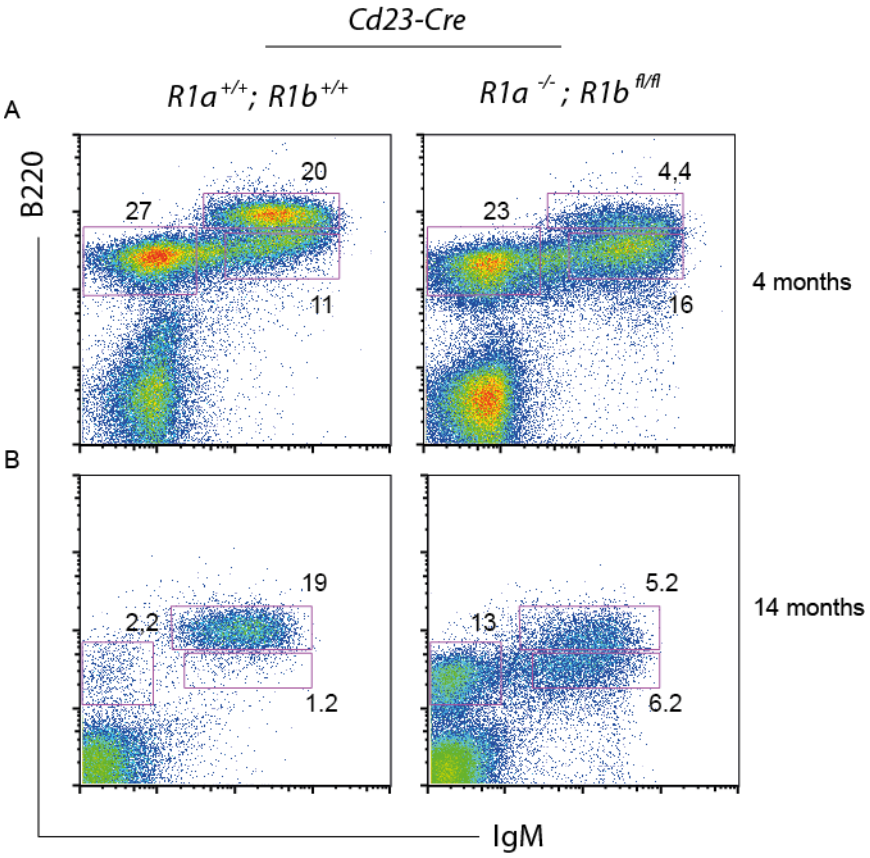

Figure 32. *Ring1a*$^{-/-}$*Ring1b*$^{-/-}$ mice display more sustained B cell production and lower frequencies of recirculating B cells.

Flow cytometric analysis of bone marrow B cell suspensions from age-matched young (A) and aged (B) control and experimental animals. Frequencies of the indicated gates are representative of 4 independent experiments.

The reduction in the number of PRC1 mutant FO B cells, coupled to their aberrant maturation could potentiate early B cell development as a feedback compensatory mechanism. Indeed, flow cytometric analysis of BM cells from control and PRC1 mutant mice revealed lower frequencies of IgM^{+} B220^{+} recirculating B cells in the latter samples (Figure 32A). Morever, similar analysis on 14-month-old animals revealed a substantial higher frequency of progenitor B cells in the BM of PRC1 mutant animals as compared with those from age-matched control mice (Figure

32B). These results suggest that PRC1 inactivation in mature B cells activates a compensatory mechanism based on potentiation of early B-cell lymphopoiesis in order to normalize the peripheral B cell pool.

3.3.4. PRC1 regulates the transcriptome profile of mature B cells

In an attempt to identify the molecular mechanism underlying the developmental aberrancies observed in PRC1 mutant mice, we performed transcriptome analysis of splenic $CD19^+$ B cells of mutant and control mice. Such analysis revealed extensive alterations in the gene expression profile of B cells in response to PRC1 inactivation. Specifically, most differentially expressed genes were up-regulated in PRC1 mutant B cells (n=343, 88%), whereas only a handful (n=48, 12%) were down-regulated (Figure 33).

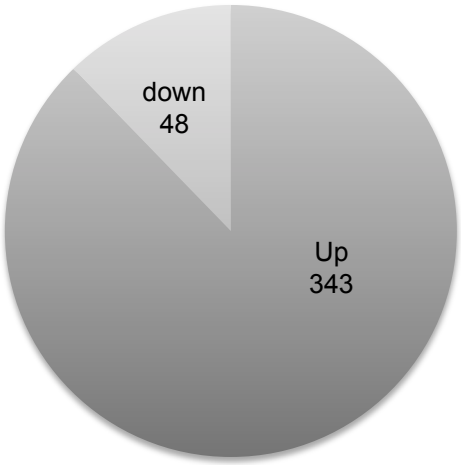

Figure 33. Gene deregulation in *Ring1a*$^{-/-}$*Ring1b*$^{-/-}$ $CD19^+$ cells.

Relative distribution of up- and down-regulated genes in transcriptome obtained from $CD19^+$ cells of 3 mutant and 3 control animals. Results were filtered according to 0,5<FC>1,5 and p-value<0,05.

We performed gene ontology (GO) analysis to identify gene categories significantly overrepresented among up- and down regulated genes in PRC1 mutant B cells. In mature B cells, PRC1 was specifically required to repress genes involved in various developmental processes (Figure 34). Instead, PRC1 acted as a positive regulator in the expression of genes controlling cell cycle regulation and S phase progression (Figure 34B).

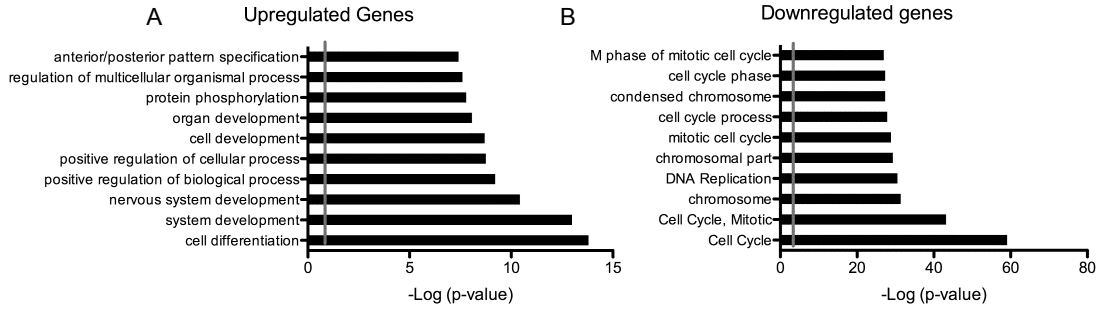

Figure 34. Up-and down-regulated genes in *Ring1a;Ring1b* double mutant B cells belong to different functional GO categories.

Gene ontology analysis of categories enriched within up-regulated (A) and down-regulated genes (B).

Next, we tried to assess whether genes de-regulated upon loss of *Ring1a* and *Ring1b* were direct PcG targets in peripheral B cells. To this end, since data concerning genome-wide occupancy of PRC1 in B cells was lacking, we intersected the list of differentially expressed genes in PRC1 mutant B cells to that of H3K27me3/PRC2 targets in splenic mature B cells (FO and MZ B cells) recently established by our group (C. Carrisi, F. Zanardi and S. Casola unpublished data; Figure 35). This analysis showed that 45% of genes de-repressed in PRC1 mutant B cells are marked by H3K27me3 and therefore bound by PRC2 (165 out of 387) in peripheral B cells, thereby representing *bona fide* PcG target genes. Instead,

only 22% (132 out of 609) of the down-regulated genes were also marked by H3K27me3, suggesting that most of them are controlled indirectly by PRC1. These results are consistent with PRC1 acting predominantly to promote transcriptional repression in mature B cells.

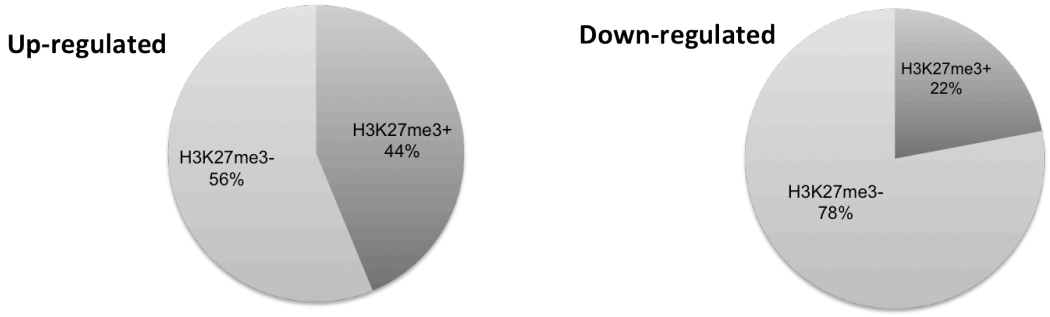

Figure 35. Relative enrichment for H3K27me3-marked loci among genes up- and down- regulated in CD19^{+} cells from *Ring1a/Ring1b* mutants.

Pie charts displaying relative enrichment of H3K27me3 loci among genes deregulated following loss of PRC1, Lists of up- and down- regulated genes were intersected with lists of H3K27me3 genome-wide occupancy and enrichment calculated based on the proportion of genes marked by H3K27me3 within each category. Preferential enrichment for H3K27me3 targets among up-regulated genes was found to be highly significant (*p*-value <0.0001), whereas the enrichment for loci targeted by H3K27me3 and down-regulated following PRC1 loss did not reach statistical significance (*p*-value=0.485)

3.4. PRC1 and B cell immunity

3.4.1. PRC1 inactivation in GC B cell founders impairs germinal center responses

Expression of PRC1 components is conserved in B cells recruited into the germinal center (GC) reaction during a T cell-dependent immune response (L. D'Artista, F. Mainoldi and S. Casola, unpublished data). To assess the effects of B cell-specific PRC1 inactivation on GC responses, we immunized controls and *Ring1a*$^{-/-}$*;Ring1b*$^{ff/fl}$*;Cd23-cre* compound mutants with alum-precipitated 4-nytrohenyl-acetyl (NP) coupled to chicken gamma globulin (CGG). GC responses were analyzed at day 14 post-immunization. PRC1 conditional mutant mice displayed a significant reduction in the frequency and numbers of splenic CD19^{+}FAS^{hi}CD38^{lo} GC B cells as compared to controls (Figure 36 and Figure 37).

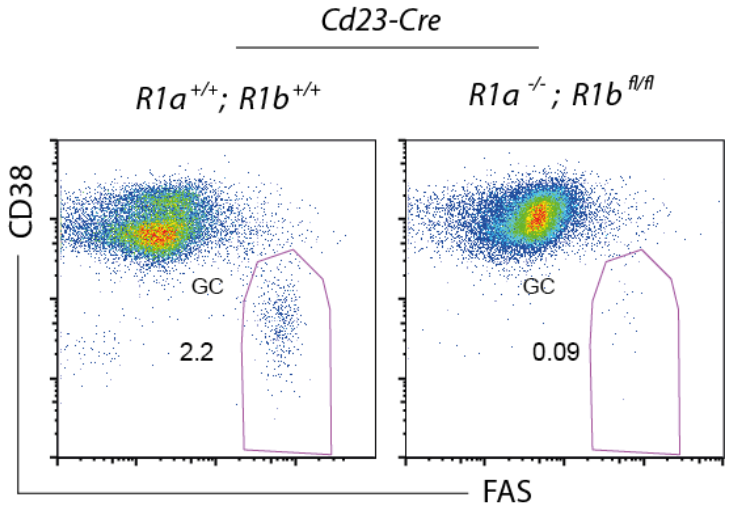

Figure 36. GC B cell development is impaired upon loss of *Ring1a* and *Ring1b*.

Flow cytometric analysis displaying GC B cell frequencies at day 14 post NP-CGG immunization in control (left) and experimental *Ring1a*$^{-/-}$;*Ring1b*$^{ff/fl}$;*Cd23-cre* (right) animals. Frequencies of the indicated gates are representative of 8 independent experiments.

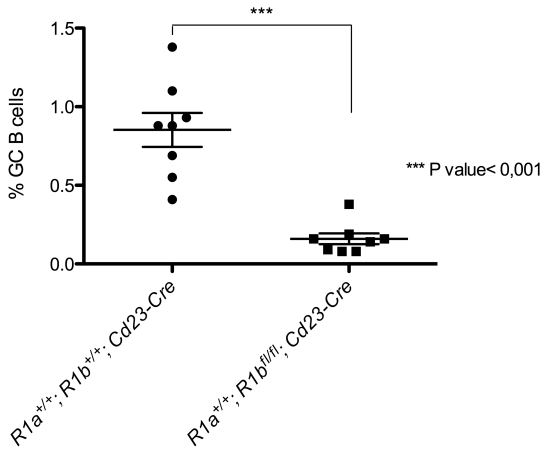

Figure 37. GC B cell numbers are reduced upon PRC1 inactivation.

To confirm these results, we performed histological analysis of the GC master regulator Bcl6 on splenic sections of animals immunized with the T cell-dependent sheep red blood cell (SRBC) antigen, which induces a faster and more robust immune response as compared with NP (Figure 38) (Luster et al., 1988).

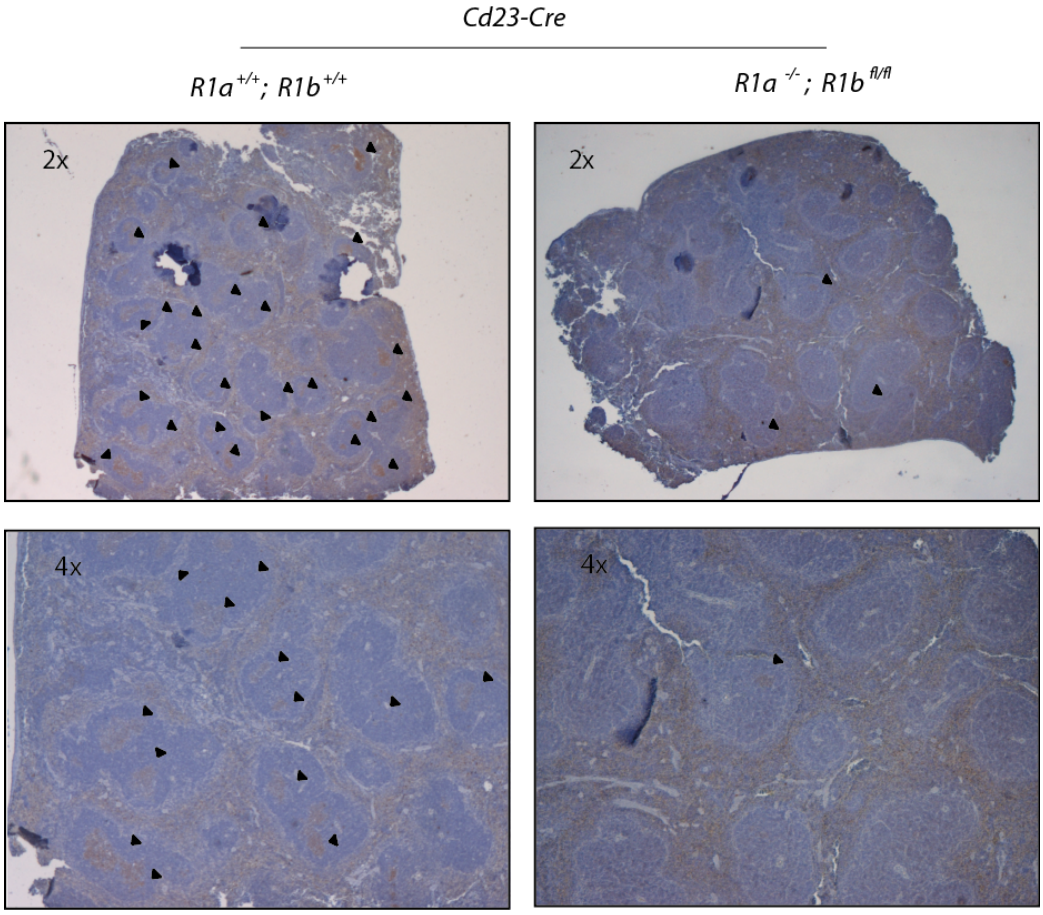

Figure 38. Significant reduction of GC number in PRC1 mutants.

Spleen samples were collected from sheep red blood cells-immunized mutant (n=3) and control (n=2) animals at day 8 post-immunization with SRBCs. Paraffin-embedded sections were stained for the GC reaction master regulator Bcl6. Representative stainings for control and mutant animals are shown with arrowheads indicating $Bcl6^{+}$ foci.

Quantification of Bcl6^{+} GCs revealed a significant reduction in their number in spleen sections of PRC1 mutants as compared to controls (Figure 39). Instead, average GCs size remained unchanged after *Ring1a/Ring1b* loss.

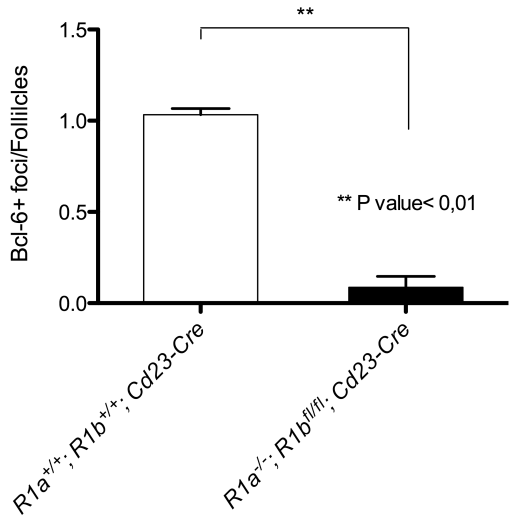

Figure 39. Significant reduction in GC frequency in *Ring1a/Ring1b* mutants.

To assess whether the remaining B cells detected in the GCs of mutant animals had undergone Cre-mediated recombination at the *Ring1b* locus, we performed quantitative PCR (q-PCR) analysis on genomic DNA extracted from sorted cells. Whereas up to 80% of FO B cells in *Ring1a$^{-/-}$; Ring1b$^{ff/fl}$;Cd23-cre* mice showed efficient deletion of the floxed segment, the frequency of *Ring1b* mutant B cells dropped to 60% when isolated from the GC (Figure 40).

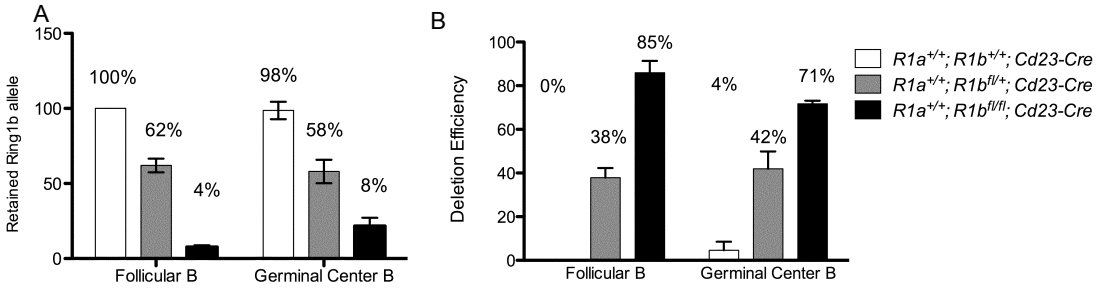

Figure 40. Status of the *Ring1b* gene in GC B cells from *Ring1a*$^{-/-}$*Ring1b*$^{fl/fl}$ *Cd23-cre* mutant and control mice.

Q-PCR was performed on genomic DNA with primers annealing to the *Ring1b* region encoding the fragment excised upon Cre-mediated recombination. Data shown in (A) represent the percentage of retained *Ring1b* allele in follicular and germinal center B cells. Data shown in (B) represent deletion efficiency. Data are representative of 3 independent experiments analyzed and are presented as mean +/- SEM.

This result is consistent with the preferential expansion of PRC1 proficient B cells carrying in most cases only one recombined *Ring1b* allele within the GC compartment. To address this hypothesis, *Ring1a*$^{-/-}$*Ring1b*$^{fl/fl}$*Cd23-cre* animals were bred to the Rosa26-EYFP (R26-EYFP$^{fl\text{-}STOP}$) Cre reporter strain. In R26-EYFP mice, EYFP expression is induced upon Cre-mediated excision of a transcription termination sequence (STOP cassette), flanked by *loxP* sites (Srinivas et al., 2001) (Figure 41).

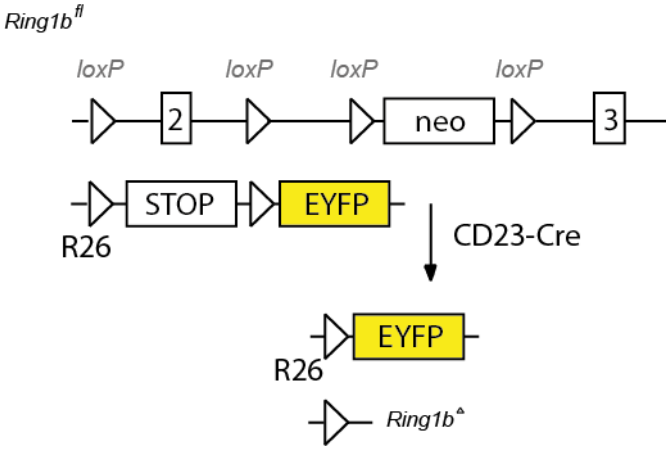

Figure 41. Schematic view of the R26-EYFPfl-STOP reporter system.

Flow cytometric analysis of GC B cells from NP-CGG immunized controls (*Ring1a*$^{-/-}$*;Ring1b*$^{fl/+}$*;Cd23-cre R26-EYFP*) and PRC1 conditional mutants (*Ring1a*$^{-/-}$*; Ring1b*$^{ff/fl}$*;Cd23-cre*;*R26-EYFP)* revealed a strong reduction of YFP/Cre-expressing cells as a result of *Ring1a/Ring1b* double inactivation (Figure 42).

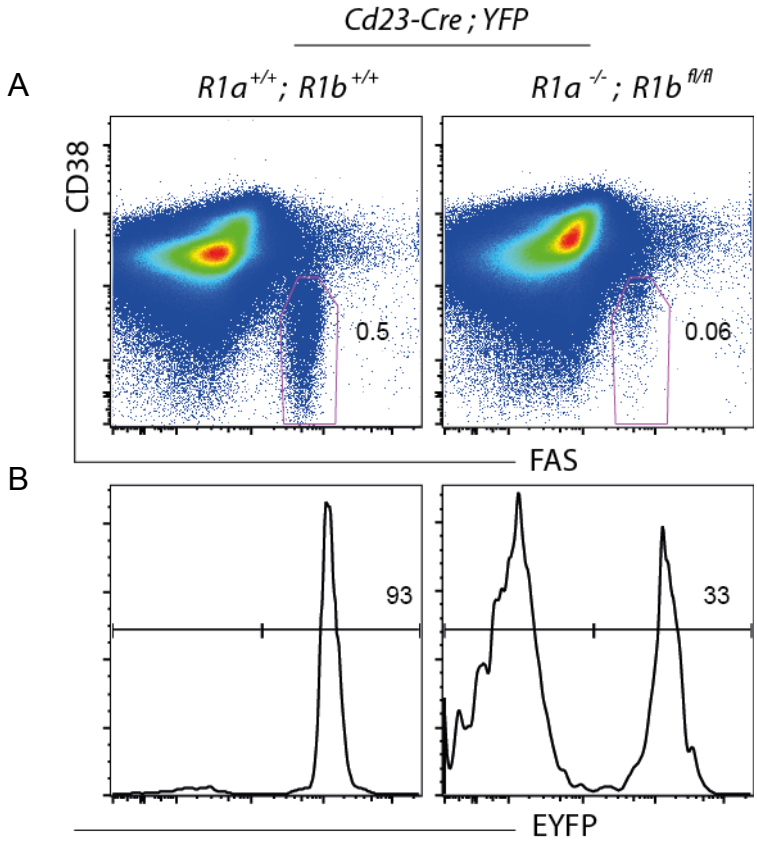

Figure 42. *Ring1a*$^{-/-}$*Ring1b*$^{-/-}$ GC B cells are counter-selected *in vivo*.

Flow cytometric analysis of CD19^{+} splenic GC B cells from control and mutant animals. Numbers indicate the percentage of GC B cells (A). (B) Histogram plot displaying percentages of *EYFP*-expressing cells within the GC compartment. Data shown are representative of 3 independent experiments.

3.4.2. PRC1 inactivation triggers counter-selection of mutant GC B cells

To exclude that the defects seen in GC responses of *Ring1a*$^{-/-}$*;Ring1b*$^{lf/fl}$*;Cd23-cre* mutants resulted from developmental defects of PRC1 mutant GC B cell founders, we crossed *Ring1a*$^{-/-}$*Ring1b*$^{fl/fl}$ mice to *Cγ1-cre* transgenic animals. In compound

mutants, PRC1 inactivation is specifically induced in GC B cells undergoing IgG1 class-switch recombination (Casola et al., 2006) (Figure 43).

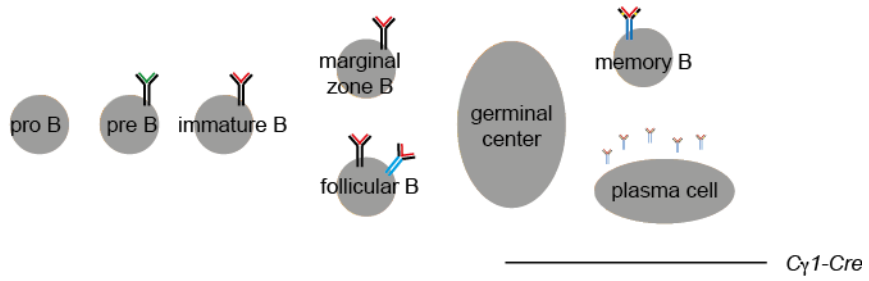

Figure 43 . Schematic view of B cell development and timing of *Cγ1-cre*-mediated deletion.

In apparent contrast to what observed in *Ring1a*$^{-/-}$*; Ring1b*$^{fl/fl}$*;Cd23-cre* animals, mice deprived of PRC1 specifically in GC B cells formed GCs with efficiency comparable to that of their WT counterparts (Figure 44).

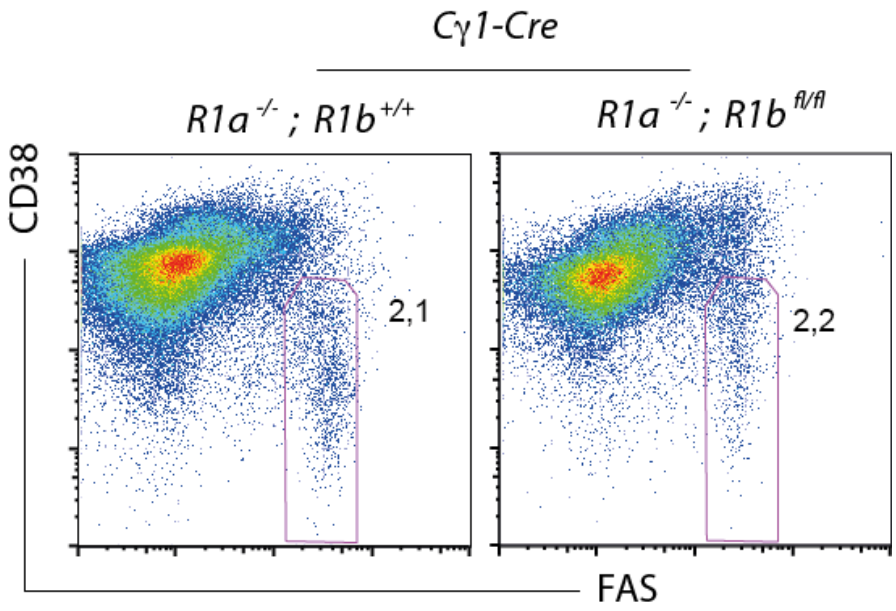

Figure 44. Efficiency of GC formation by *Ring1a*$^{-/-}$; *Ring1b*$^{fl/fl}$; *Cγ1-cre* animals is comparable to that of controls.

Flow cytometric analysis displaying GC B cell frequencies at day 14 post NP-CGG immunization following *Cγ1-cre*-mediated deletion. Data shown are representative of 6 independent experiments.

To assess the efficiency of Cre-mediated recombination in *Ring1a*$^{-/-}$; *Ring1b*$^{fl/fl}$; *Cγ1-cre* GC B cells, we performed genomic q-PCR analysis for the *Ring1b* floxed segment on sorted cells. Strikingly, *Ring1b* inactivation in GC B cells caused a dramatic counter-selection of mutant cells, leading to the preferential rapid outgrowth of PRC1 proficient B cells that failed to express Cre recombinase (Figure 45).

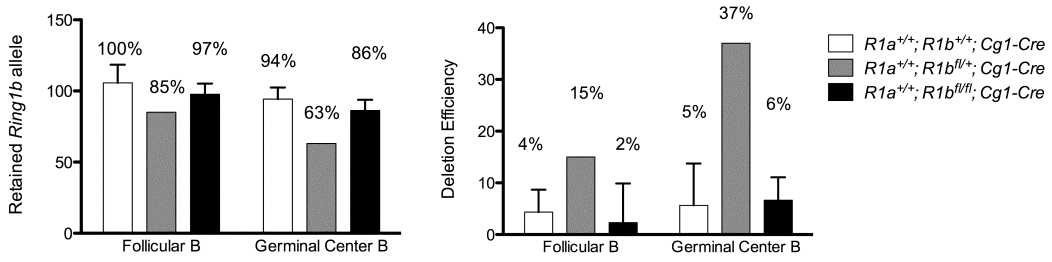

Figure 45. Status of the *Ring1b* gene in GC B cells from *Ring1a*$^{-/-}$*Ring1b*$^{fl/fl}$ *Cγ1-cre* mutant and control mice.

Q-PCR was performed on genomic DNA with primers annealing to the *Ring1b* region coding for the fragment excised upon Cre-mediated recombination. Data shown in (A) represent the percentage of retained *Ring1b* allele in follicular and germinal center B cells. Data shown in (B) represent deletion efficiency. Data are representative of 3 mice/genotype analyzed and data are presented as mean +/- SEM.

When expression of Cre recombinase was induced in the vast majority of GC B cells, such as when *Ring1a*$^{-/-}$*/Ring1b*$^{fl/fl}$ mice were bred to the *Aicda-cre* strain (Figure 46) (Crouch et al., 2007), the reduction in GC B cell frequencies and numbers became very substantial (Figure 47).

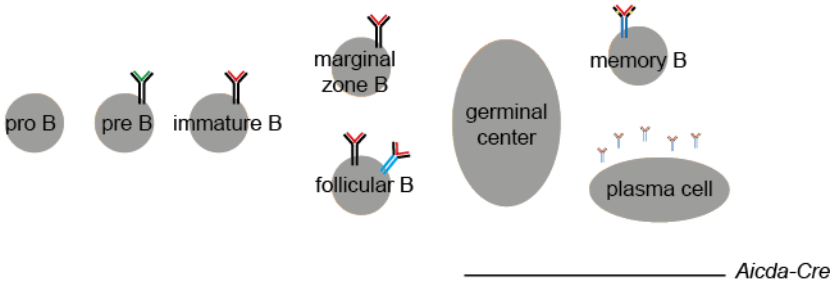

Figure 46. Schematic view of B cell development and timing of *Aicda-cre*-mediated deletion.

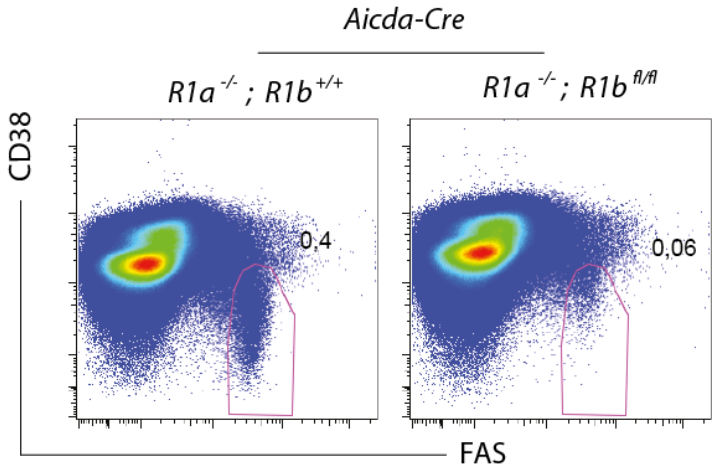

Figure 47. Impaired GC formation in *Ring1a*$^{-/-}$*Ring1b*$^{fl/fl}$ *Aicda-cre* animals.

Flow cytometric analysis displaying GC B cell frequencies at day 14 post NP-CGG immunization following *Aicda-cre*-mediated deletion. Data are representative of 3 independent experiments.

All together, these results indicate that inhibition of PRC1 in GC B cells or their direct progenitors prevents their ability to clonally expand in response to the recognition of cognate antigen.

3.4.3. Antibody responses are compromised upon PRC1 inactivation

In order to assess the role of PRC1 in the establishment of an antibody response to foreign antigens, we immunized mutant *Ring1a*$^{-/-}$*;Ring1b*$^{fl/fl}$*;Cγ1-cre* mutants and controls with the T cell-dependent antigen NP-CGG.

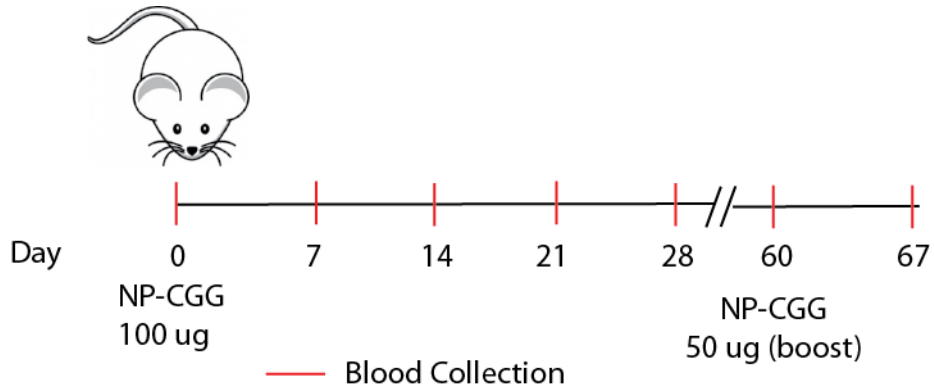

Figure 48. Sera collection scheme for the analysis of primary and secondary antibody responses.

Blood sera samples were collected at different time points after immunization (Figure 48) and antigen-specific IgM and IgG1 titers were determined by Enzyme/linked immunosorbent assay (ELISA). NP-specific Ig titers were significantly reduced in response to GC B cell-specific inactivation of PRC1. The reduction affected mainly IgG1 serum titers, in accordance with the preferential expression of the *Cγ1-cre* transgene in IgG1-class switched B cells (Figure 49A and B). The impairment in antibody responses in PRC1 mutant mice was already detected 7 days after primary immunization and became increasingly evident at later time points.

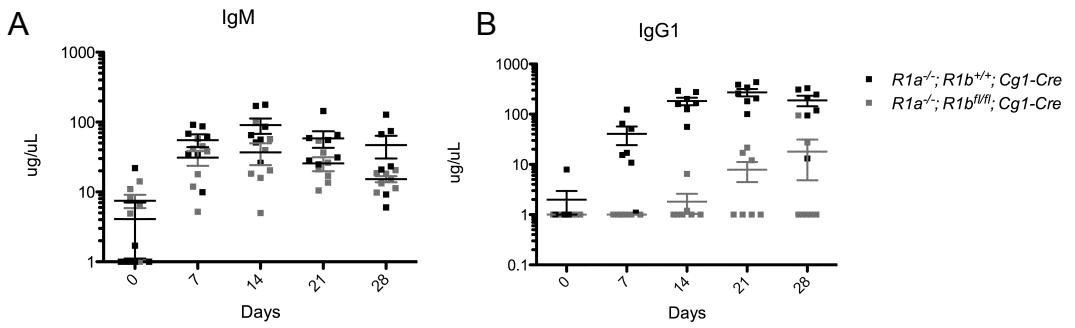

Figure 49. PRC1-deficient mice display an impaired antibody response.

ELISA analysis of blood sera collected from control and mutant mice at the indicated time points following NP-CGG immunization.

We also measured how PRC1 mutant mice responded to antigenic re-challenges in recall responses. Specifically, PRC1 control and mutant (*Ring1a$^{-/-}$;Ring1b$^{fl/fl}$;Cγ1-cre)* animals were immunized with NP-CGG and re-challenged 60 days later with lower doses of the same antigen, when the primary response had faded away and high affinity memory B cells had been generated. Blood sera were collected 7 days following secondary immunization and high-affinity NP-specific IgG1 antibodies quantified by ELISA assay. Data revealed that PRC1 inactivation caused an over 10-fold reduction in high-affinity antibody responses (Figure 50).

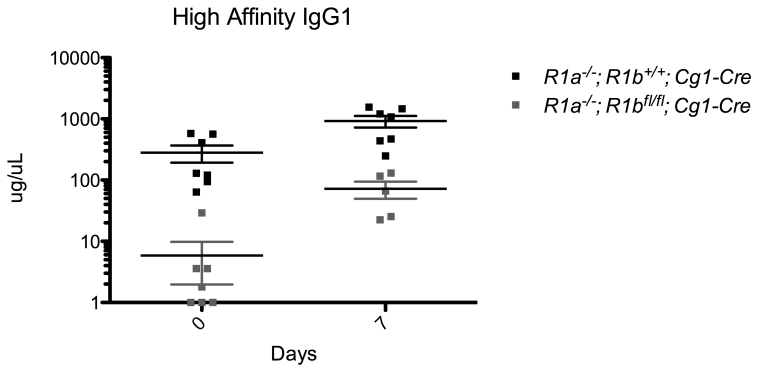

Figure 50. PRC1-deficient mice display impaired recall resposes.

ELISA analysis of blood sera collected from control and mutant mice at the indicated time points following NP-CGG boost.

3.4.4. PRC1 is required for memory B cell formation

The reduction in antibody titers produced during secondary immunizations suggested an impairment in memory B cell formation in *Ring1a/Ring1b* double mutants. To test this hypothesis, we measured the proportion of memory B cells in the spleen 60 days after NP-CGG immunization (Figure 51).

Figure 51. Timeline for the analysis of memory B cell formation.

Antigen-specific memory B cells were identified by flow cytometric analysis as $CD19^{+}NIP^{+}PNA^{lo}Ig\kappa^{lo}IgG1^{+}$. In *Ring1a*$^{-/-}$*;Ring1b*$^{fl/fl}$*;Cγ1-cre* mice, we observed a 30-fold reduction in the frequency of antigen-specific IgG1 memory B cells as compared to controls (Figure 52 and Figure 53).

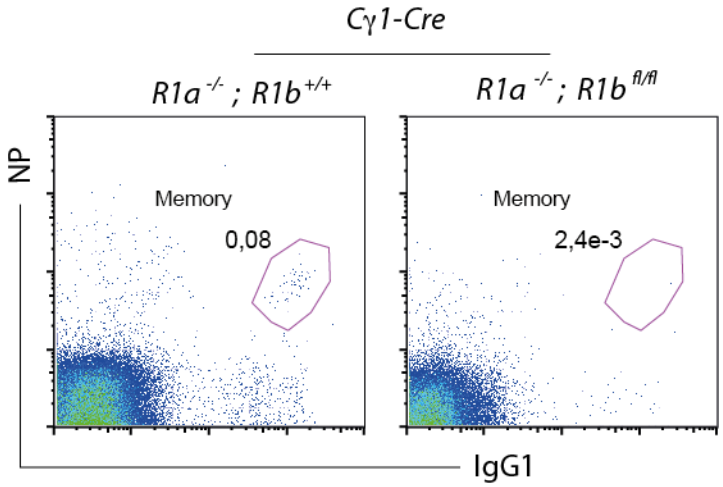

Figure 52. Frequency of memory B cells in *Ring1a*$^{-/-}$*Ring1b*$^{fl/fl}$ *Cγ1-cre* animals is lower than that of controls.

Flow cytometric analysis displaying frequency of memory B cells at day 60 post NP-CGG immunization in control (left) and mutant (right) animals. Data are representative of 6 independent experiments.

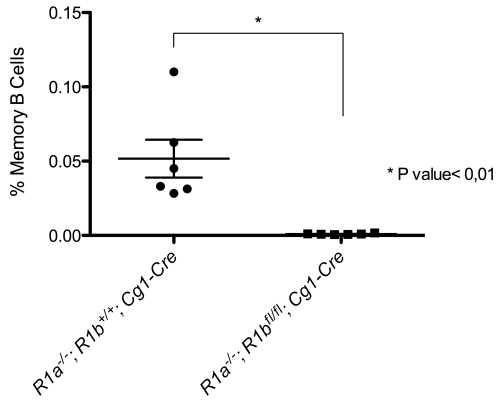

Figure 53. Frequency of memory B cells is lower in *Ring1a/Ring1b* mutants compared to controls.

Frequencies of $CD19^{+}PNA^{lo}\kappa^{lo}NP^{+}IgG1^{+}$ cells in control (left) and mutant (right) animals, each shown as a single dot. Data are presented +/- SEM.

The strong reduction in memory B cells detected 2 months after primary immunization could have resulted from a defect in their formation and/or maintenance. To address this question, *Ring1a$^{-/-}$;Ring1b$^{fl/fl}$;Cγ1-cre* experimental and control mice were immunized with NP-CGG and the frequency of newly generated IgG1 memory B cells was analyzed by flow cytometry at day 14 post immunization, at the peak of the GC response. At this time, the frequency of memory B cells was significantly lower in PRC1 mutant animals in comparison to controls (0,08% vs 0,003%) (Figure 54).

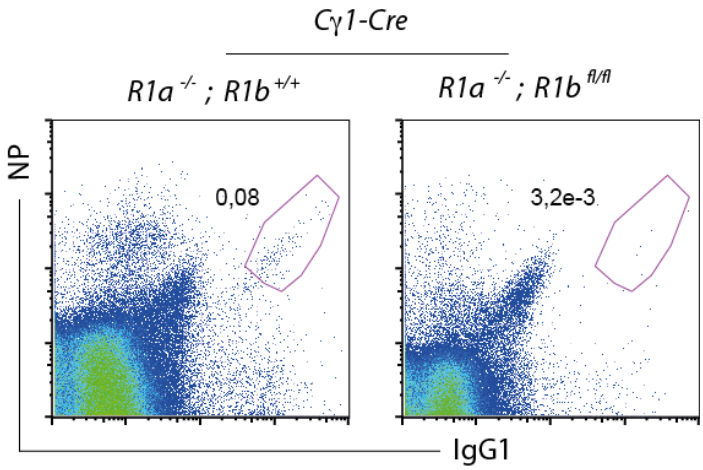

Figure 54. Absence of *Ring1a* and *Ring1b* interferes with memory B cell formation.

Flow cytometric analysis displaying frequency of memory B cells at day 14 post NP-CGG immunization in control (left) and mutant (right) animals. Data are representative of 4 animals/genotype.

We therefore conclude that *Ring1a* and *Ring1b* are essential for the formation of antigen-specific, high affinity long-lived memory B cells.

3.5. How does PRC1 regulate B cell function?

3.5.1. PRC1 protects GC B cells from apoptosis

The significant counter-selection of PRC1 mutant B cells seen in the GC could depend on impaired survival of the cells. To test this hypothesis, we first activated primary B cells from controls and *Ring1a*$^{-/-}$*;Ring1b*$^{fl/fl}$*;Cd23-cre* compound mutants with bacterial lipopolysaccharide (LPS) to closely monitor their behavior *in vitro*. Three days after stimulation, B cells were stained with fluorescent-labeled VAD-FMK (CaspGLOW^{TM}), which binds to active caspases, and analyzed by flow cytometry. Inactivation of PRC1 increased by approximately 1.5-fold the proportion of apoptotic B cells in response to LPS stimulation (Figure 55).

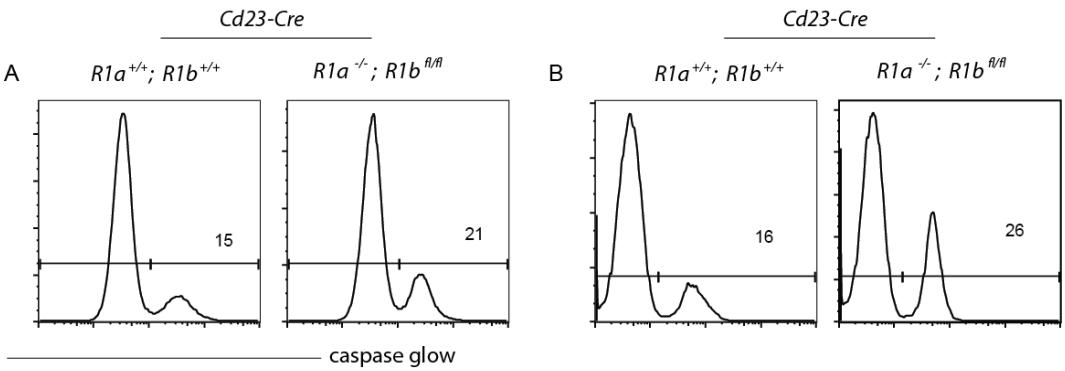

Figure 55. Increased apoptosis upon *in vitro* stimulation of *Ring1a*$^{-/-}$*Ring1b*$^{-/-}$ cells.

Flow cytometric analysis of Caspase glow^{+} cells from *Ring1a*$^{-/-}$*;Ring1b*$^{fl/fl}$*;Cd23-cre* and control cultures at day 3 of LPS and IL-4 (A) and LPS (B) stimulation. Data are representative of 3 independent experiments.

On the basis of these results, similar analyses were performed *in vivo* on *Ring1a*$^{-/-}$*;Ring1b*$^{ff/fl}$*;Cd23-cre* mutant and control animals, which were immunized with alum-NP-CGG. Assessment of the fraction of Caspase GLOW^{+} B cells among

$CD19^{+}FAS^{hi}CD38^{lo}$ GC B cells was performed at the peak of the response. Flow cytometric analysis revealed a significant increase in the frequency of apoptotic GC B cells in response to PRC1 inactivation (Figure 56 and Figure 57).

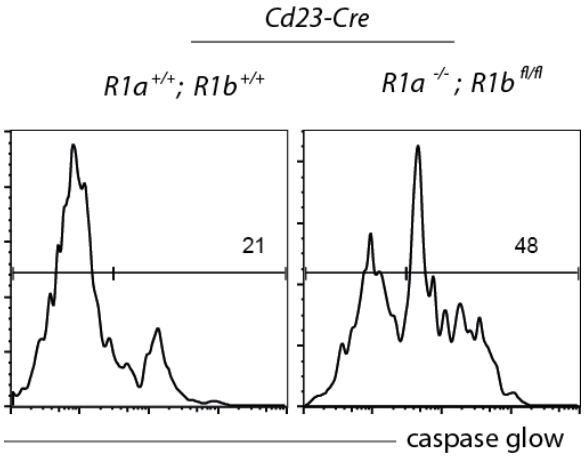

Figure 56. Apoptosis in GC B cells.

Flow cytometric analysis of the fraction of Caspase $glow^{+}$ cells within the $CD19^{+}CD38^{lo}FAS^{hi}$ GC compartment of control (left) and mutant (right) animals at day 14 post NP-CGG immunization. Data shown are representative of 6 independent experiments.

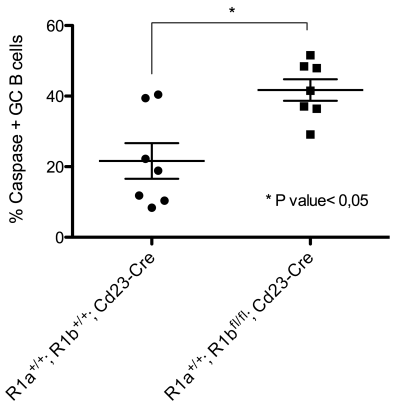

Figure 57. Increased frequency of apoptotic GC B cells upon lack of *Ring1a* and *Ring1b*.

To investigate the possible mechanisms responsible for the heightened apoptosis of PRC1 mutant GC B cells we quantified transcripts of several pro- (*Apaf1*, *Bad*, *Bak1*, *Bax*, *Bcl2l11*, *Bid*, *Casp7*, *Diablo*, *Foxo3*, *Moap1*, *Pmaip1*, *Trp53bp2*) and anti-apoptotic (*Bcl2*, *Cflar*, *Mdm4*, *Pdcd6ip*, *Mcl-1*) factors. Except for *Foxo3*, expression of the main pro-apoptotic factors, including several BCL2 family members were unaffected (*Bax*, *Bax1*, *Bim, Bcl2l11*) or down-regulated (*Bad*) in PRC1 mutant GC B cells. Instead, transcripts coding for anti-apoptotic proteins *Mcl1* and *Bcl2* were substantially up-regulated in *Ring1a/Ring1b* double mutant GC B cells (Figure 58).

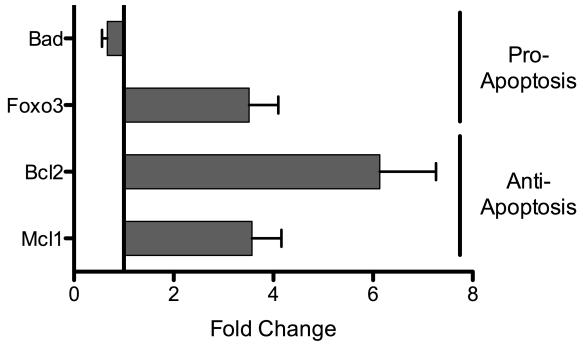

Figure 58. Loss of PRC1 leads to de-regulation of pro- and anti-apoptotic genes in GC B cells.

Q-PCR of transcript levels for the indicated genes in GC B cells sorted from 11 *Ring1a*$^{-/-}$*;Ring1b*$^{ff/fl}$*;Cd23-cre* mutant and 11 *Ring1a*$^{+/+-}$*;Ring1*$^{+/+}$*;Cd23-cre* control animals. Transcript levels were normalized using Rplp0. Genes were filtered based on number of samples where consistent up- or down-regulation was detected in >= 5 samples and if 0,5<FC>1,5. Bars represent mean values +/- SEM.

All together, our data assign to PRC1 a critical role in the protection of GC B cells from programmed cell death, which is independent of the activation of the mitochondrial pathway.

3.5.2. Does AID contribute to apoptosis of PRC1 mutant B cells?

Recent work in our laboratory has shown that Activation-Induced Cytidine Deaminase (AID) is a major trigger of cell death in GC B cells lacking the catalytic subunit of PRC2, *Ezh2* (Caganova et al., 2013). Moreover, we could also show that apoptosis of *Ezh2* mutant B cells correlated with the induction of genotoxic stress. To test whether AID contributed to the apoptosis of PRC1 mutant B cells, we initially measured the fraction of Ig class-switched B cells generated *in vitro* after LPS+/- IL-4 stimulation as a readout of AID activity. Flow cytometric analysis revealed a reduction in the proportion of PRC1 mutant B cells that switched to either become IgG3-(LPS) and IgG1-(LPS+IL-4) expressing B cells (Figure 59).

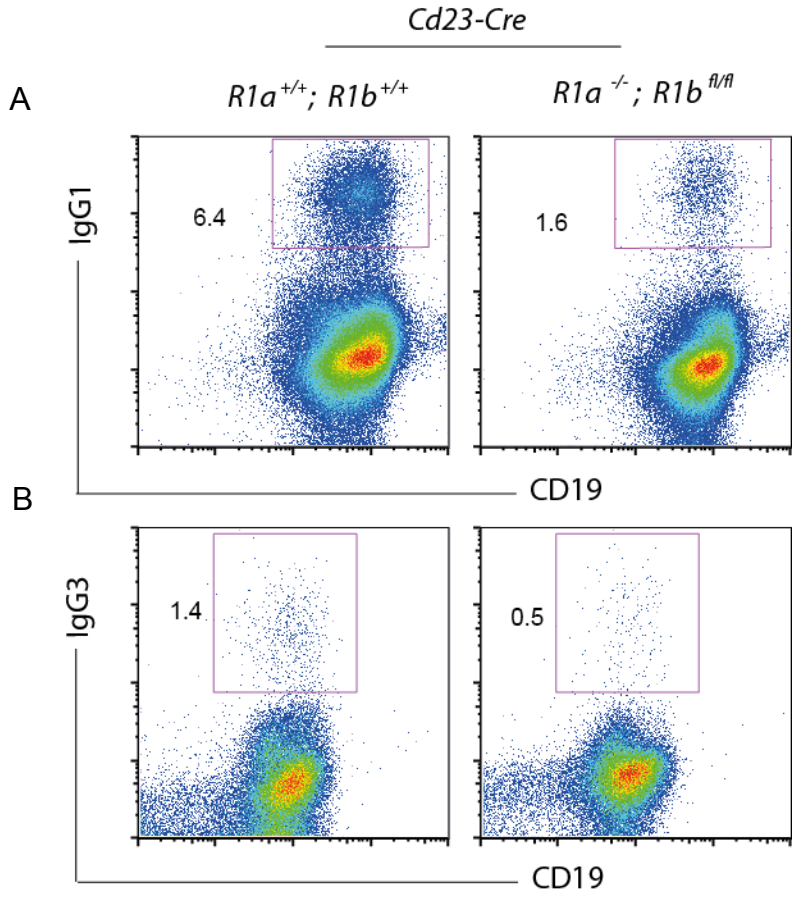

Figure 59. Reduction in frequency of isotype-switched cells in *Ring1a*$^{-/-}$*Ring1b*$^{-/-}$ cultures.

Flow cytometric analysis displaying frequency of (A) CD19^{+}IgG1^{+} and (B) CD19^{+}IgG3^{+} cells at day 3 following stimulation of purified naïve B cells with LPS and IL-4 or LPS alone, respectively, in control (left) and mutant (right) animals. Data are representative of 3 independent experiments.

This result is compatible with a scenario in which induction of AID prior to class-switching reduces the viability of activated B cells lacking functional PRC1, as a consequence of impaired ability to cope with AID-induced DNA double-strand breaks. To corroborate this hypothesis, PRC1 mutant and control B cells were activated *in vitro* with an agonistic antibody against the Toll-like receptor RP-105. Similarly to LPS, stimulation through RP-105 induces intense B cell proliferation

but, in contrast to endotoxin, it does not induce AID expression (Ogata et al., 2000). Importantly, stimulation of PRC1 mutant B cells through RP-105 led to a robust mitogenic response (data not shown) without any detectable effect on apoptosis (Figure 60).

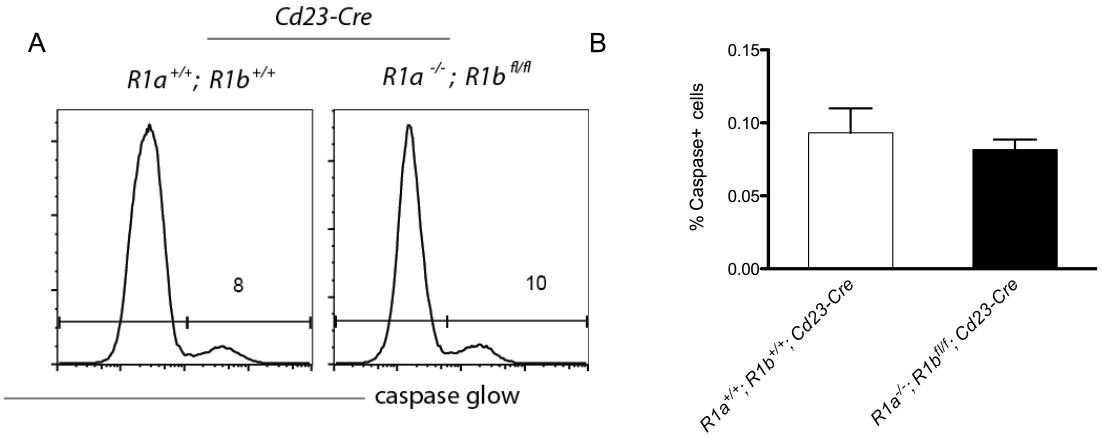

Figure 60. Lack of AID induction prevents apoptosis of *Ring1a*$^{-/-}$*Ring1b*$^{-/-}$ cells.

(A) Representative histogram plot displaying frequency of apoptotic cells at day 3 of RP-105 treatment. (B) Frequency of caspase positive cells presented as mean +/- SEM of 3 independent experiments.

3.5.3. PRC1 facilitates G1-to-S transition in activated B cells

Given the high proliferative rate that characterizes B cells recruited into the GC reaction and considering the well-documented role of PcG proteins in regulating transcription of the *Cdkn2a* locus, we determined whether PRC1 inactivation affected expression of cell-cycle regulators in mutant GC B cells. To this end, we immunized *Ring1a*$^{-/-}$*;Ring1b*$^{ff/fl}$*;Cd23-cre* and control mice with NP-CGG and compared mRNA expression between control and mutant GC B cells sorted at day 14 post immunization (Figure 61).

We found that *Cdkn2a/*p16^{INK4A}/p19^{ARF}, *Cdkn1a/*p21^{CIP1} and *Cdkn1b/*p27^{KIP1} transcripts, encoding for inhibitors of cyclin-dependent protein kinases (Cdk) regulating G1-to-S transition were significantly up- regulated in PRC1 mutant GC B cells. At the same time, we also detected up-regulation of loci encoding positive regulators of cell cycle progression, namely *Ccnd2* and *Ccng1*.

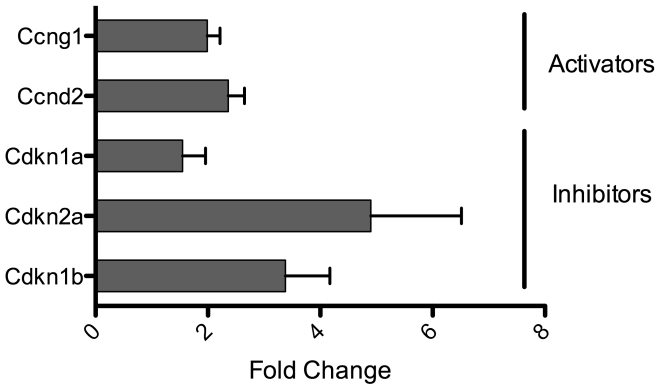

Figure 61. Loss of PRC1 leads to aberrant expression of cell cycle regulators.

Q-PCR of transcript levels for the indicated genes in GC B cells sorted from 11 mutants and 11 control animals. Transcript levels were normalized using Rplp0. Genes were filtered based on number of samples where consistent up- or down-regulation was detected in >= 5 samples and if 0,5<FC>1,5. Bars represent mean values +/- SEM.

In order to investigate whether transcriptional de-regulation of genes modulating cell cycle progression would affect proliferation of mutant PRC1 cells, and to overcome limitations due to the low cellularity observed in GCs of *Ring1a*$^{-/-}$*;Ring1b*$^{ff/fl}$*;Cd23-cre*, we employed an *in vitro* primary B cell culture system that generates highly proliferating GC B cell-like (iGB) cells (Figure 62) (Nojima et al., 2011).

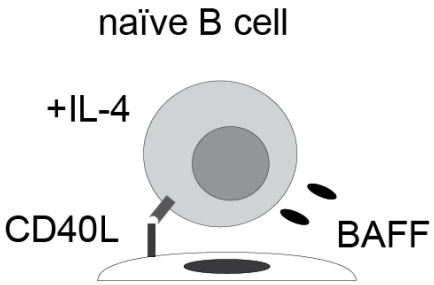

Figure 62. *In vitro* system to generate GC-like B cells from MACS-isolated naïve splenic B cells.

Briefly, resting splenic B cells from *Ring1a*$^{-/-}$*;Ring1b*$^{fl/fl}$*;Cγ1-cre* and control animals were purified by magnetic cell sorting and stimulated with soluble BAFF, IL-4 and membrane-bound CD40L. Using this experimental approach, we achieved efficient and rapid induction of the Cγ1-cre transgene, which in turn led to inactivation of PRC1 in the majority of *Ring1a*$^{-/-}$*;Ring1b*$^{fl/fl}$ activated B cells (Figure 63).

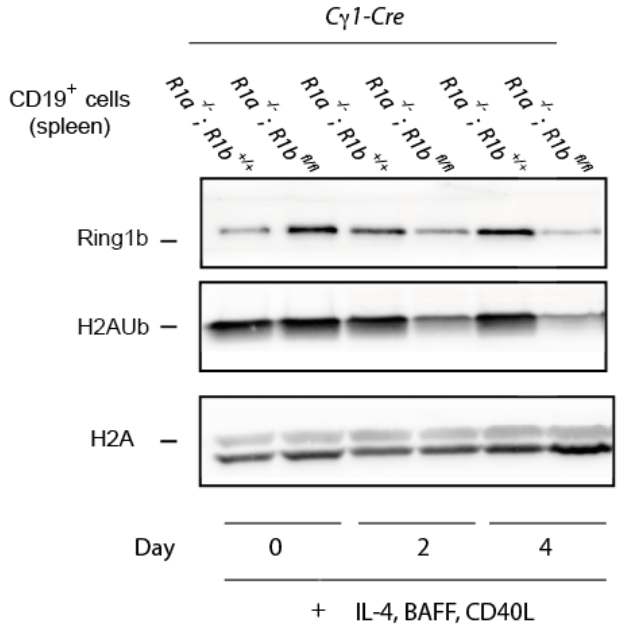

Figure 63. Efficient deletion of Ring1b and loss of H2AK119Ub in the iGB culture system.

Immunoblot analysis of splenic CD19^{+} cells isolated from spleens of *Ring1a*$^{-/-}$*; Ring1b*$^{fl/fl}$*; Cγ1-cre* mutant and control animals and cultured for the indicated number of days in the presence of membrane-bound CD40L, soluble BAFF and IL-4. Results shown are representative of 2 independent experiments.

Cell cycle distribution was determined by flow cytometric analysis on control and PRC1 mutant B cells at different days after stimulation following a brief pulse with BrdU and labeling of the cells with propidium iodide (PI) to determine the DNA content. Acute loss of PRC1 led to a progressive accumulation of activated B cells in the G_0/G_1 phase of the cell cycle (Figure 64).

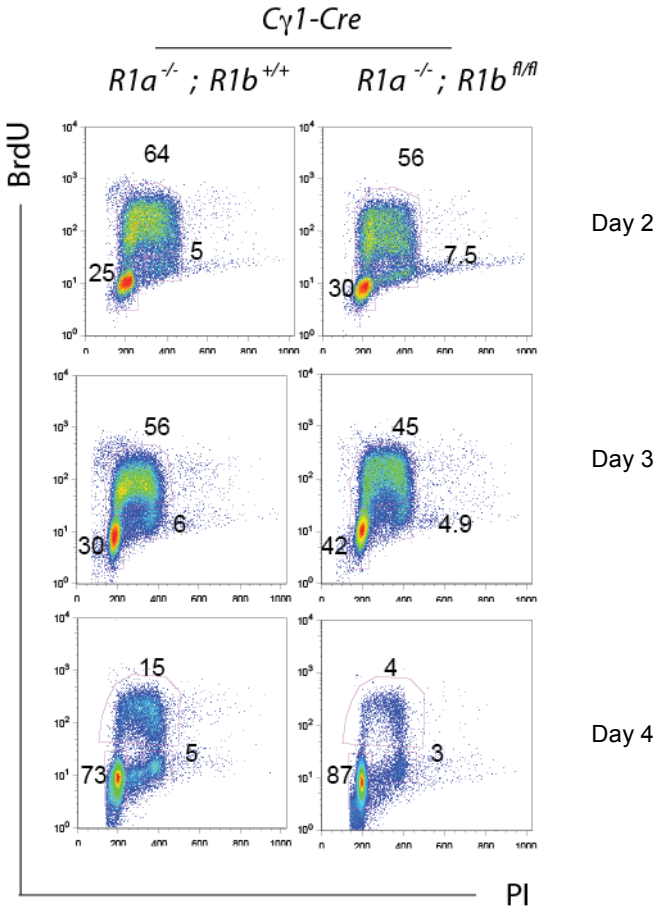

Figure 64. Loss of *Ring1a* and *Ring1b* affects cell cycle progression *in vitro*.

Flow cytometric analysis of cell cycle distribution of control (left) and mutant (right) induced GC B cells. Data shown are representative of data obtained in 3 independent experiments.

In order to determine whether the arrest in cell cycle progression was likely to originate from de-regulation of cell cycle modulators, we analyzed transcript levels for *Cdkn2a/*p16^{INK4A}/p19^{ARF}, *Cdkn1a/*p21^{CIP1} and *Cdkn1b/*p27^{KIP1} from control and PRC1 mutant cultures. Preliminary data show results similar to those obtained *in vivo* (Figure 65).

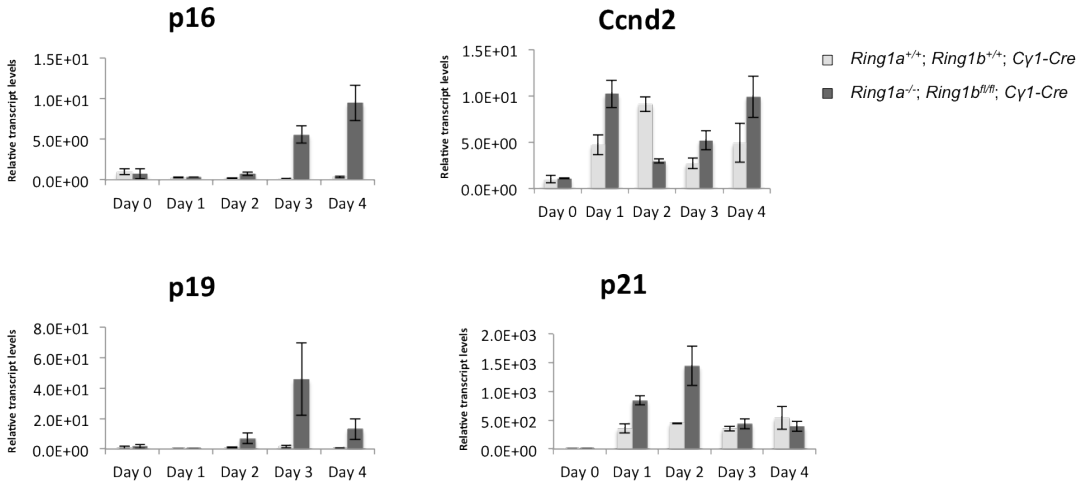

Figure 65. Loss of PRC1 de-regulates expression of cell cycle regulators *in vitro*.

Representative Q-PCR analysis of one of two independent experiments displaying aberrant modulation of cell cycle regulators following PRC1 loss *in vitro*. Cells were collected at the indicated time points following activation. Transcript levels were normalized using Rplp0 and expression levels of controls at day 0 of activation (*Ring1a*$^{+/+}$*;Ring1b*$^{+/+}$*;Cγ1-cre*, light gray bars). Mutant transcript levels are represented with dark grey bars. Error bars represent standard deviation across three technical replicates.

Together, this suggests on the one hand that PRC1 supports proliferation of GC B cells through the repression of Cdk inhibitors that regulate G1-to-S transition. On the other hand, transcripts coding for cyclin-D2 and -G1 were also increased in PRC1 mutant GC B cells and in iGB cultures (*Ccnd2* only), indicating a more complex regulation of the cell-cycle operated by *Ring1a/Ring1b* in GC B cells.

3.5.4. Bcl6 function is altered in PRC1 mutant GC B cells.

Among the genes up- regulated in PRC1 mutant GC B cells, we found several targets of the transcriptional repressor Bcl6, which is essential for GC B cell responses (Dent et al., 1997) (Ye et al., 1997) (Fukuda et al., 1997). These included genes coding for chemokine receptors (*Ccr7* and *Gpr183)*, cell-cycle regulators (*Cdkn1a*, *Cdkn1b*, *Cdkn2a*, and *Ccnd2*), developmental regulators (*Prmd1*, *Id2*) and modulators of survival/apoptosis (*Bcl2*) (Figure 66).

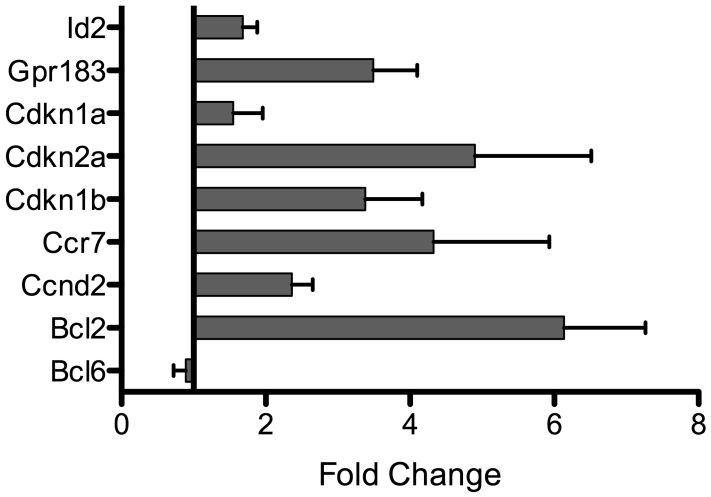

Figure 66. De-regulation of Bcl-6 target genes in GC B cells following loss of PRC1.

Q-PCR of transcript levels for the indicated genes in GC B cells sorted from 11 mutants and 11 control animals. Transcript levels were normalized using Rplp0. Genes were filtered based on number of samples where consistent up- or down-regulation was detected in >= 5 samples and if 0,5<FC>1,5. Bars represent mean values +/- SEM.

We tested the possibility that the reduction in GC B cell numbers observed in PRC1 conditional mutants was dependent on an impairment in Bcl6 expression and/or function. We quantified Bcl6 transcripts in PRC1 mutant GC B cells. RT-qPCR analyses revealed a modest yet reproducible reduction in *Bcl6* mRNA levels

in PRC1 mutant B cells (Figure 66). Since a substantial number of genes repressed by Bcl6 in GC B cells is also targeted by H3K27me3/PRC2 (Velichutina et al., 2010), we explored the possibility that PRC1 could contribute to Bcl6-mediated gene silencing. This hypothesis was supported by recent evidence showing that PRC1 can form a macromolecular complex with the Bcl6 co-repressor BCOR (Gearhart et al., 2006). Therefore, we tested whether PRC1 interacted directly with Bcl6 in the Bcl6-expressing A20 lymphoma cell line. To this aim, we performed immunoprecipitation assays with an anti-Ring1b antibody using protein extracts from A20 lymphoma cells. Immunoblotting analysis of immunoprecipitated material confirmed the interaction of Ring1b with BCOR, but failed to identify Bcl6 within the same complex (Figure 67). These results are compatible with a scenario in which PRC1 supports Bcl6 repressor activity through an indirect mechanism.

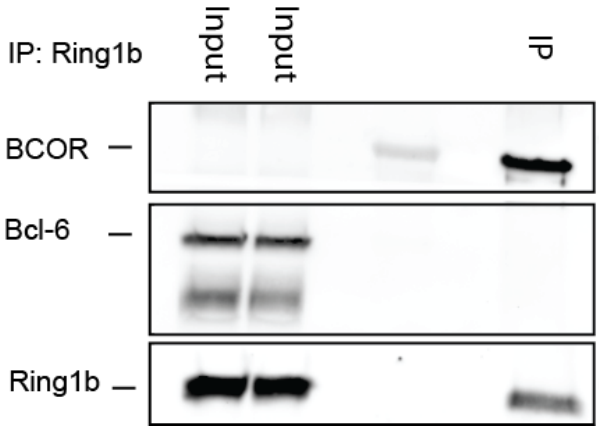

Figure 67. Ring1b and Bcl6 do not interact.

Immunoblot analysis of mmunoprecipitated material from the A20 cell line. Endogenous Ring1b was immunoprecipitated with 5 µg of anti-Ring1b antibody from 1 mg protein lysate obtained from A20 cells. The blot shown is representative of 3 independent experiments.

3.5.5. PRC1 regulates plasma cell differentiation onset

The ultimate goal of an immune response is the generation of terminally differentiated plasma cells that secrete neutralizing antibodies to mediate pathogen clearance. Plasma cells differentiate from GC B cells, but can also arise in a T cell-independent fashion. In the GC, PC differentiation is triggered in B cells that have undergone several rounds of proliferation and mutation of their Ig genes as a result of a stringent selection process (Victora et al., 2010). What prevents premature activation of the PC program in GC B cells remains yet poorly defined. We have recently identified through genome-wide mapping of H3K27me3 targets, the master regulator of PC development IRF4 as a target of H3K27me3/PRC2 in GC B cells (Caganova et al., 2013). In order to assess the contribution of *Ring1a* and *Ring1b* to the repression of Irf4 in GC B cells, the fraction of Irf4-expressing GC B cells in *Ring1a*$^{-/-}$*;Ring1b*$^{ff/fl}$*;Cd23-cre* and control animals immunized with NP-CGG was determined by FACS analysis. We found that PRC1 inactivation caused a substantial increase in the proportion of IRF4^{hi} GC B cells in comparison to controls (Figure 68 and Figure 69).

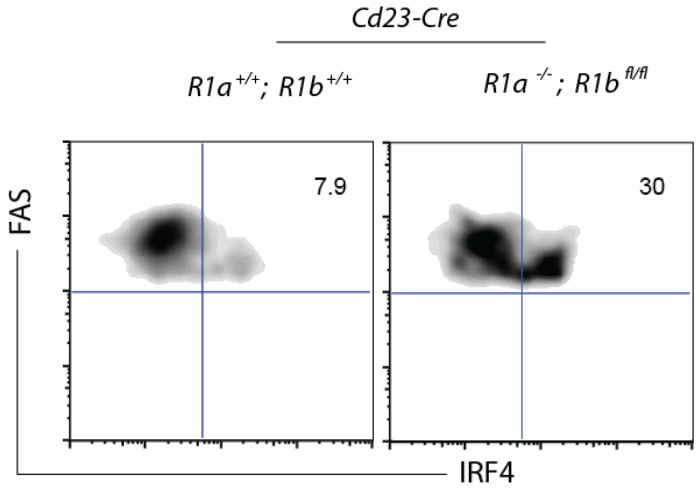

Figure 68. Absence of *Ring1a* and *Ring1b* accelerates plasma cell development.

Flow cytometric analysis of the fraction of Irf4^{hi} cells within the CD19^{+}CD38^{lo}FAS^{hi} GC compartment of control (left) and mutant (right) animals at day 14 post NP-CGG immunization. Data shown are representative of 14 independent experiments.

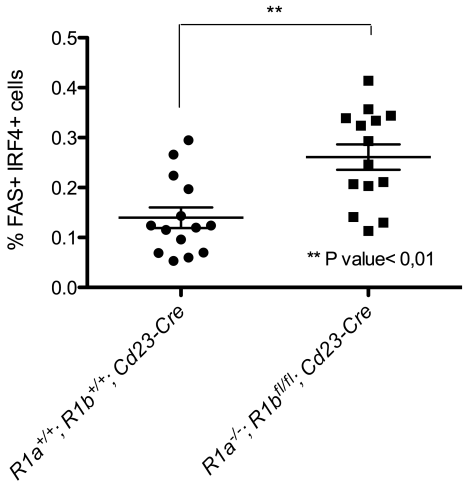

Figure 69. Increased fraction of Irf4-expressing cells in GCs of mutant animals.

The increase in Irf4 expression in PRC1 mutant GC B cells correlated with an up-regulation of transcripts for *Irf4* and for another determinant of plasma cell differentiation, namely *Prdm1/Blimp1* (Figure 70).

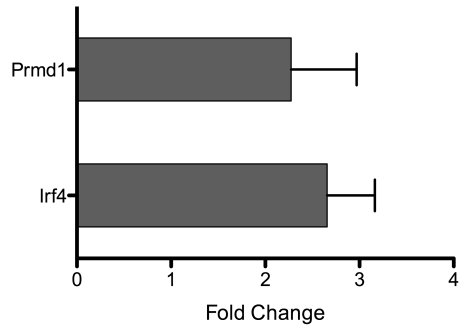

Figure 70. Loss of PRC1 in GC B cells leads to de-repression of plasma cell fate determinants.

Q-PCR of transcript levels for the indicated genes in GC B cells sorted from 11 mutants and 11 control animals. Transcript levels were normalized using Rplp0. Genes were filtered based on number of samples where consistent up- or down-regulation was detected in >= 5 samples and if 0,5<FC>1,5. Bars represent mean values +/- SEM.

These results suggest that in the absence of *Ring1a* and *Ring1b,* GC B cells activate prematurely the plasma cell program, hampering thereby their ability to persist within this compartment.

In order to monitor the early steps of PC differentiation under conditions of PRC1 deficiency, we performed *in vitro* stimulations with LPS +/- IL-4 of PRC1 control *(Ring1a$^{+/+}$;Ring1b$^{+/+}$;Cd23-cre*) and mutant *(Ring1a$^{-/-}$;Ring1b$^{ff/fl}$;Cd23-cre*) primary B cells to induce terminal differentiation. Upon stimulation with endotoxin, Ring1b protein levels increased between day 2 and day 3 of activation, which correlated with a substantial increase in the levels of H2AK119Ub (Figure 71).

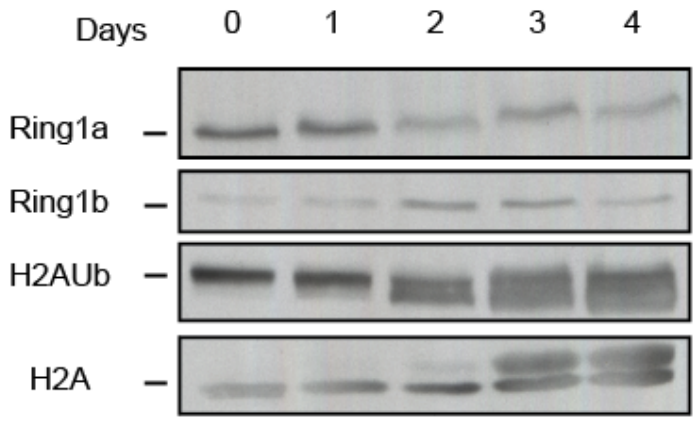

Figure 71. Expression of PRC1 members is modulated during B cell activation *in vitro*.

Immunoblot analysis of Ring1a, Ring1b and H2AK119Ub levels in $CD19^{+}$ splenic B cells isolated from C57/J animals. B cells were activated with LPS+IL-4 and harvested at the indicated time points. Data shown are representative of 3 independent experiments.

To assess the differentiation potential of PRC1 control and mutant B cells, flow cytometric analysis of LPS cultures was performed 3 days after stimulation. Strikingly, inactivation of PRC1 led to a substantial increase in the fraction of B cells that up-regulated the PC marker syndecan-1/CD138 (Figure 72 and Figure 73).

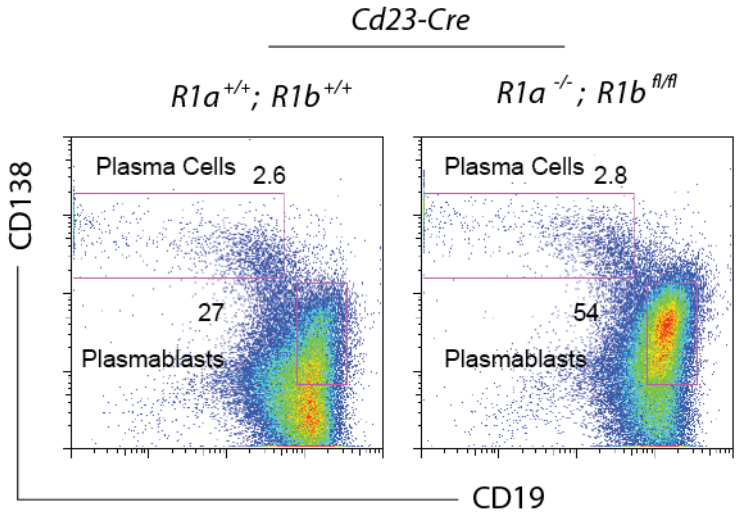

Figure 72. Premature appearance of CD138^{+} plasmablasts in LPS+IL-4-stimulated *Ring1a$^{-/-}$Ring1b$^{-/-}$* cultures.

Representative flow cytometric analysis displaying frequency of CD19^{+}CD138^{+} cells at day 3 following stimulation of purified naïve B cells with LPS +/- IL-4 in control (left) and mutant (right) animals. Data are representative of 7 independent experiments.

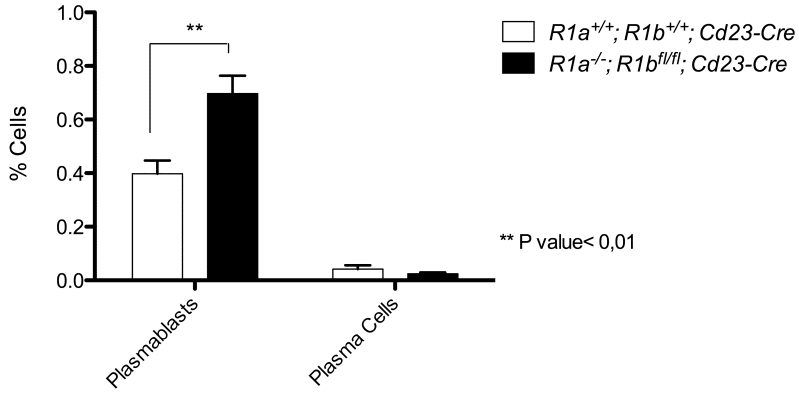

Figure 73. Frequency of plasmablasts and plasma cells upon *in vitro* stimulation of *Ring1a$^{-/-}$Ring1b$^{-/-}$* cells.

Frequency of CD138^{+} CD19^{+} plasmablasts and of CD138^{+} CD19^{lo} plasma cells at day 3 of LPS +/- IL-4 activation. Data are shown +/- SEM and are representative of 7 (plasmablasts) and 5 (plasma cells) independent experiments.

This was associated with increased expression in PRC1 mutant B cell cultures of *Irf4*, *Xbp1* and *Prmd1* transcription factors that are required for plasma cell development (Figure 74).

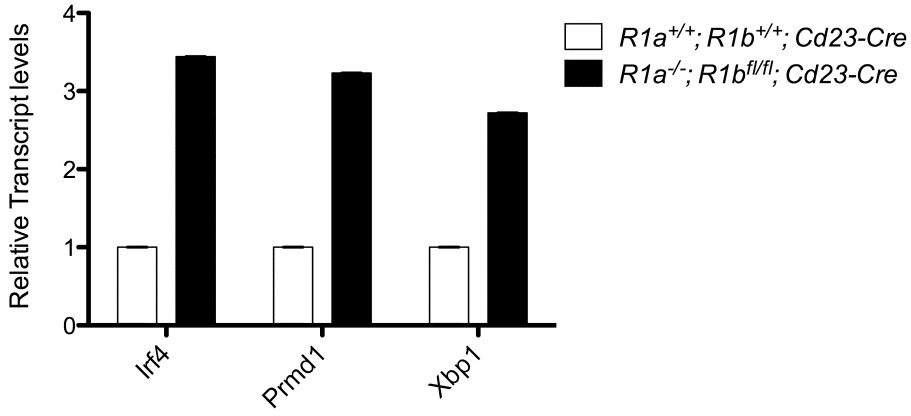

Figure 74. Increased expression of plasma cell master regulators in mutant cells activated with LPS and IL-4.

Q-PCR analsyis was performed on RNA extracted from cells at day 3 of LPS and IL-4 activation. Data are representative of 3 independent experiments and are presented as mean +/- SEM.

$CD138^+$ B cells in PRC1 mutant cultures retained expression of the pan-B cell marker and PAX-5 target CD19, representing thereby early plasmablasts. In contrast, the subset of $CD19^{lo}CD138^{hi}$ PCs was only marginally affected by PRC1 inactivation. These results indicate that loss of PRC1 facilitates onset of terminal B cell differentiation both *in vivo* and *in vitro*.

3.6. PRC1 is necessary to sustain PC function

Next, we assessed whether PRC1 inactivation affected plasma cell generation *in vivo*. To this end, we immunized control *(Ring1a$^{+/+}$;Ring1b$^{+/+}$;Cd23-cre*) and PRC1 conditional mutants *(Ring1a$^{-/-}$;Ring1b$^{ff/fl}$;Cd23-cre*) with alum-precipitated NP-CGG and assessed the fraction of splenic CD19^{lo}IRF4^{hi} cells generated 14 days later. Flow cytometric analyses revealed comparable frequencies of plasma cells in PRC1 mutant and control mice (Figure 75 and Figure 76).

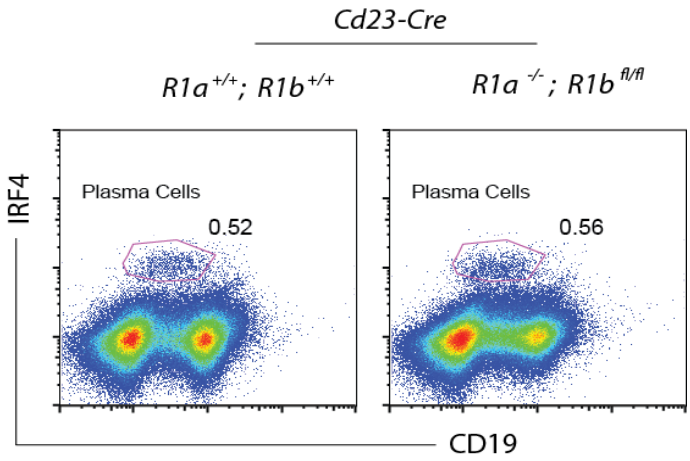

Figure 75. Plasma cells frequency in *Ring1a/Ring1b* mutants is comparable to that of controls.

Flow cytometric analysis displaying frequency of CD19^{+}IRF4^{+} cells at day 14 following NP-CGG immunization in control (left) and mutant (right) animals. Data are representative of 14 independent experiments.

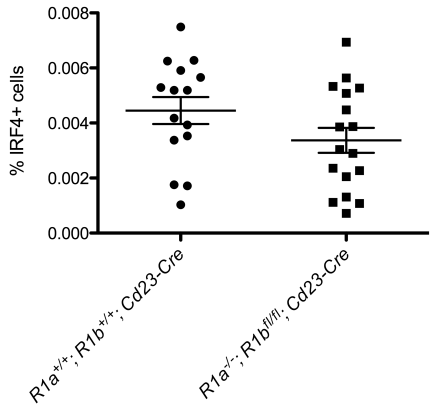

Figure 76. . Plasma cell frequency is not affected by loss of *Ring1a* and *Ring1b*.

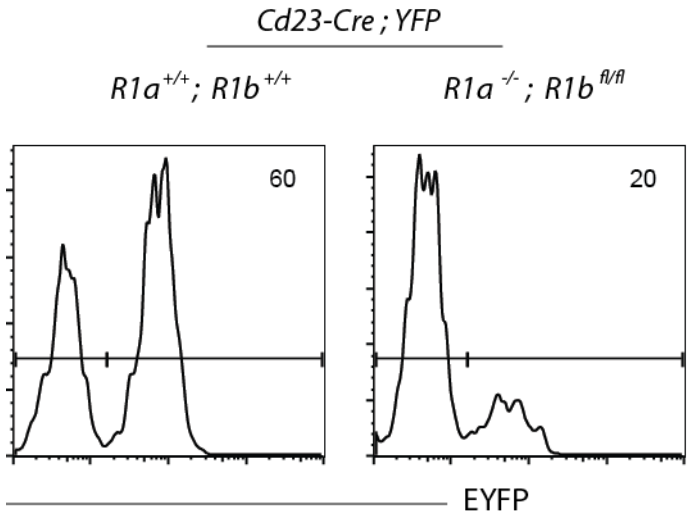

Figure 77. *Ring1a*$^{-/-}$*Ring1b*$^{-/-}$ plasma cells cells are counter-selected *in vivo*.

Histogram plot displaying frequency of EYFP-expressing cells within the plasma cell compartment in control (left) and mutant (right) animals. Data are representative of 3 independent experiments.

To address whether PCs in PRC1 conditional mutant mice had undergone Cre-mediated recombination at the *Ring1b* locus, I took advantage of the R26-EYFP Cre reporter allele. Specifically, we measured the frequency of YFP^{+} cells among CD19^{lo}IRF4^{hi} PCs in the spleen of PRC1 proficient (*Ring1a*$^{-/-}$*;Ring1b*$^{fl/+}$*;Cd23-cre*;*R26-EYFP)* and mutant (*Ring1a*$^{-/-}$*;Ring1b*$^{ff/fl}$*;Cd23-cre*;*R26-EYFP)* animals

after NP-CGG immunization. Strikingly, whereas most PCs expressed YFP in control animals, the counterparts in PRC1 mutants had to a large extent escaped Cre-mediated recombination (Figure 77). Counter-selection of PRC1 mutant cells within the plasma cell compartment was further confirmed by analysis of iGB cells induced to differentiate towards the plasma cell fate. Briefly, following a 4-day treatment, IL-4 was substituted with interleukin 21 (IL-21) in established iGB cultures, to induce plasma cell differentiation (Nojima et al., 2011).

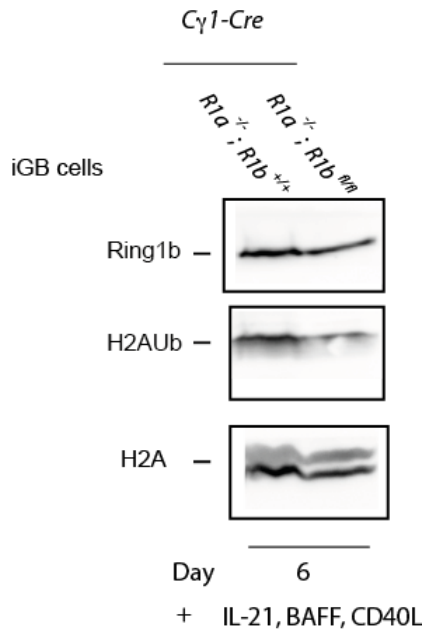

Figure 78. Counter-selection of *Ring1b* mutant cells upon induction of the plasma cell program.

Immunoblot analysis displaying levels of Ring1b and H2AK119Ub following induction of the plasma cell program through IL-21 stimulation of iGB cells established after 4 days of culture in the presence of IL-4.

Immunoblot analysis of iGB cells after 2 days of exposure to IL-21 showed a strong counter-selection of PRC1 mutant cells, with *Ring1b* proficient cells taking

over the culture (Figure 78). Together, *in vitro* and *in vivo* results indicate that PRC1 is required to sustain the developmental program that underlies the function of antibody-secreting plasma cells.

4. Discussion

This study has addressed the role of the catalytic subunits of PRC1, *Ring1a* and *Ring1b*, in B cell development and their contribution to adaptive B cell immune responses. Using a conditional gene targeting approach, we have initially explored the function of *Ring1b* in B lineage cells. Our lab could show that *Ring1b* inactivation alone had no detectable consequences on the development of B cells (L. D'Artista and S. Casola, unpublished data). In accordance with this, *Ring1b* mutant B cells had almost wild-type levels of H2AK119Ub, suggesting that *Ring1b* close homologue, *Ring1a*, may be the main catalytic subunit of PRC1 in B cells. However, *Ring1a* gene-targeted animals showed normal B cell development. This led us to hypothesize functional redundancy between Ring1a and Ring1b proteins in developing B cells. We addressed this possibility by generating compound $Ring1a^{-/-}Ring1b^{fl/fl}$ mutant animals crossed to *Cre* transgenic strains allowing PRC1 ablation at defined stages of B cell development. These experiments showed that concomitant ablation of *Ring1* proteins caused major defects at multiple stages of B cell differentiation.

4.1. PRC1 in early B cell development

PRC1 inactivation induced in pro-B cells by the *Mb1-cre* transgene caused a significant block in the transition from pro-B to the pre-B cells. Impairment in the transit through this differentiation step may reflect defective V(D)J recombination. A similar mechanism was described in *Ezh2* mutants, where defects in V_H gene rearrangements caused impaired transition from the pro- to the pre-B cell stage, resulting in a reduced peripheral B cell pool (Su et al., 2003). A causal relationship between defective IgH rearrangement and impairment in B cell production following loss of PcG is also supported by previous work carried out on *Bmi1*$^{-/-}$ animals in our lab (F. Alberghini and S. Casola, unpublished data). In these animals, the block in transition from the pro-B to the pre-B cell stage was substantially rescued by the expression of a pre-rearranged B1-8f Ig heavy chain in progenitor cells (Lam et al., 1997).

The early developmental block could also depend on the inability of *Ring1a/Ring1b* mutant progenitors to cope with DNA double strand breaks (DSBs) induced by RAG proteins during V(D)J recombination. Involvement of PRC1 members in DNA DSBs repair is supported by a number of studies reporting the presence of Polycomb members and repressive histone modifications including H2AK119Ub at sites of DNA breaks (Facchino et al., 2010) (Ismail et al., 2010) (Ginjala et al., 2011) (Chagraoui et al., 2011) (Chou et al., 2010). In these studies, early recruitment of PRC1 members Bmi1 and Ring1b followed by ubiquitination of histones H2A and H2AX was observed to promote DNA repair (Ismail et al., 2010). Supporting an important role for PcG proteins in DNA repair, absence of Polycomb members results in enhanced sensitivity to ionizing radiation and increased levels of spontaneous DNA breaks (Facchino et al., 2010) (Chagraoui et al., 2011) (Caganova et al., 2013). Together, this indicates an important role for PcG

proteins in DNA repair and supports a scenario whereby absence of PRC1 impairs B cell differentiation by preventing efficient repair of RAG-induced DNA DSBs. This is likely to result from de-repression of loci encoding the main cell cycle-dependent kinase (Cdk) inhibitors, which encode tumor suppressors that mediate cell cycle arrest, senescence and apoptosis (Fan et al., 2011) (Park et al., 2003) (Bruggeman et al., 2005) (Velichutina et al., 2010). This hypothesis is supported by a large body of evidence showing substantial rescue of PcG-deficient cells upon inactivation of the Polycomb target *Cdkn2a/* $p16^{INK4A}$/ $p19^{ARF}$ locus (Park et al., 2003) (Bruggeman et al., 2005). In support of this, our lab could recently show that the block in pro-B to the pre-B cell transition observed in $Ezh2^{-/-}$ animals is substantially relieved by concomitant inactivation of *Cdkn2a* (M. Caganova and S. Casola, unpublished data). To conclude, several mechanisms may account for the defects observed in PRC1 deficient progenitors. The partial recovery of the defects of Polycomb mutant B cell progenitors via inactivation of Cdk inhibitors or by-pass of V(D)J recombination suggests that PRC1 exerts a critical control at multiple levels to promote early B cell differentiation (M. Caganova and S. Casola, unpublished data and F. Alberghini and S. Casola, unpublished data).

4.2. PRC1 in peripheral B cell maturation

Since PRC1 function has remained largely unexplored in differentiated cells, this study focused primarily on the contribution of PRC1 in mature B cells before and after their encounter with a foreign antigen. Using the *Cd23-cre* mouse strain, we achieved over 90% efficiency of *Ring1b* inactivation starting from late transitional/immature B cells that also carried a *Ring1a* mutant allele. By studying resting B cells, we ruled out any effect of PRC1 inactivation on cell cycle

progression and addressed how PRC1 regulates peripheral B cell maturation in a cell autonomous fashion.

PRC1 inactivation in late transitional B cells had marginal effects on total B cell numbers in secondary lymphoid organs. Instead, it caused a substantial mis-regulation of surface markers on mutant B cells, pointing to a defect in their differentiation. Indeed, loss of PRC1 combined the immunophenotype of immature B cells, characterized by the expression of CD93/AA4.1, HSA/CD24 and high levels of CD95/FAS, with that of mature B cells featuring high levels of CD21 and BAFF-R expression. Moreover, mutant B cells were proficient in the homing to B cell follicles and formed a marginal zone in the spleen. In spite of the normal number and localization of *Ring1a/Ring1b* mutant peripheral B cells, the analysis of B cell development at different ages unveiled sustained bone marrow B cell production in aged *Ring1a/Ring1b* deficient animals as compared to controls. Such condition may represent a compensatory homeostatic mechanism responding to a shorter life- span of peripheral B cells, as previously observed in other mouse mutants showing defects in peripheral B cell development (Keren et al., 2011). Experiments to determine the life- span of PRC1 deficient B cells are ongoing at the moment. Importantly, recent evidence implicates *Ring1b* in the maintenance of the quiescent state characterizing mature lymphocytes. In their work, Frangini and colleagues unveil a previously unreported role for Ring1b as a transcriptional activator in a complex involving Bmi1 and the Aurora B kinase. In resting B cells, Ring1b was bound to a substantial number of transcriptionally active genes in combination with Aurora B, which contributed to inhibit Ring1b-dependent H2AK119Ub. Ring1b/Aurora B kinase targets included several genes necessary to help the survival of resting lymphocytes. These results have led to the hypothesis that Ring1b is necessary to support lymphocyte quiescence through the positive regulation of quiescence-associated genes (Frangini et al.,

2013). The extended B cell lymphopoiesis observed in *Ring1a/Ring1b* mutant mice sustains a model whereby PRC1 controls viability of quiescent mature B cells. On the other hand, in contrast to what described by Frangini and co-workers, the majority of differentially expressed genes were up- regulated in resting PRC1 mutant B cells. This result is in line with the function of PRC1 as a transcriptional repressor. Moreover, the comparison with genome-wide occupancy of H3K27me3 in peripheral B cells (C. Carrisi and S. Casola, unpublished data) revealed that 45% of the up-regulated genes in PRC1 mutant B cells were marked by H3K27me3, and thus target of PRC2. This suggests that close to half of the genes de-regulated in PRC1 mutant B cells represent *bona fide* Polycomb targets, which require PRC1 for stable repression. Genes de-regulated following PRC1 removal were enriched among Gene Ontology categories enriched for developmental regulators, in line with previous data obtained from analyses on Polycomb mutant ES and differentiated cells (Boyer et al., 2006) (Morey et al., 2013) (Ezhkova et al., 2011). In particular, we observed the substantial re-activation of genes expressed in stem and progenitor cells, including several members of the *Hox* gene family, and genes expressed in the neuronal lineage (Terunuma et al., 2004). Interestingly, *Ring1a/Ring1b* resting mutant B cells showed high transcript levels for *Hoxa9* and *Meis1*, which in myeloid progenitors is sufficient to induce malignant transformation (Kroon et al., 1998; Lawrence et al., 1999). Surprisingly, even aged PRC1 conditional mutant animals did not suffer from any form of B cell malignancy, indicating either that the oncogenic role of *Hoxa9/Meis1* is restricted to the myeloid lineage and/or that B cell transformation requires intact PRC1 activity.

In spite of the de-repression of lineage- and stage-inappropriate genes, PRC1 inactivation did not overtly affect B cell identity. PRC1 mutant $CD23^{+}$ B cells did neither revert to an earlier developmental stage nor suffered from trans-

differentiation to other lineages, as confirmed by the lack of expression of the Cre-reporter YFP allele in other hematopoietic lineages assessed in *Ring1a*$^{-/-}$*;Ring1b*$^{fl/fl}$*;Cd23-cre*;*R26-EYFP* compound mutants. These results are thus discordant with the substantial reprogramming of mature B cells undergoing conditional inactivation of the transcription factor *Pax5* (Cobaleda et al., 2007a).

In conclusion, results obtained so far suggest that PRC1 supports maintenance of peripheral B cells cell identity, but place its activity hierarchically downstream of TFs sustaining B cell identity such as *Pax5* (Cobaleda et al., 2007a).

4.3. PRC1 in immune responses

Next, we analyzed the effects of PRC1 inactivation on resting B cells upon their recruitment into an immune response after recognition of a T-cell dependent antigen. We employed the *Cg1-cre* transgene to specifically inactivate PRC1 in GC B cells. The striking counter-selection of *Ring1a/Ring1b* double mutant GC B cells indicated an essential role for PRC1 in these cells. This was confirmed in a second set of experiments in which the *Cγ1-cre* transgene was replaced by *Aicda-cre*. In the latter animals, the higher efficiency of Cre-mediated recombination compared to *Cγ1-cre* led to a significant loss of GC B cell numbers in secondary lymphoid organs of immunized mice. Similar results were also observed in compound mutants in which PRC1 was deleted using the *Cd23-cre* transgene in pre-GC B cells. In accordance with the observed defect in GC formation, PRC1 conditional mutant mice displayed impaired primary antibody responses following immunization with the T cell-dependent antigen NP-CGG. In addition, *Ring1a/Ring1b* inactivation led to a severe impairment in memory B cell formation, as revealed by the reduction in antigen-specific IgG1^{+} B cells two weeks following

primary immunization. A defect in B cell memory differentiation was confirmed by the failure of PRC1 mutant animals to produce high-affinity antigen-specific antibodies in recall immune responses. To investigate the mechanisms involved in the reduction in GC B cells, we investigated the effects of *Ring1a/Ring1b* loss on apoptosis, proliferation and differentiation of GC B cells. The detection of an increased fraction of GC B cells expressing active forms of caspase(s) indicated a higher susceptibility of PRC1 mutant GC B cells to programmed cell death. We hypothesized that PRC1 inactivation sensitized cells to mitochondrial apoptosis. Therefore, we investigated the expression of the *Noxa/Mcl1* axis, which is the major regulator of GC B cell apoptosis (Vikstrom et al., 2010). Loss of PRC1 activity failed to up-regulate *Pmaip1/Noxa*. Moreover, quite surprisingly, we consistently detected increased levels of *Mcl-1* transcripts in *Ring1a/Ring1b* double mutant GC B cells. Therefore, these results seem to exclude a contribution of mitochondrial apoptosis in the death of PRC1 defective GC B cells. Increased apoptosis may also be brought about by inability of the cells to cope with genotoxic damage. Several recent studies have shown that PRC1 components are rapidly recruited to sites of DNA breaks, where they contribute to the repair process (Ginjala et al., 2011) (Ismail et al., 2010). Thus, it is possible that GC B cells lacking PRC1 acquire increased sensitivity to genotoxic stress. A likely candidate for the induction of genotoxic damage in GC B cells is AID. Here, upon onset of Ig class switch recombination, AID is recruited to the IgH locus, where it promotes the accumulation of DNA DSBs at high frequency. This allows the replacement of the Cμ constant region coding sequence with that of another isotype though a process that is primarily mediated by non-homologous end joining proteins (Xu et al., 2012). Loss of PRC1 may impair the repair of DNA breaks at IgH constant region genes, ultimately causing the death of the cells. In support of this hypothesis, *in vitro* Ig CSR assays revealed a smaller percentage of Ig switched B

cells in PRC1 mutant cultures. Moreover, heightened apoptosis of PRC1 deficient B cells was primarily observed under culture conditions, such as LPS stimulation, when AID is strongly induced. In contrast, stimulation of PRC1 mutant B cells with mitogens that fail to induce AID expression (such as stimulation through the Toll-like receptor RP-105) had minor effects on their death (Ogata et al., 2000). A genetic proof for the role AID in the induction of apoptosis of Polycomb mutant cells has recently come from our laboratory studying the effects of *Ezh2* inactivation on GC B cells (Caganova et al., 2013). Inactivation of *Ezh2* in GC B cells led to a significant increase in the fraction of apoptotic cells. Such phenotype was fully normalized by concomitant inactivation of AID. The involvement of AID in the acquired sensitivity of Polycomb mutant GC B cells may also result from excessive recruitment of the deaminase to genomic off-target sites. Indeed, previous work has shown that AID recruitment is favored by the presence of epigenetic marks associated to active transcription such as H3K4me3. In contrast, genome-wide recruitment of AID is limited by the presence of repressive histone marks such as H3K27me3 (Yamane et al., 2011). It remains to be seen whether PRC1 and its associated repressive mark H2AK119Ub may contribute to prevent/limit genome-wide AID attack.

The impairment in GC B cell responses resulting from PRC1 inactivation may also stem from proliferation defects. Given the technical limitations associated with the analysis of PRC1 mutant GC B cells *in vivo*, due to their strong counter-selection, we took advantage of a recently developed *in vitro* culture system to generate GC B-like (iGB) cells from primary resting $CD19^{+}$ splenic B cells after activation with membrane-bound CD40L, BAFF and IL-4 (Nojima et al., 2011). Under these experimental conditions, we achieved acute *in vitro* PRC1 inactivation in activated *Ring1a*$^{-/-}$; *Ring1b*$^{fl/fl}$*; Cγ1-cre* B cells. Cell cycle distribution analysis of CD40-stimulated PRC1 mutant B cells revealed a prominent defect in the G1-to-S

transition. In search of the mechanisms underlying the observed phenotypes, we measured the expression of several cell-cycle regulators in PRC1 proficient and mutant B cell cultures. Concomitant loss of *Ring1a* and *Ring1b* in CD40-activated B cells led to the consistent up-regulation of Cdk inhibitors $p16^{INK4A}$ and $p21^{CIP1}$, which are known Polycomb targets. Our lab has recently shown that $p16^{INK4A}$ encoded by the *Cdkn2a* locus is not responsible for the G1-to-S transition defect observed in activated B cells lacking *Ezh2*. Indeed, the numbers of GC B cells and the proliferative defects observed in *in vitro*- generated iGB cells lacking functional *Ezh2* could not be rescued by concomitant loss of *Cdkn2a (Caganova et al., 2013)*. Along the same line, despite the up-regulation of $p21^{CIP1}$ detected in both PRC1 and *Ezh2* mutant GC B cells, *Cdkn1a* transcripts remained unaltered in G_0/G_1 arrested *Ezh2* mutant iGB cells (Caganova et al., 2013). The latter result is in contrast with recent work by the Melnick group that showed a partial rescue in the proliferation defects of *Ezh2*-inhibited human B lymphoma cells following *p21* knock-down(Beguelin et al., 2013). All together, these results point to additional contributions made by PRC1 in the regulation of S-phase entry in B cells.

A defect in G1-to-S transition may result from the interference with the function of the E2F family of transcription factors (Wu et al., 2001). *Ezh2* is a downstream target of E2F transcriptional activity required for cell proliferation (Bracken et al., 2003). Importantly, a master regulatory analysis recently performed in our lab on genes down-regulated in PRC1 mutant resting B cells revealed a significant enrichment for an *E2f1* gene signature (F. Alberghini, F. Zanardi, S. Casola, data not shown). In a similar fashion, a gene signature associated with *E2f2* function, which exerts a negative regulation on cell-cycle progression (Infante et al., 2008) was enriched among the genes up-regulated in PRC1 mutant B cells.

The loss of GC B cells following acute PRC1 inactivation could also be contributed by uncoordinated activation of developmental programs underlying the exit of B

cells from the GC. This could result from a premature activation of the plasma cell program and/or by interference with the activities of transcriptional repressors such as Bcl6 that sustain the GC B cell response (Fukuda et al., 1997). To this end, we quantified mRNA levels for transcription factors playing a crucial role in terminal B cell differentiation. Inactivation of PRC1 in GC B cells led to a consistent up-regulation of *Blimp1* and Irf4, which represent major determinants of plasma cell (PC) development (Shapiro-Shelef et al., 2003) (Klein et al., 2006). To have a closer look at the initial stages of PC development in the absence of PRC1, we performed *in vitro* LPS stimulation assays. Loss of *Ring1a/Ring1b* caused a substantial increase in the fraction of $CD19^{+}CD138^{+}$ plasma blasts generated after endotoxin stimulation. Similarly to what had been observed in GC B cells, *in vitro*-activated PRC1 mutant B cells showed substantial higher expression of *Blimp1* and *Irf4*. The finding that *Irf4* and *Blimp1* loci are marked by H3K27me3 in both mouse and human GC B cells (Caganova et al., 2013) supports a scenario whereby Ezh2 controls onset of PC differentiation in GCs by directly regulating the expression of PC lineage determinants. Similar results were confirmed by our group and by Melnick and colleagues analyzing human Diffuse Large B lymphoma cell lines after treatment with a highly specific small molecule inhibitor to Ezh2 (Beguelin et al., 2013; Caganova et al., 2013). The observation that, similarly to *Ezh2* inhibition, *Ring1a/Ring1b* inactivation facilitated PC differentiation strongly argues for the coordinated activity of PRC1 and PRC2 in the temporal control of GC B cell differentiation.

Lastly, PRC1 may sustain the persistence of B cells within the GC by supporting the repressor activity of the GC B cell master regulator Bcl6. This hypothesis is supported by the observation that several genes that were de-regulated in PcG mutant B cells are highly significant Bcl6 targets (*Ccr7*, *Gpr183*, *Cdkn1a*, *Cdkn1b*, *Cdkn2a*, *Ccnd2, Prmd1*, *Id2* and *Bcl2)* (Basso et al., 2010). We hypothesized that

PRC1 could directly interact with Bcl6 to support its repressor function in GC B cells. To address this, we performed immunoprecipitation assays using protein extracts from GC-derived A20 B lymphoma cells. These studies failed to detect physical interaction between PRC1 and Bcl6, supporting a model whereby PRC1 influences indirectly the repression by Bcl6 on common targets. Indeed, recent work has identified the Bcl6 co-repressor BCOR as an essential component of PRC1 (Gao et al., 2012) (Gearhart et al., 2006) (Sanchez et al., 2007). Future studies will reveal the degree of overlap between Bcl6 and PRC1 targets and which of them requires the interaction between Bcl6 and BCOR for stable repression (Huang et al., 2013). The functional relationship between Polycomb- and Bcl6-mediated gene silencing is supported by recent work by our group and others showing a substantial degree of overlap between H3K27me3/Ezh2 and Bcl6 targets in both human and mouse GC B cells (Caganova et al., 2013) (Velichutina et al., 2010). Moreover, we could show that Ezh2 is required to sustain Bcl6 repressive activity (but not its expression) in GC B cells (Caganova et al., 2013).

4.4. PRC1 in B cell terminal differentiation

In spite of the facilitated onset of plasma cell differentiation, the generation of *bona fide* antibody-secreting $CD19^{lo}CD138^{+}$ PCs was impaired in the absence of PRC1 both *in vitro* and *in vivo* after immunization with a T-cell dependent antigen. These results suggest that PRC1 exerts a dual role during terminal differentiation. In GC B cells, PRC1 prevents premature activation of the PC program, possibly through a direct repression of *Blimp1* and *Irf4* expression. Once PCs are generated, PRC1 is required to sustain their function. This may be achieved by guaranteeing stable repression of B-cell specific genes and those expressed in other lineages. This

hypothesis is supported by the frequent dysregulation of lineage-inappropriate genes when PcG function is inhibited (Ezhkova et al., 2009) (Ezhkova et al., 2011). Inactivation of *Ring1a/Ring1b* in B cells also had a major impact on the generation of long-lived memory B cells. The loss of memory B cells resulting from inactivation of PRC1 in pre-GC B cells (using the *Cd23-cre* transgene) or in the vast majority of GC B cells (*Aicda-cre*) is likely the consequence of the disaggregation of the GC reaction. Instead, using the *Cg1-cre* transgene, which allowed the preferential outgrowth of GC B cells that retained PRC1 function, we could determine the effects of PRC1 inactivation in newly generated IgG1-switched memory B cells. Loss of PRC1 almost completely abolished the pool of long-lived antigen-specific IgG1 memory B cells, highlighting an essential contribution of *Ring1a/Ring1b* to memory B cell maintenance.

Together, data presented in this PhD thesis indicate that PRC1 is critical at multiple stages of B cell differentiation, affecting both cycling and resting B cell subsets. Phenotypes observed from the analysis of conditional PRC1 mutant mice are to a large extent overlapping with those observed in mutants for *Ezh2*, the main catalytic subunit of PRC2. These results are in agreement with the model based on concerted activity of the two PRCs in ensuring transcriptional silencing of the majority of their targets. Our data also suggest that deposition of H3K27me3 alone is not sufficient to achieve heritable gene repression, which is strictly dependent on the over imposing activity of PRC1.

Acknoledgements

I would like to thank all the people without whom this work wouldn't have been possible:

Our collaborators Dr. Miguel Angel Vidal Caballero and Dr. Haruhiko Koseki for sharing Ring1b^{fl} animals.

Federica Mainoldi, for the ELISA analysis and assistance with the iGB culture.

Federica Pisati, for patiently teaching me how to perform and analyse immunofluorescent and immunohistochemical assays.

Federica Zanardi, for the bioinformatical analyses.

Marieta Caganova, for the help that she gave me and important contributions to the work presented in this thesis.

I would like to thank the people from the IFOM-IEO Campus facilities, who support everyday's work with their skill and expertise:

Mouse facility (Alberto Gobbi, Manuela Capillo)

Sorting facility- past and present members (Simona Ronzoni, Lorenzo Raeli, Anna Sciullo, Elisa Zatta, Sara Martone)

Imaging facility (Dario Parazzoli, Amanda Oldani, Rocco D Antuono)

Microarray facility (Gabriele Bucci)

DNA sequencing facility (Milena Ficarazzi)

Real Time PCR facility (Valentina Dall'olio)

Cell culture facility

I would like to thank all the people I have met so far and who supported me during my academic career:

Dr. Heinz Jacobs and Dr. Peter Krjiger for their enthusiasm and for making me discovery immunology, research and The Netherlands in the best possible way.

Dr. Karòli Szhuai and Dr. Asta Björk Jonsdòttir, for teaching me immunofluorescence and for the beautiful time I had during the time spent in their laboratory.

I would like to thank all the SCAs for their invaluable support, for making everyday life in the lab fun and for their help, which is provided whenever needed. So, thank you Gabriele, Federica M., Federica Z., Mahshid, Valentina, Chiara, Giulia and Rashmi.

I would also like to thank all the people in Lab F, in particular Valentina De Lorenzi and Gian Maria Sarra-Ferraris, for their friendship and help with the immuno-precipitation experiments.

I also thank:

My co-supervisors for useful help and suggestions: Dr. Gioacchino Natoli and Prof. Matthias Merkenschlager for scientific discussions and support;

My examiners Dr. Diego Pasini and Dr. Marc Schmidt-.Supprian for reading my thesis and for their evaluation and comments.

I address the biggest “THANK YOU” to my supervisor, Dr. Stefano Casola, for his curiosity, his criticism, his never-ending enthusiasm, and for the LONG and fruitful

discussions that paved the ground for this work. I thank him for supporting this PhD work with his positive thinking and his intuition.

Agnese, Vale, thank you. During the past years, your friendship helped me through difficult times and rejoiced every moment. Our evenings together, our lunches, our shopping expeditions and eating marathons (Vale ☺) have added inestimable value to these years.

Family, thank you all. Mum, dad, sister. This thesis is yours as much as it is mine. Thank you for being a shelter and providing me with a safe harbor in difficult times. Thank you for supporting all my endeavors, and for your never-ending faith in me. Mum, thank you for the LONG and numerous calls of all these years and for your listening and advice. Dad, thank you for your love, your protection and because you'd turn the world upside down for me. Sister, thank you for your laughter and for all the fun we have together. You always find a way to make me smile, and that helps more than a 1000 words.

Famiglia, grazie a tutti. Mamma, papà, sorella. Questa tesi è tanto vostra quanto mia. Grazie, perchè siete il mio porto sicuro in tempi difficili, e so di poter sempre contare su di voi. Grazie per aver supportato le mie azioni e le mie scelte, e per la vostra infinita fiducia in me. Mamma, grazie per le LUNGHE e numerose chiamate di questi anni, per il tuo ascolto e I tuoi consigli. Papà, grazie per il tuo amore per me, perchè mi proteggi e rivolteresti il mondo per me. Sorella, grazie per le tue risate e per quanto ci divertiamo insieme. Trovi sempre un sistema per farmi sorridere, e questo spesso aiuta più di mille parole.

Thank you, Enrico. Your love and care sustained me all along and pervade everything. Thank you for giving me strength when mine is not enough, and for supporting and encouraging every step I take. Thank you for your silent help, and for your never-ending patience. Thank you for staying by my side despite knowing me so well ;). Thank you for all the happiness and light you have brought in my life.

Reference List

Adolfsson, J., Borge, O.J., Bryder, D., Theilgaard-Monch, K., Astrand-Grundstrom, I., Sitnicka, E., Sasaki, Y., and Jacobsen, S.E. (2001). Upregulation of Flt3 expression within the bone marrow Lin(-)Sca1(+)c-kit(+) stem cell compartment is accompanied by loss of self-renewal capacity. Immunity *15*, 659-669.

Adolfsson, J., Mansson, R., Buza-Vidas, N., Hultquist, A., Liuba, K., Jensen, C.T., Bryder, D., Yang, L., Borge, O.J., Thoren, L.A.*, et al.* (2005). Identification of Flt3+ lympho-myeloid stem cells lacking erythro-megakaryocytic potential a revised road map for adult blood lineage commitment. Cell *121*, 295-306.

Agherbi, H., Gaussmann-Wenger, A., Verthuy, C., Chasson, L., Serrano, M., and Djabali, M. (2009). Polycomb mediated epigenetic silencing and replication timing at the INK4a/ARF locus during senescence. PLoS One *4*, e5622.

Akasaka, T., Tsuji, K., Kawahira, H., Kanno, M., Harigaya, K., Hu, L., Ebihara, Y., Nakahata, T., Tetsu, O., Taniguchi, M.*, et al.* (1997). The role of mel-18, a mammalian Polycomb group gene, during IL-7-dependent proliferation of lymphocyte precursors. Immunity *7*, 135-146.

Allman, D., Lindsley, R.C., DeMuth, W., Rudd, K., Shinton, S.A., and Hardy, R.R. (2001a). Resolution of three nonproliferative immature splenic B cell subsets reveals multiple selection points during peripheral B cell maturation. J Immunol *167*, 6834-6840.

Allman, D., Lindsley, R.C., DeMuth, W., Rudd, K., Shinton, S.A., and Hardy, R.R. (2001b). Resolution of three nonproliferative immature splenic B cell subsets reveals multiple selection points during peripheral B cell maturation. J Immunol *167*, 6834-6840.

Allman, D.M., Ferguson, S.E., and Cancro, M.P. (1992). Peripheral B cell maturation. I. Immature peripheral B cells in adults are heat-stable antigenhi and exhibit unique signaling characteristics. J Immunol *149*, 2533-2540.

Allman, D.M., Ferguson, S.E., Lentz, V.M., and Cancro, M.P. (1993). Peripheral B cell maturation. II. Heat-stable antigen(hi) splenic B cells are an immature developmental intermediate in the production of long-lived marrow-derived B cells. J Immunol *151*, 4431-4444.

Alugupalli, K.R., Leong, J.M., Woodland, R.T., Muramatsu, M., Honjo, T., and Gerstein, R.M. (2004). B1b lymphocytes confer T cell-independent long-lasting immunity. Immunity *21*, 379-390.

Angelin-Duclos, C., Cattoretti, G., Lin, K.I., and Calame, K. (2000). Commitment of B lymphocytes to a plasma cell fate is associated with Blimp-1 expression in vivo. J Immunol *165*, 5462-5471.

Arpin, C., Dechanet, J., Van Kooten, C., Merville, P., Grouard, G., Briere, F., Banchereau, J., and Liu, Y.J. (1995). Generation of memory B cells and plasma cells in vitro. Science *268*, 720-722.

Attwooll, C., Oddi, S., Cartwright, P., Prosperini, E., Agger, K., Steensgaard, P., Wagener, C., Sardet, C., Moroni, M.C., and Helin, K. (2005). A novel repressive E2F6 complex containing the polycomb group protein, EPC1, that interacts with EZH2 in a proliferation-specific manner. J Biol Chem *280*, 1199-1208.

Basso, K., and Dalla-Favera, R. (2010). BCL6: master regulator of the germinal center reaction and key oncogene in B cell lymphomagenesis. Adv Immunol *105*, 193-210.

Basso, K., Saito, M., Sumazin, P., Margolin, A.A., Wang, K., Lim, W.K., Kitagawa, Y., Schneider, C., Alvarez, M.J., Califano, A.*, et al.* (2010). Integrated biochemical and computational approach identifies BCL6 direct target genes controlling multiple pathways in normal germinal center B cells. Blood *115*, 975-984.

Beguelin, W., Popovic, R., Teater, M., Jiang, Y., Bunting, K.L., Rosen, M., Shen, H., Yang, S.N., Wang, L., Ezponda, T.*, et al.* (2013). EZH2 is required for germinal center formation and somatic EZH2 mutations promote lymphoid transformation. Cancer Cell *23*, 677-692.

Berland, R., and Wortis, H.H. (2003). Normal B-1a cell development requires B cell-intrinsic NFATc1 activity. Proc Natl Acad Sci U S A *100*, 13459-13464.

Bernstein, B.E., Mikkelsen, T.S., Xie, X., Kamal, M., Huebert, D.J., Cuff, J., Fry, B., Meissner, A., Wernig, M., Plath, K.*, et al.* (2006). A bivalent chromatin structure marks key developmental genes in embryonic stem cells. Cell *125*, 315-326.

Bloyer, S., Cavalli, G., Brock, H.W., and Dura, J.M. (2003). Identification and characterization of polyhomeotic PREs and TREs. Dev Biol *261*, 426-442.

Bossen, C., and Schneider, P. (2006). BAFF, APRIL and their receptors: structure, function and signaling. Semin Immunol *18*, 263-275.

Bouillet, P., Metcalf, D., Huang, D.C., Tarlinton, D.M., Kay, T.W., Kontgen, F., Adams, J.M., and Strasser, A. (1999). Proapoptotic Bcl-2 relative Bim required for certain apoptotic responses, leukocyte homeostasis, and to preclude autoimmunity. Science *286*, 1735-1738.

Boyer, L.A., Lee, T.I., Cole, M.F., Johnstone, S.E., Levine, S.S., Zucker, J.P., Guenther, M.G., Kumar, R.M., Murray, H.L., Jenner, R.G., *et al.* (2005). Core transcriptional regulatory circuitry in human embryonic stem cells. Cell *122*, 947-956.

Boyer, L.A., Plath, K., Zeitlinger, J., Brambrink, T., Medeiros, L.A., Lee, T.I., Levine, S.S., Wernig, M., Tajonar, A., Ray, M.K., *et al.* (2006). Polycomb complexes repress developmental regulators in murine embryonic stem cells. Nature *441*, 349-353.

Bracken, A.P., Pasini, D., Capra, M., Prosperini, E., Colli, E., and Helin, K. (2003). EZH2 is downstream of the pRB-E2F pathway, essential for proliferation and amplified in cancer. Embo J *22*, 5323-5335.

Brown, J.L., Mucci, D., Whiteley, M., Dirksen, M.L., and Kassis, J.A. (1998). The Drosophila Polycomb group gene pleiohomeotic encodes a DNA binding protein with homology to the transcription factor YY1. Mol Cell *1*, 1057-1064.

Bruggeman, S.W., Valk-Lingbeek, M.E., van der Stoop, P.P., Jacobs, J.J., Kieboom, K., Tanger, E., Hulsman, D., Leung, C., Arsenijevic, Y., Marino, S., *et al.* (2005). Ink4a and Arf differentially affect cell proliferation and neural stem cell self-renewal in Bmi1-deficient mice. Genes Dev *19*, 1438-1443.

Caganova, M., Carrisi, C., Varano, G., Mainoldi, F., Zanardi, F., Germain, P.L., George, L., Alberghini, F., Ferrarini, L., Talukder, A.K., *et al.* (2013). Germinal center dysregulation by histone methyltransferase EZH2 promotes lymphomagenesis. The Journal of clinical investigation.

Cales, C., Roman-Trufero, M., Pavon, L., Serrano, I., Melgar, T., Endoh, M., Perez, C., Koseki, H., and Vidal, M. (2008). Inactivation of the polycomb group protein Ring1B unveils an antiproliferative role in hematopoietic cell expansion and cooperation with tumorigenesis associated with Ink4a deletion. Mol Cell Biol *28*, 1018-1028.

Calfon, M., Zeng, H., Urano, F., Till, J.H., Hubbard, S.R., Harding, H.P., Clark, S.G., and Ron, D. (2002). IRE1 couples endoplasmic reticulum load to secretory capacity by processing the XBP-1 mRNA. Nature *415*, 92-96.

Campisi, J., and d'Adda di Fagagna, F. (2007). Cellular senescence: when bad things happen to good cells. Nature reviews Molecular cell biology *8*, 729-740.

Caretti, G., Di Padova, M., Micales, B., Lyons, G.E., and Sartorelli, V. (2004). The Polycomb Ezh2 methyltransferase regulates muscle gene expression and skeletal muscle differentiation. Genes Dev *18*, 2627-2638.

Cariappa, A., Boboila, C., Moran, S.T., Liu, H., Shi, H.N., and Pillai, S. (2007). The recirculating B cell pool contains two functionally distinct, long-lived, posttransitional, follicular B cell populations. J Immunol *179*, 2270-2281.

Casanova, M., Preissner, T., Cerase, A., Poot, R., Yamada, D., Li, X., Appanah, R., Bezstarosti, K., Demmers, J., Koseki, H.*, et al.* (2011). Polycomblike 2 facilitates the recruitment of PRC2 Polycomb group complexes to the inactive X chromosome and to target loci in embryonic stem cells. Development *138*, 1471-1482.

Casola, S. (2007). Control of peripheral B-cell development. Curr Opin Immunol *19*, 143-149.

Casola, S., Cattoretti, G., Uyttersprot, N., Koralov, S.B., Seagal, J., Hao, Z., Waisman, A., Egert, A., Ghitza, D., and Rajewsky, K. (2006). Tracking germinal center B cells expressing germ-line immunoglobulin gamma1 transcripts by conditional gene targeting. Proc Natl Acad Sci U S A *103*, 7396-7401.

Casola, S., Otipoby, K.L., Alimzhanov, M., Humme, S., Uyttersprot, N., Kutok, J.L., Carroll, M.C., and Rajewsky, K. (2004). B cell receptor signal strength determines B cell fate. Nature immunology *5*, 317-327.

Cattoretti, G., Pasqualucci, L., Ballon, G., Tam, W., Nandula, S.V., Shen, Q., Mo, T., Murty, V.V., and Dalla-Favera, R. (2005). Deregulated BCL6 expression recapitulates the pathogenesis of human diffuse large B cell lymphomas in mice. Cancer Cell *7*, 445-455.

Chagraoui, J., Hebert, J., Girard, S., and Sauvageau, G. (2011). An anticlastogenic function for the Polycomb Group gene Bmi1. Proc Natl Acad Sci U S A *108*, 5284-5289.

Chang, S.K., Arendt, B.K., Darce, J.R., Wu, X., and Jelinek, D.F. (2006). A role for BLyS in the activation of innate immune cells. Blood *108*, 2687-2694.

Chang, S.K., Mihalcik, S.A., and Jelinek, D.F. (2008). B lymphocyte stimulator regulates adaptive immune responses by directly promoting dendritic cell maturation. J Immunol *180*, 7394-7403.

Chou, D.M., Adamson, B., Dephoure, N.E., Tan, X., Nottke, A.C., Hurov, K.E., Gygi, S.P., Colaiacovo, M.P., and Elledge, S.J. (2010). A chromatin localization screen reveals poly (ADP ribose)-regulated recruitment of the repressive polycomb and NuRD complexes to sites of DNA damage. Proc Natl Acad Sci U S A *107*, 18475-18480.

Chung, J.B., Sater, R.A., Fields, M.L., Erikson, J., and Monroe, J.G. (2002). CD23 defines two distinct subsets of immature B cells which differ in their responses to T cell help signals. Int Immunol *14*, 157-166.

Cinamon, G., Zachariah, M.A., Lam, O.M., Foss, F.W., Jr., and Cyster, J.G. (2008). Follicular shuttling of marginal zone B cells facilitates antigen transport. Nature immunology *9*, 54-62.

Cobaleda, C., Jochum, W., and Busslinger, M. (2007a). Conversion of mature B cells into T cells by dedifferentiation to uncommitted progenitors. Nature *449*, 473-477.

Cobaleda, C., Schebesta, A., Delogu, A., and Busslinger, M. (2007b). Pax5: the guardian of B cell identity and function. Nat Immunol *8*, 463-470.

Crabtree, G.R., and Olson, E.N. (2002). NFAT signaling: choreographing the social lives of cells. Cell *109 Suppl*, S67-79.

Crouch, E.E., Li, Z., Takizawa, M., Fichtner-Feigl, S., Gourzi, P., Montano, C., Feigenbaum, L., Wilson, P., Janz, S., Papavasiliou, F.N.*, et al.* (2007). Regulation of AID expression in the immune response. J Exp Med *204*, 1145-1156.

Crowley, J.E., Scholz, J.L., Quinn, W.J., 3rd, Stadanlick, J.E., Treml, J.F., Treml, L.S., Hao, Y., Goenka, R., O'Neill, P.J., Matthews, A.H.*, et al.* (2008). Homeostatic control of B lymphocyte subsets. Immunol Res *42*, 75-83.

Cui, K., Zang, C., Roh, T.Y., Schones, D.E., Childs, R.W., Peng, W., and Zhao, K. (2009). Chromatin signatures in multipotent human hematopoietic stem cells indicate the fate of bivalent genes during differentiation. Cell Stem Cell *4*, 80-93.

d'Adda di Fagagna, F. (2008). Living on a break: cellular senescence as a DNA-damage response. Nat Rev Cancer *8*, 512-522.

Darce, J.R., Arendt, B.K., Wu, X., and Jelinek, D.F. (2007). Regulated expression of BAFF-binding receptors during human B cell differentiation. J Immunol *179*, 7276-7286.

del Mar Lorente, M., Marcos-Gutierrez, C., Perez, C., Schoorlemmer, J., Ramirez, A., Magin, T., and Vidal, M. (2000). Loss- and gain-of-function mutations show a polycomb group function for Ring1A in mice. Development *127*, 5093-5100.

Dellino, G.I., Schwartz, Y.B., Farkas, G., McCabe, D., Elgin, S.C., and Pirrotta, V. (2004). Polycomb silencing blocks transcription initiation. Mol Cell *13*, 887-893.

Delogu, A., Schebesta, A., Sun, Q., Aschenbrenner, K., Perlot, T., and Busslinger, M. (2006). Gene repression by Pax5 in B cells is essential for blood cell homeostasis and is reversed in plasma cells. Immunity *24*, 269-281.

Dent, A.L., Shaffer, A.L., Yu, X., Allman, D., and Staudt, L.M. (1997). Control of inflammation, cytokine expression, and germinal center formation by BCL-6. Science *276*, 589-592.

Dhordain, P., Lin, R.J., Quief, S., Lantoine, D., Kerckaert, J.P., Evans, R.M., and Albagli, O. (1998). The LAZ3(BCL-6) oncoprotein recruits a SMRT/mSIN3A/histone deacetylase containing complex to mediate transcriptional repression. Nucleic Acids Res *26*, 4645-4651.

Dietrich, N., Lerdrup, M., Landt, E., Agrawal-Singh, S., Bak, M., Tommerup, N., Rappsilber, J., Sodersten, E., and Hansen, K. (2012). REST-mediated recruitment of polycomb repressor complexes in mammalian cells. PLoS Genet *8*, e1002494.

Difilippantonio, M.J., Zhu, J., Chen, H.T., Meffre, E., Nussenzweig, M.C., Max, E.E., Ried, T., and Nussenzweig, A. (2000). DNA repair protein Ku80 suppresses chromosomal aberrations and malignant transformation. Nature *404*, 510-514.

Dogan, I., Bertocci, B., Vilmont, V., Delbos, F., Megret, J., Storck, S., Reynaud, C.A., and Weill, J.C. (2009). Multiple layers of B cell memory with different effector functions. Nat Immunol *10*, 1292-1299.

Eastman, Q.M., Leu, T.M., and Schatz, D.G. (1996). Initiation of V(D)J recombination in vitro obeying the 12/23 rule. Nature *380*, 85-88.

Eskeland, R., Leeb, M., Grimes, G.R., Kress, C., Boyle, S., Sproul, D., Gilbert, N., Fan, Y., Skoultchi, A.I., Wutz, A.*, et al.* (2010). Ring1B compacts chromatin structure and represses gene expression independent of histone ubiquitination. Mol Cell *38*, 452-464.

Ezhkova, E., Lien, W.H., Stokes, N., Pasolli, H.A., Silva, J.M., and Fuchs, E. (2011). EZH1 and EZH2 cogovern histone H3K27 trimethylation and are essential for hair follicle homeostasis and wound repair. Genes Dev *25*, 485-498.

Ezhkova, E., Pasolli, H.A., Parker, J.S., Stokes, N., Su, I.H., Hannon, G., Tarakhovsky, A., and Fuchs, E. (2009). Ezh2 orchestrates gene expression for the stepwise differentiation of tissue-specific stem cells. Cell *136*, 1122-1135.

Facchino, S., Abdouh, M., Chatoo, W., and Bernier, G. (2010). BMI1 confers radioresistance to normal and cancerous neural stem cells through recruitment of the DNA damage response machinery. J Neurosci *30*, 10096-10111.

Fagarasan, S., and Honjo, T. (2003). Intestinal IgA synthesis: regulation of front-line body defences. Nat Rev Immunol *3*, 63-72.

Fan, T., Jiang, S., Chung, N., Alikhan, A., Ni, C., Lee, C.C., and Hornyak, T.J. (2011). EZH2-dependent suppression of a cellular senescence phenotype in melanoma cells by inhibition of p21/CDKN1A expression. Mol Cancer Res *9*, 418-429.

Farcas, A.M., Blackledge, N.P., Sudbery, I., Long, H.K., McGouran, J.F., Rose, N.R., Lee, S., Sims, D., Cerase, A., Sheahan, T.W.*, et al.* (2012). KDM2B links the Polycomb Repressive Complex 1 (PRC1) to recognition of CpG islands. Elife *1*, e00205.

Forsberg, E.C., Serwold, T., Kogan, S., Weissman, I.L., and Passegue, E. (2006). New evidence supporting megakaryocyte-erythrocyte potential of flk2/flt3+ multipotent hematopoietic progenitors. Cell *126*, 415-426.

Francis, N.J., Kingston, R.E., and Woodcock, C.L. (2004). Chromatin compaction by a polycomb group protein complex. Science *306*, 1574-1577.

Frangini, A., Sjoberg, M., Roman-Trufero, M., Dharmalingam, G., Haberle, V., Bartke, T., Lenhard, B., Malumbres, M., Vidal, M., and Dillon, N. (2013). The Aurora B Kinase and the Polycomb Protein Ring1B Combine to Regulate Active Promoters in Quiescent Lymphocytes. Mol Cell *51*, 647-661.

Fujita, N., Jaye, D.L., Geigerman, C., Akyildiz, A., Mooney, M.R., Boss, J.M., and Wade, P.A. (2004). MTA3 and the Mi-2/NuRD complex regulate cell fate during B lymphocyte differentiation. Cell *119*, 75-86.

Fukuda, T., Yoshida, T., Okada, S., Hatano, M., Miki, T., Ishibashi, K., Okabe, S., Koseki, H., Hirosawa, S., Taniguchi, M.*, et al.* (1997). Disruption of the Bcl6 gene results in an impaired germinal center formation. J Exp Med *186*, 439-448.

Gao, Z., Zhang, J., Bonasio, R., Strino, F., Sawai, A., Parisi, F., Kluger, Y., and Reinberg, D. (2012). PCGF homologs, CBX proteins, and RYBP define functionally distinct PRC1 family complexes. Mol Cell *45*, 344-356.

Gass, J.N., Gifford, N.M., and Brewer, J.W. (2002). Activation of an unfolded protein response during differentiation of antibody-secreting B cells. The Journal of biological chemistry *277*, 49047-49054.

Gautier, L., Cope, L., Bolstad, B.M., and Irizarry, R.A. (2004). affy--analysis of Affymetrix GeneChip data at the probe level. Bioinformatics *20*, 307-315.

Gearhart, M.D., Corcoran, C.M., Wamstad, J.A., and Bardwell, V.J. (2006). Polycomb group and SCF ubiquitin ligases are found in a novel BCOR complex that is recruited to BCL6 targets. Mol Cell Biol *26*, 6880-6889.

Ginjala, V., Nacerddine, K., Kulkarni, A., Oza, J., Hill, S.J., Yao, M., Citterio, E., van Lohuizen, M., and Ganesan, S. (2011). BMI1 is recruited to DNA breaks and contributes to DNA damage-induced H2A ubiquitination and repair. Mol Cell Biol *31*, 1972-1982.

Gorman, J.R., and Alt, F.W. (1998). Regulation of immunoglobulin light chain isotype expression. Adv Immunol *69*, 113-181.

Grau, D.J., Chapman, B.A., Garlick, J.D., Borowsky, M., Francis, N.J., and Kingston, R.E. (2011). Compaction of chromatin by diverse Polycomb group proteins requires localized regions of high charge. Genes Dev *25*, 2210-2221.

Gupta, R.A., Shah, N., Wang, K.C., Kim, J., Horlings, H.M., Wong, D.J., Tsai, M.C., Hung, T., Argani, P., Rinn, J.L.*, et al.* (2010). Long non-coding RNA HOTAIR reprograms chromatin state to promote cancer metastasis. Nature *464*, 1071-1076.

Haas, K.M., Poe, J.C., Steeber, D.A., and Tedder, T.F. (2005). B-1a and B-1b cells exhibit distinct developmental requirements and have unique functional roles in innate and adaptive immunity to S. pneumoniae. Immunity *23*, 7-18.

Hagman, J., and Lukin, K. (2006). Transcription factors drive B cell development. Curr Opin Immunol *18*, 127-134.

Hardy, R.R. (2006). B-1 B cell development. J Immunol *177*, 2749-2754.

Hatzi, K., Jiang, Y., Huang, C., Garrett-Bakelman, F., Gearhart, M.D., Giannopoulou, E.G., Zumbo, P., Kirouac, K., Bhaskara, S., Polo, J.M.*, et al.* (2013). A Hybrid Mechanism of Action for BCL6 in B Cells Defined by Formation of Functionally Distinct Complexes at Enhancers and Promoters. Cell Rep *4*, 578-588.

Herranz, N., Pasini, D., Diaz, V.M., Franci, C., Gutierrez, A., Dave, N., Escriva, M., Hernandez-Munoz, I., Di Croce, L., Helin, K.*, et al.* (2008). Polycomb complex 2 is required for E-cadherin repression by the Snail1 transcription factor. Mol Cell Biol *28*, 4772-4781.

Herz, H.M., and Shilatifard, A. (2010). The JARID2-PRC2 duality. Genes Dev *24*, 857-861.

Ho, S.N., Thomas, D.J., Timmerman, L.A., Li, X., Francke, U., and Crabtree, G.R. (1995). NFATc3, a lymphoid-specific NFATc family member that is calcium-regulated and exhibits distinct DNA binding specificity. J Biol Chem *270*, 19898-19907.

Hobeika, E., Thiemann, S., Storch, B., Jumaa, H., Nielsen, P.J., Pelanda, R., and Reth, M. (2006). Testing gene function early in the B cell lineage in mb1-cre mice. Proc Natl Acad Sci U S A *103*, 13789-13794.

Hozumi, K., Negishi, N., Suzuki, D., Abe, N., Sotomaru, Y., Tamaoki, N., Mailhos, C., Ish-Horowicz, D., Habu, S., and Owen, M.J. (2004). Delta-like 1 is necessary for the generation of marginal zone B cells but not T cells in vivo. Nat Immunol *5*, 638-644.

Hu, D., Garruss, A.S., Gao, X., Morgan, M.A., Cook, M., Smith, E.R., and Shilatifard, A. (2013). The Mll2 branch of the COMPASS family regulates bivalent promoters in mouse embryonic stem cells. Nat Struct Mol Biol *20*, 1093-1097.

Huang, C., Hatzi, K., and Melnick, A. (2013). Lineage-specific functions of Bcl-6 in immunity and inflammation are mediated by distinct biochemical mechanisms. Nat Immunol *14*, 380-388.

Hunkapiller, J., Shen, Y., Diaz, A., Cagney, G., McCleary, D., Ramalho-Santos, M., Krogan, N., Ren, B., Song, J.S., and Reiter, J.F. (2012). Polycomb-like 3 promotes polycomb repressive complex 2 binding to CpG islands and embryonic stem cell self-renewal. PLoS Genet *8*, e1002576.

Huynh, K.D., and Bardwell, V.J. (1998). The BCL-6 POZ domain and other POZ domains interact with the co-repressors N-CoR and SMRT. Oncogene *17*, 2473-2484.

Ikuta, K., and Weissman, I.L. (1992). Evidence that hematopoietic stem cells express mouse c-kit but do not depend on steel factor for their generation. Proceedings of the National Academy of Sciences of the United States of America *89*, 1502-1506.

Infante, A., Laresgoiti, U., Fernandez-Rueda, J., Fullaondo, A., Galan, J., Diaz-Uriarte, R., Malumbres, M., Field, S.J., and Zubiaga, A.M. (2008). E2F2 represses cell cycle regulators to maintain quiescence. Cell Cycle *7*, 3915-3927.

Ismail, I.H., Andrin, C., McDonald, D., and Hendzel, M.J. (2010). BMI1-mediated histone ubiquitylation promotes DNA double-strand break repair. J Cell Biol *191*, 45-60.

Iwakoshi, N.N., Lee, A.H., Vallabhajosyula, P., Otipoby, K.L., Rajewsky, K., and Glimcher, L.H. (2003). Plasma cell differentiation and the unfolded protein response intersect at the transcription factor XBP-1. Nature immunology *4*, 321-329.

Jacobs, J.J., Kieboom, K., Marino, S., DePinho, R.A., and van Lohuizen, M. (1999). The oncogene and Polycomb-group gene bmi-1 regulates cell proliferation and senescence through the ink4a locus. Nature *397*, 164-168.

Johnson, K., Pflugh, D.L., Yu, D., Hesslein, D.G., Lin, K.I., Bothwell, A.L., Thomas-Tikhonenko, A., Schatz, D.G., and Calame, K. (2004). B cell-specific loss of histone 3 lysine 9 methylation in the V(H) locus depends on Pax5. Nature immunology *5*, 853-861.

Kaji, T., Ishige, A., Hikida, M., Taka, J., Hijikata, A., Kubo, M., Nagashima, T., Takahashi, Y., Kurosaki, T., Okada, M*., et al.* (2012). Distinct cellular pathways select germline-encoded and somatically mutated antibodies into immunological memory. J Exp Med *209*, 2079-2097.

Kajiume, T., Ninomiya, Y., Ishihara, H., Kanno, R., and Kanno, M. (2004). Polycomb group gene mel-18 modulates the self-renewal activity and cell cycle status of hematopoietic stem cells. Exp Hematol *32*, 571-578.

Kallies, A., Hasbold, J., Tarlinton, D.M., Dietrich, W., Corcoran, L.M., Hodgkin, P.D., and Nutt, S.L. (2004). Plasma cell ontogeny defined by quantitative changes in blimp-1 expression. The Journal of experimental medicine *200*, 967-977.

Kamijo, T., Weber, J.D., Zambetti, G., Zindy, F., Roussel, M.F., and Sherr, C.J. (1998). Functional and physical interactions of the ARF tumor suppressor with p53 and Mdm2. Proc Natl Acad Sci U S A *95*, 8292-8297.

Kawabe, T., Naka, T., Yoshida, K., Tanaka, T., Fujiwara, H., Suematsu, S., Yoshida, N., Kishimoto, T., and Kikutani, H. (1994). The immune responses in CD40-deficient mice: impaired immunoglobulin class switching and germinal center formation. Immunity *1*, 167-178.

Keren, Z., Naor, S., Nussbaum, S., Golan, K., Itkin, T., Sasaki, Y., Schmidt-Supprian, M., Lapidot, T., and Melamed, D. (2011). B-cell depletion reactivates B lymphopoiesis in the BM and rejuvenates the B lineage in aging. Blood *117*, 3104-3112.

Kiani, A., Rao, A., and Aramburu, J. (2000). Manipulating immune responses with immunosuppressive agents that target NFAT. Immunity *12*, 359-372.

Klein, U., Casola, S., Cattoretti, G., Shen, Q., Lia, M., Mo, T., Ludwig, T., Rajewsky, K., and Dalla-Favera, R. (2006). Transcription factor IRF4 controls plasma cell differentiation and class-switch recombination. Nature immunology *7*, 773-782.

Klein, U., and Dalla-Favera, R. (2008a). Germinal centres: role in B-cell physiology and malignancy. Nat Rev Immunol *8*, 22-33.

Klein, U., and Dalla-Favera, R. (2008b). Germinal centres: role in B-cell physiology and malignancy. Nat Rev Immunol *8*, 22-33.

Klein, U., Tu, Y., Stolovitzky, G.A., Keller, J.L., Haddad, J., Jr., Miljkovic, V., Cattoretti, G., Califano, A., and Dalla-Favera, R. (2003). Transcriptional analysis of the B cell germinal center reaction. Proc Natl Acad Sci U S A *100*, 2639-2644.

Kometani, K., Nakagawa, R., Shinnakasu, R., Kaji, T., Rybouchkin, A., Moriyama, S., Furukawa, K., Koseki, H., Takemori, T., and Kurosaki, T. (2013). Repression of the transcription factor Bach2 contributes to predisposition of IgG1 memory B cells toward plasma cell differentiation. Immunity *39*, 136-147.

Kornberg, R.D., and Lorch, Y. (1999). Twenty-five years of the nucleosome, fundamental particle of the eukaryote chromosome. Cell *98*, 285-294.

Kotake, Y., Nakagawa, T., Kitagawa, K., Suzuki, S., Liu, N., Kitagawa, M., and Xiong, Y. (2011). Long non-coding RNA ANRIL is required for the PRC2 recruitment to and silencing of p15(INK4B) tumor suppressor gene. Oncogene *30*, 1956-1962.

Kraus, M., Alimzhanov, M.B., Rajewsky, N., and Rajewsky, K. (2004). Survival of resting mature B lymphocytes depends on BCR signaling via the Igalpha/beta heterodimer. Cell *117*, 787-800.

Kroon, E., Krosl, J., Thorsteinsdottir, U., Baban, S., Buchberg, A.M., and Sauvageau, G. (1998). Hoxa9 transforms primary bone marrow cells through specific collaboration with Meis1a but not Pbx1b. Embo J *17*, 3714-3725.

Ku, M., Koche, R.P., Rheinbay, E., Mendenhall, E.M., Endoh, M., Mikkelsen, T.S., Presser, A., Nusbaum, C., Xie, X., Chi, A.S.*, et al.* (2008). Genomewide analysis of PRC1 and PRC2 occupancy identifies two classes of bivalent domains. PLoS Genet *4*, e1000242.

Kuroda, K., Han, H., Tani, S., Tanigaki, K., Tun, T., Furukawa, T., Taniguchi, Y., Kurooka, H., Hamada, Y., Toyokuni, S.*, et al.* (2003). Regulation of marginal zone B cell development by MINT, a suppressor of Notch/RBP-J signaling pathway. Immunity *18*, 301-312.

Kwon, H., Thierry-Mieg, D., Thierry-Mieg, J., Kim, H.P., Oh, J., Tunyaplin, C., Carotta, S., Donovan, C.E., Goldman, M.L., Tailor, P.*, et al.* (2009). Analysis of interleukin-21-induced Prdm1 gene regulation reveals functional cooperation of STAT3 and IRF4 transcription factors. Immunity *31*, 941-952.

Kwon, K., Hutter, C., Sun, Q., Bilic, I., Cobaleda, C., Malin, S., and Busslinger, M. (2008). Instructive role of the transcription factor E2A in early B lymphopoiesis and germinal center B cell development. Immunity *28*, 751-762.

Lam, K.P., Kuhn, R., and Rajewsky, K. (1997). In vivo ablation of surface immunoglobulin on mature B cells by inducible gene targeting results in rapid cell death. Cell *90*, 1073-1083.

Landeira, D., Sauer, S., Poot, R., Dvorkina, M., Mazzarella, L., Jorgensen, H.F., Pereira, C.F., Leleu, M., Piccolo, F.M., Spivakov, M.*, et al.* (2010). Jarid2 is a PRC2 component in embryonic stem cells required for multi-lineage differentiation and recruitment of PRC1 and RNA Polymerase II to developmental regulators. Nat Cell Biol *12*, 618-624.

Lawrence, H.J., Rozenfeld, S., Cruz, C., Matsukuma, K., Kwong, A., Komuves, L., Buchberg, A.M., and Largman, C. (1999). Frequent co-expression of the HOXA9 and MEIS1 homeobox genes in human myeloid leukemias. Leukemia *13*, 1993-1999.

Lee, K., Tirasophon, W., Shen, X., Michalak, M., Prywes, R., Okada, T., Yoshida, H., Mori, K., and Kaufman, R.J. (2002). IRE1-mediated unconventional mRNA splicing and S2P-mediated ATF6 cleavage merge to regulate XBP1 in signaling the unfolded protein response. Genes Dev *16*, 452-466.

Lee, T.I., Jenner, R.G., Boyer, L.A., Guenther, M.G., Levine, S.S., Kumar, R.M., Chevalier, B., Johnstone, S.E., Cole, M.F., Isono, K.*, et al.* (2006). Control of developmental regulators by Polycomb in human embryonic stem cells. Cell *125*, 301-313.

Li, C.L., and Johnson, G.R. (1995). Murine hematopoietic stem and progenitor cells: I. Enrichment and biologic characterization. Blood *85*, 1472-1479.

Li, X., Su, K., Ji, C., Szalai, A.J., Wu, J., Zhang, Y., Zhou, T., Kimberly, R.P., and Edberg, J.C. (2008). Immune opsonins modulate BLyS/BAFF release in a receptor-specific fashion. J Immunol *181*, 1012-1018.

Li, Z., Otevrel, T., Gao, Y., Cheng, H.L., Seed, B., Stamato, T.D., Taccioli, G.E., and Alt, F.W. (1995). The XRCC4 gene encodes a novel protein involved in DNA double-strand break repair and V(D)J recombination. Cell *83*, 1079-1089.

Lin, H., and Grosschedl, R. (1995). Failure of B-cell differentiation in mice lacking the transcription factor EBF. Nature *376*, 263-267.

Lin, K.I., Angelin-Duclos, C., Kuo, T.C., and Calame, K. (2002). Blimp-1-dependent repression of Pax-5 is required for differentiation of B cells to immunoglobulin M-secreting plasma cells. Molecular and cellular biology *22*, 4771-4780.

Lin, Y., Wong, K., and Calame, K. (1997). Repression of c-myc transcription by Blimp-1, an inducer of terminal B cell differentiation. Science *276*, 596-599.

Liu, J., Cao, L., Chen, J., Song, S., Lee, I.H., Quijano, C., Liu, H., Keyvanfar, K., Chen, H., Cao, L.Y.*, et al.* (2009). Bmi1 regulates mitochondrial function and the DNA damage response pathway. Nature *459*, 387-392.

Liu, Y.J. (1997). Sites of B lymphocyte selection, activation, and tolerance in spleen. J Exp Med *186*, 625-629.

Loder, F., Mutschler, B., Ray, R.J., Paige, C.J., Sideras, P., Torres, R., Lamers, M.C., and Carsetti, R. (1999). B cell development in the spleen takes place in discrete steps and is determined by the quality of B cell receptor-derived signals. J Exp Med *190*, 75-89.

Lopes-Carvalho, T., and Kearney, J.F. (2004). Development and selection of marginal zone B cells. Immunol Rev *197*, 192-205.

Lu, R., Medina, K.L., Lancki, D.W., and Singh, H. (2003). IRF-4,8 orchestrate the pre-B-to-B transition in lymphocyte development. Genes & development *17*, 1703-1708.

Luster, M.I., Munson, A.E., Thomas, P.T., Holsapple, M.P., Fenters, J.D., White, K.L., Jr., Lauer, L.D., Germolec, D.R., Rosenthal, G.J., and Dean, J.H. (1988). Development of a testing battery to assess chemical-induced immunotoxicity: National Toxicology Program's guidelines for immunotoxicity evaluation in mice. Fundam Appl Toxicol *10*, 2-19.

Mackay, F., and Leung, H. (2006). The role of the BAFF/APRIL system on T cell function. Semin Immunol *18*, 284-289.

Maillard, I., Fang, T., and Pear, W.S. (2005). Regulation of lymphoid development, differentiation, and function by the Notch pathway. Annu Rev Immunol *23*, 945-974.

Majewski, I.J., Blewitt, M.E., de Graaf, C.A., McManus, E.J., Bahlo, M., Hilton, A.A., Hyland, C.D., Smyth, G.K., Corbin, J.E., Metcalf, D*., et al.* (2008). Polycomb repressive complex 2 (PRC2) restricts hematopoietic stem cell activity. PLoS Biol *6*, e93.

Martin, F., and Kearney, J.F. (2002). Marginal-zone B cells. Nat Rev Immunol *2*, 323-335.

Martin, S.W., and Goodnow, C.C. (2002). Burst-enhancing role of the IgG membrane tail as a molecular determinant of memory. Nat Immunol *3*, 182-188.

Martinez-Valdez, H., Guret, C., de Bouteiller, O., Fugier, I., Banchereau, J., and Liu, Y.J. (1996). Human germinal center B cells express the apoptosis-inducing genes Fas, c-myc, P53, and Bax but not the survival gene bcl-2. J Exp Med *183*, 971-977.

Maruyama, M., Lam, K.P., and Rajewsky, K. (2000). Memory B-cell persistence is independent of persisting immunizing antigen. Nature *407*, 636-642.

Matsuzawa, A., Tseng, P.H., Vallabhapurapu, S., Luo, J.L., Zhang, W., Wang, H., Vignali, D.A., Gallagher, E., and Karin, M. (2008). Essential cytoplasmic translocation of a cytokine receptor-assembled signaling complex. Science *321*, 663-668.

McBlane, J.F., van Gent, D.C., Ramsden, D.A., Romeo, C., Cuomo, C.A., Gellert, M., and Oettinger, M.A. (1995). Cleavage at a V(D)J recombination signal requires only RAG1 and RAG2 proteins and occurs in two steps. Cell *83*, 387-395.

McCabe, M.T., Ott, H.M., Ganji, G., Korenchuk, S., Thompson, C., Van Aller, G.S., Liu, Y., Graves, A.P., Della Pietra, A., 3rd, Diaz, E*., et al.* (2012). EZH2 inhibition as a therapeutic strategy for lymphoma with EZH2-activating mutations. Nature *492*, 108-112.

Medina, K.L., Pongubala, J.M., Reddy, K.L., Lancki, D.W., Dekoter, R., Kieslinger, M., Grosschedl, R., and Singh, H. (2004). Assembling a gene regulatory network for specification of the B cell fate. Dev Cell *7*, 607-617.

Melek, M., Gellert, M., and van Gent, D.C. (1998). Rejoining of DNA by the RAG1 and RAG2 proteins. Science *280*, 301-303.

Mills, J.R., Hippo, Y., Robert, F., Chen, S.M., Malina, A., Lin, C.J., Trojahn, U., Wendel, H.G., Charest, A., Bronson, R.T.*, et al.* (2008). mTORC1 promotes survival through translational control of Mcl-1. Proceedings of the National Academy of Sciences of the United States of America *105*, 10853-10858.

Mittrucker, H.W., Matsuyama, T., Grossman, A., Kundig, T.M., Potter, J., Shahinian, A., Wakeham, A., Patterson, B., Ohashi, P.S., and Mak, T.W. (1997). Requirement for the transcription factor LSIRF/IRF4 for mature B and T lymphocyte function. Science *275*, 540-543.

Montecino-Rodriguez, E., Leathers, H., and Dorshkind, K. (2006). Identification of a B-1 B cell-specified progenitor. Nat Immunol *7*, 293-301.

Morey, L., Aloia, L., Cozzuto, L., Benitah, S.A., and Di Croce, L. (2013). RYBP and Cbx7 define specific biological functions of polycomb complexes in mouse embryonic stem cells. Cell Rep *3*, 60-69.

Morgan, B., Sun, L., Avitahl, N., Andrikopoulos, K., Ikeda, T., Gonzales, E., Wu, P., Neben, S., and Georgopoulos, K. (1997). Aiolos, a lymphoid restricted transcription factor that interacts with Ikaros to regulate lymphocyte differentiation. EMBO J *16*, 2004-2013.

Morin, R.D., Johnson, N.A., Severson, T.M., Mungall, A.J., An, J., Goya, R., Paul, J.E., Boyle, M., Woolcock, B.W., Kuchenbauer, F.*, et al.* (2010). Somatic mutations altering EZH2 (Tyr641) in follicular and diffuse large B-cell lymphomas of germinal-center origin. Nat Genet *42*, 181-185.

Morshead, K.B., Ciccone, D.N., Taverna, S.D., Allis, C.D., and Oettinger, M.A. (2003). Antigen receptor loci poised for V(D)J rearrangement are broadly associated with BRG1 and flanked by peaks of histone H3 dimethylated at lysine 4. Proceedings of the National Academy of Sciences of the United States of America *100*, 11577-11582.

Muramatsu, M., Kinoshita, K., Fagarasan, S., Yamada, S., Shinkai, Y., and Honjo, T. (2000). Class switch recombination and hypermutation require activation-induced cytidine deaminase (AID), a potential RNA editing enzyme. Cell *102*, 553-563.

Neff, T., Sinha, A.U., Kluk, M.J., Zhu, N., Khattab, M.H., Stein, L., Xie, H., Orkin, S.H., and Armstrong, S.A. (2012). Polycomb repressive complex 2 is required for MLL-AF9 leukemia. Proc Natl Acad Sci U S A *109*, 5028-5033.

Nevins, J.R. (2001). The Rb/E2F pathway and cancer. Hum Mol Genet *10*, 699-703.

Niu, H., Ye, B.H., and Dalla-Favera, R. (1998). Antigen receptor signaling induces MAP kinase-mediated phosphorylation and degradation of the BCL-6 transcription factor. Genes & development *12*, 1953-1961.

Nojima, T., Haniuda, K., Moutai, T., Matsudaira, M., Mizokawa, S., Shiratori, I., Azuma, T., and Kitamura, D. (2011). In-vitro derived germinal centre B cells differentially generate memory B or plasma cells in vivo. Nat Commun *2*, 465.

Norvell, A., Mandik, L., and Monroe, J.G. (1995). Engagement of the antigen-receptor on immature murine B lymphocytes results in death by apoptosis. J Immunol *154*, 4404-4413.

Norvell, A., and Monroe, J.G. (1996). Acquisition of surface IgD fails to protect from tolerance-induction. Both surface IgM- and surface IgD-mediated signals induce apoptosis of immature murine B lymphocytes. J Immunol *156*, 1328-1332.

Nutt, S.L., Heavey, B., Rolink, A.G., and Busslinger, M. (1999). Commitment to the B-lymphoid lineage depends on the transcription factor Pax5. Nature *401*, 556-562.

Nutt, S.L., and Kee, B.L. (2007). The transcriptional regulation of B cell lineage commitment. Immunity *26*, 715-725.

O'Carroll, D., Erhardt, S., Pagani, M., Barton, S.C., Surani, M.A., and Jenuwein, T. (2001). The polycomb-group gene Ezh2 is required for early mouse development. Mol Cell Biol *21*, 4330-4336.

Ochiai, K., Maienschein-Cline, M., Simonetti, G., Chen, J., Rosenthal, R., Brink, R., Chong, A.S., Klein, U., Dinner, A.R., Singh, H.*, et al.* (2013). Transcriptional regulation of germinal center B and plasma cell fates by dynamical control of IRF4. Immunity *38*, 918-929.

Ogata, H., Su, I., Miyake, K., Nagai, Y., Akashi, S., Mecklenbrauker, I., Rajewsky, K., Kimoto, M., and Tarakhovsky, A. (2000). The toll-like receptor protein RP105 regulates lipopolysaccharide signaling in B cells. J Exp Med *192*, 23-29.

Ogawa, H., Ishiguro, K., Gaubatz, S., Livingston, D.M., and Nakatani, Y. (2002). A complex with chromatin modifiers that occupies E2F- and Myc-responsive genes in G0 cells. Science *296*, 1132-1136.

Oguro, H., Yuan, J., Ichikawa, H., Ikawa, T., Yamazaki, S., Kawamoto, H., Nakauchi, H., and Iwama, A. (2010). Poised lineage specification in multipotential hematopoietic stem and progenitor cells by the polycomb protein Bmi1. Cell Stem Cell *6*, 279-286.

Opferman, J.T., Letai, A., Beard, C., Sorcinelli, M.D., Ong, C.C., and Korsmeyer, S.J. (2003). Development and maintenance of B and T lymphocytes requires antiapoptotic MCL-1. Nature *426*, 671-676.

Osipovich, O., Milley, R., Meade, A., Tachibana, M., Shinkai, Y., Krangel, M.S., and Oltz, E.M. (2004). Targeted inhibition of V(D)J recombination by a histone methyltransferase. Nature immunology *5*, 309-316.

Parekh, S., Polo, J.M., Shaknovich, R., Juszczynski, P., Lev, P., Ranuncolo, S.M., Yin, Y., Klein, U., Cattoretti, G., Dalla Favera, R*., et al.* (2007). BCL6 programs lymphoma cells for survival and differentiation through distinct biochemical mechanisms. Blood *110*, 2067-2074.

Park, I.K., Qian, D., Kiel, M., Becker, M.W., Pihalja, M., Weissman, I.L., Morrison, S.J., and Clarke, M.F. (2003). Bmi-1 is required for maintenance of adult self-renewing haematopoietic stem cells. Nature *423*, 302-305.

Pasini, D., Bracken, A.P., Jensen, M.R., Lazzerini Denchi, E., and Helin, K. (2004). Suz12 is essential for mouse development and for EZH2 histone methyltransferase activity. Embo J *23*, 4061-4071.

Pasini, D., Cloos, P.A., Walfridsson, J., Olsson, L., Bukowski, J.P., Johansen, J.V., Bak, M., Tommerup, N., Rappsilber, J., and Helin, K. (2010). JARID2 regulates binding of the Polycomb repressive complex 2 to target genes in ES cells. Nature *464*, 306-310.

Patke, A., Mecklenbrauker, I., Erdjument-Bromage, H., Tempst, P., and Tarakhovsky, A. (2006). BAFF controls B cell metabolic fitness through a PKC beta- and Akt-dependent mechanism. J Exp Med *203*, 2551-2562.

Phan, R.T., and Dalla-Favera, R. (2004). The BCL6 proto-oncogene suppresses p53 expression in germinal-centre B cells. Nature *432*, 635-639.

Phan, R.T., Saito, M., Kitagawa, Y., Means, A.R., and Dalla-Favera, R. (2007a). Genotoxic stress regulates expression of the proto-oncogene Bcl6 in germinal center B cells. Nat Immunol *8*, 1132-1139.

Phan, R.T., Saito, M., Kitagawa, Y., Means, A.R., and Dalla-Favera, R. (2007b). Genotoxic stress regulates expression of the proto-oncogene Bcl6 in germinal center B cells. Nature immunology *8*, 1132-1139.

Pierce, S.K., and Liu, W. (2013). Encoding Immunological Memory in the Initiation of B-Cell Receptor Signaling. Cold Spring Harb Symp Quant Biol.

Plath, K., Fang, J., Mlynarczyk-Evans, S.K., Cao, R., Worringer, K.A., Wang, H., de la Cruz, C.C., Otte, A.P., Panning, B., and Zhang, Y. (2003). Role of histone H3 lysine 27 methylation in X inactivation. Science *300*, 131-135.

Polo, J.M., Ci, W., Licht, J.D., and Melnick, A. (2008). Reversible disruption of BCL6 repression complexes by CD40 signaling in normal and malignant B cells. Blood *112*, 644-651.

Raaphorst, F.M., van Kemenade, F.J., Blokzijl, T., Fieret, E., Hamer, K.M., Satijn, D.P., Otte, A.P., and Meijer, C.J. (2000a). Coexpression of BMI-1 and EZH2 polycomb group genes in Reed-Sternberg cells of Hodgkin's disease. Am J Pathol *157*, 709-715.

Raaphorst, F.M., van Kemenade, F.J., Fieret, E., Hamer, K.M., Satijn, D.P., Otte, A.P., and Meijer, C.J. (2000b). Cutting edge: polycomb gene expression patterns reflect distinct B cell differentiation stages in human germinal centers. J Immunol *164*, 1-4.

Rajewsky, K. (1996). Clonal selection and learning in the antibody system. Nature *381*, 751-758.

Ranuncolo, S.M., Polo, J.M., Dierov, J., Singer, M., Kuo, T., Greally, J., Green, R., Carroll, M., and Melnick, A. (2007). Bcl-6 mediates the germinal center B cell phenotype and lymphomagenesis through transcriptional repression of the DNA-damage sensor ATR. Nature immunology *8*, 705-714.

Ranuncolo, S.M., Polo, J.M., and Melnick, A. (2008a). BCL6 represses CHEK1 and suppresses DNA damage pathways in normal and malignant B-cells. Blood Cells Mol Dis *41*, 95-99.

Ranuncolo, S.M., Wang, L., Polo, J.M., Dell'Oso, T., Dierov, J., Gaymes, T.J., Rassool, F., Carroll, M., and Melnick, A. (2008b). BCL6-mediated attenuation of DNA damage sensing triggers growth arrest and senescence through a p53-dependent pathway in a cell context-dependent manner. The Journal of biological chemistry *283*, 22565-22572.

Reimold, A.M., Iwakoshi, N.N., Manis, J., Vallabhajosyula, P., Szomolanyi-Tsuda, E., Gravallese, E.M., Friend, D., Grusby, M.J., Alt, F., and Glimcher, L.H. (2001). Plasma cell differentiation requires the transcription factor XBP-1. Nature *412*, 300-307.

Reimold, A.M., Ponath, P.D., Li, Y.S., Hardy, R.R., David, C.S., Strominger, J.L., and Glimcher, L.H. (1996). Transcription factor B cell lineage-specific activator protein regulates the gene for human X-box binding protein 1. The Journal of experimental medicine *183*, 393-401.

Revilla, I.D.R., Bilic, I., Vilagos, B., Tagoh, H., Ebert, A., Tamir, I.M., Smeenk, L., Trupke, J., Sommer, A., Jaritz, M., *et al.* (2012). The B-cell identity factor Pax5 regulates distinct transcriptional programmes in early and late B lymphopoiesis. Embo J *31*, 3130-3146.

Ringrose, L., Rehmsmeier, M., Dura, J.M., and Paro, R. (2003). Genome-wide prediction of Polycomb/Trithorax response elements in Drosophila melanogaster. Dev Cell *5*, 759-771.

Rinn, J.L., Kertesz, M., Wang, J.K., Squazzo, S.L., Xu, X., Brugmann, S.A., Goodnough, L.H., Helms, J.A., Farnham, P.J., Segal, E., *et al.* (2007). Functional demarcation of active and silent chromatin domains in human HOX loci by noncoding RNAs. Cell *129*, 1311-1323.

Roman-Trufero, M., Mendez-Gomez, H.R., Perez, C., Hijikata, A., Fujimura, Y., Endo, T., Koseki, H., Vicario-Abejon, C., and Vidal, M. (2009). Maintenance of undifferentiated state and self-renewal of embryonic neural stem cells by Polycomb protein Ring1B. Stem Cells *27*, 1559-1570.

Saito, T., Chiba, S., Ichikawa, M., Kunisato, A., Asai, T., Shimizu, K., Yamaguchi, T., Yamamoto, G., Seo, S., Kumano, K., *et al.* (2003). Notch2 is preferentially expressed in mature B cells and indispensable for marginal zone B lineage development. Immunity *18*, 675-685.

Sanchez, C., Sanchez, I., Demmers, J.A., Rodriguez, P., Strouboulis, J., and Vidal, M. (2007). Proteomics analysis of Ring1B/Rnf2 interactors identifies a novel complex with the Fbxl10/Jhdm1B histone demethylase and the Bcl6 interacting corepressor. Mol Cell Proteomics *6*, 820-834.

Sasaki, Y., Casola, S., Kutok, J.L., Rajewsky, K., and Schmidt-Supprian, M. (2004). TNF family member B cell-activating factor (BAFF) receptor-dependent and -independent roles for BAFF in B cell physiology. J Immunol *173*, 2245-2252.

Sasaki, Y., Derudder, E., Hobeika, E., Pelanda, R., Reth, M., Rajewsky, K., and Schmidt-Supprian, M. (2006). Canonical NF-kappaB activity, dispensable for B cell development, replaces BAFF-receptor signals and promotes B cell proliferation upon activation. Immunity *24*, 729-739.

Scheeren, F.A., Naspetti, M., Diehl, S., Schotte, R., Nagasawa, M., Wijnands, E., Gimeno, R., Vyth-Dreese, F.A., Blom, B., and Spits, H. (2005). STAT5 regulates the self-renewal capacity and differentiation of human memory B cells and controls Bcl-6 expression. Nat Immunol *6*, 303-313.

Schiemann, B., Gommerman, J.L., Vora, K., Cachero, T.G., Shulga-Morskaya, S., Dobles, M., Frew, E., and Scott, M.L. (2001). An essential role for BAFF in the normal

development of B cells through a BCMA-independent pathway. Science *293*, 2111-2114.

Schoeftner, S., Sengupta, A.K., Kubicek, S., Mechtler, K., Spahn, L., Koseki, H., Jenuwein, T., and Wutz, A. (2006). Recruitment of PRC1 function at the initiation of X inactivation independent of PRC2 and silencing. Embo J *25*, 3110-3122.

Scholz, J.L., Crowley, J.E., Tomayko, M.M., Steinel, N., O'Neill, P.J., Quinn, W.J., 3rd, Goenka, R., Miller, J.P., Cho, Y.H., Long, V.*, et al.* (2008). BLyS inhibition eliminates primary B cells but leaves natural and acquired humoral immunity intact. Proc Natl Acad Sci U S A *105*, 15517-15522.

Sciammas, R., and Davis, M.M. (2004). Modular nature of Blimp-1 in the regulation of gene expression during B cell maturation. J Immunol *172*, 5427-5440.

Sciammas, R., Shaffer, A.L., Schatz, J.H., Zhao, H., Staudt, L.M., and Singh, H. (2006). Graded expression of interferon regulatory factor-4 coordinates isotype switching with plasma cell differentiation. Immunity *25*, 225-236.

Shaffer, A.L., Lin, K.I., Kuo, T.C., Yu, X., Hurt, E.M., Rosenwald, A., Giltnane, J.M., Yang, L., Zhao, H., Calame, K.*, et al.* (2002). Blimp-1 orchestrates plasma cell differentiation by extinguishing the mature B cell gene expression program. Immunity *17*, 51-62.

Shaffer, A.L., Shapiro-Shelef, M., Iwakoshi, N.N., Lee, A.H., Qian, S.B., Zhao, H., Yu, X., Yang, L., Tan, B.K., Rosenwald, A.*, et al.* (2004). XBP1, downstream of Blimp-1, expands the secretory apparatus and other organelles, and increases protein synthesis in plasma cell differentiation. Immunity *21*, 81-93.

Shapiro-Shelef, M., Lin, K.I., McHeyzer-Williams, L.J., Liao, J., McHeyzer-Williams, M.G., and Calame, K. (2003). Blimp-1 is required for the formation of immunoglobulin secreting plasma cells and pre-plasma memory B cells. Immunity *19*, 607-620.

Shapiro-Shelef, M., Lin, K.I., Savitsky, D., Liao, J., and Calame, K. (2005). Blimp-1 is required for maintenance of long-lived plasma cells in the bone marrow. J Exp Med *202*, 1471-1476.

Shaw, J.P., Utz, P.J., Durand, D.B., Toole, J.J., Emmel, E.A., and Crabtree, G.R. (1988). Identification of a putative regulator of early T cell activation genes. Science *241*, 202-205.

Shen, X., Kim, W., Fujiwara, Y., Simon, M.D., Liu, Y., Mysliwiec, M.R., Yuan, G.C., Lee, Y., and Orkin, S.H. (2009). Jumonji modulates polycomb activity and self-renewal versus differentiation of stem cells. Cell *139*, 1303-1314.

Sherr, C.J. (2001). The INK4a/ARF network in tumour suppression. Nat Rev Mol Cell Biol *2*, 731-737.

Sing, A., Pannell, D., Karaiskakis, A., Sturgeon, K., Djabali, M., Ellis, J., Lipshitz, H.D., and Cordes, S.P. (2009). A vertebrate Polycomb response element governs segmentation of the posterior hindbrain. Cell *138*, 885-897.

Skalet, A.H., Isler, J.A., King, L.B., Harding, H.P., Ron, D., and Monroe, J.G. (2005). Rapid B cell receptor-induced unfolded protein response in nonsecretory B cells correlates with pro- versus antiapoptotic cell fate. The Journal of biological chemistry *280*, 39762-39771.

Song, H., and Cerny, J. (2003). Functional heterogeneity of marginal zone B cells revealed by their ability to generate both early antibody-forming cells and germinal centers with hypermutation and memory in response to a T-dependent antigen. The Journal of experimental medicine *198*, 1923-1935.

Souabni, A., Cobaleda, C., Schebesta, M., and Busslinger, M. (2002). Pax5 promotes B lymphopoiesis and blocks T cell development by repressing Notch1. Immunity *17*, 781-793.

Sparmann, A., and van Lohuizen, M. (2006). Polycomb silencers control cell fate, development and cancer. Nat Rev Cancer *6*, 846-856.

Squazzo, S.L., O'Geen, H., Komashko, V.M., Krig, S.R., Jin, V.X., Jang, S.W., Margueron, R., Reinberg, D., Green, R., and Farnham, P.J. (2006). Suz12 binds to silenced regions of the genome in a cell-type-specific manner. Genome Res *16*, 890-900.

Srinivas, S., Watanabe, T., Lin, C.S., William, C.M., Tanabe, Y., Jessell, T.M., and Costantini, F. (2001). Cre reporter strains produced by targeted insertion of EYFP and ECFP into the ROSA26 locus. BMC Dev Biol *1*, 4.

Stall, A.M., Adams, S., Herzenberg, L.A., and Kantor, A.B. (1992). Characteristics and development of the murine B-1b (Ly-1 B sister) cell population. Ann N Y Acad Sci *651*, 33-43.

Stock, J.K., Giadrossi, S., Casanova, M., Brookes, E., Vidal, M., Koseki, H., Brockdorff, N., Fisher, A.G., and Pombo, A. (2007). Ring1-mediated ubiquitination of H2A restrains poised RNA polymerase II at bivalent genes in mouse ES cells. Nat Cell Biol *9*, 1428-1435.

Strahl, B.D., and Allis, C.D. (2000). The language of covalent histone modifications. Nature *403*, 41-45.

Su, I.H., Basavaraj, A., Krutchinsky, A.N., Hobert, O., Ullrich, A., Chait, B.T., and Tarakhovsky, A. (2003). Ezh2 controls B cell development through histone H3 methylation and Igh rearrangement. Nat Immunol *4*, 124-131.

Su, W.J., Fang, J.S., Cheng, F., Liu, C., Zhou, F., and Zhang, J. (2013). RNF2/Ring1b negatively regulates p53 expression in selective cancer cell types to promote tumor development. Proc Natl Acad Sci U S A *110*, 1720-1725.

Sulli, G., Di Micco, R., and d'Adda di Fagagna, F. (2012). Crosstalk between chromatin state and DNA damage response in cellular senescence and cancer. Nat Rev Cancer *12*, 709-720.

Sun, J., Matthias, G., Mihatsch, M.J., Georgopoulos, K., and Matthias, P. (2003). Lack of the transcriptional coactivator OBF-1 prevents the development of systemic lupus erythematosus-like phenotypes in Aiolos mutant mice. J Immunol *170*, 1699-1706.

Sun, X.H. (2004). Multitasking of helix-loop-helix proteins in lymphopoiesis. Adv Immunol *84*, 43-77.

Tanaka, S., Miyagi, S., Sashida, G., Chiba, T., Yuan, J., Mochizuki-Kashio, M., Suzuki, Y., Sugano, S., Nakaseko, C., Yokote, K.*, et al.* (2012). Ezh2 augments leukemogenicity by reinforcing differentiation blockage in acute myeloid leukemia. Blood *120*, 1107-1117.

Tanigaki, K., Han, H., Yamamoto, N., Tashiro, K., Ikegawa, M., Kuroda, K., Suzuki, A., Nakano, T., and Honjo, T. (2002). Notch-RBP-J signaling is involved in cell fate determination of marginal zone B cells. Nat Immunol *3*, 443-450.

Tavares, L., Dimitrova, E., Oxley, D., Webster, J., Poot, R., Demmers, J., Bezstarosti, K., Taylor, S., Ura, H., Koide, H.*, et al.* (2012). RYBP-PRC1 complexes mediate H2A ubiquitylation at polycomb target sites independently of PRC2 and H3K27me3. Cell *148*, 664-678.

Terunuma, M., Jang, I.S., Ha, S.H., Kittler, J.T., Kanematsu, T., Jovanovic, J.N., Nakayama, K.I., Akaike, N., Ryu, S.H., Moss, S.J.*, et al.* (2004). GABAA receptor phospho-dependent modulation is regulated by phospholipase C-related inactive protein type 1, a novel protein phosphatase 1 anchoring protein. The Journal of neuroscience : the official journal of the Society for Neuroscience *24*, 7074-7084.

Tetsu, O., Ishihara, H., Kanno, R., Kamiyasu, M., Inoue, H., Tokuhisa, T., Taniguchi, M., and Kanno, M. (1998). mel-18 negatively regulates cell cycle progression upon B cell antigen receptor stimulation through a cascade leading to c-myc/cdc25. Immunity *9*, 439-448.

Timmerman, L.A., Healy, J.I., Ho, S.N., Chen, L., Goodnow, C.C., and Crabtree, G.R. (1997). Redundant expression but selective utilization of nuclear factor of activated T cells family members. J Immunol *159*, 2735-2740.

Tonegawa, S. (1983). Somatic generation of antibody diversity. Nature *302*, 575-581.

Trimarchi, J.M., Fairchild, B., Wen, J., and Lees, J.A. (2001). The E2F6 transcription factor is a component of the mammalian Bmi1-containing polycomb complex. Proc Natl Acad Sci U S A *98*, 1519-1524.

Tunyaplin, C., Shaffer, A.L., Angelin-Duclos, C.D., Yu, X., Staudt, L.M., and Calame, K.L. (2004). Direct repression of prdm1 by Bcl-6 inhibits plasmacytic differentiation. J Immunol *173*, 1158-1165.

Vallabhapurapu, S., Matsuzawa, A., Zhang, W., Tseng, P.H., Keats, J.J., Wang, H., Vignali, D.A., Bergsagel, P.L., and Karin, M. (2008). Nonredundant and complementary functions of TRAF2 and TRAF3 in a ubiquitination cascade that activates NIK-dependent alternative NF-kappaB signaling. Nat Immunol *9*, 1364-1370.

van der Lugt, N.M., Domen, J., Linders, K., van Roon, M., Robanus-Maandag, E., te Riele, H., van der Valk, M., Deschamps, J., Sofroniew, M., van Lohuizen, M*., et al.* (1994). Posterior transformation, neurological abnormalities, and severe hematopoietic defects in mice with a targeted deletion of the bmi-1 proto-oncogene. Genes Dev *8*, 757-769.

van der Stoop, P., Boutsma, E.A., Hulsman, D., Noback, S., Heimerikx, M., Kerkhoven, R.M., Voncken, J.W., Wessels, L.F., and van Lohuizen, M. (2008). Ubiquitin E3 ligase Ring1b/Rnf2 of polycomb repressive complex 1 contributes to stable maintenance of mouse embryonic stem cells. PLoS One *3*, e2235.

van Gent, D.C., McBlane, J.F., Ramsden, D.A., Sadofsky, M.J., Hesse, J.E., and Gellert, M. (1995). Initiation of V(D)J recombination in a cell-free system. Cell *81*, 925-934.

van Kemenade, F.J., Raaphorst, F.M., Blokzijl, T., Fieret, E., Hamer, K.M., Satijn, D.P., Otte, A.P., and Meijer, C.J. (2001). Coexpression of BMI-1 and EZH2 polycomb-group proteins is associated with cycling cells and degree of malignancy in B-cell non-Hodgkin lymphoma. Blood *97*, 3896-3901.

Vasanwala, F.H., Kusam, S., Toney, L.M., and Dent, A.L. (2002). Repression of AP-1 function: a mechanism for the regulation of Blimp-1 expression and B lymphocyte differentiation by the B cell lymphoma-6 protooncogene. J Immunol *169*, 1922-1929.

Velichutina, I., Shaknovich, R., Geng, H., Johnson, N.A., Gascoyne, R.D., Melnick, A.M., and Elemento, O. (2010). EZH2-mediated epigenetic silencing in germinal center B cells contributes to proliferation and lymphomagenesis. Blood *116*, 5247-5255.

Venkataraman, L., Francis, D.A., Wang, Z., Liu, J., Rothstein, T.L., and Sen, R. (1994). Cyclosporin-A sensitive induction of NF-AT in murine B cells. Immunity *1*, 189-196.

Verweij, C.L., Guidos, C., and Crabtree, G.R. (1990). Cell type specificity and activation requirements for NFAT-1 (nuclear factor of activated T-cells) transcriptional activity determined by a new method using transgenic mice to assay transcriptional activity of an individual nuclear factor. J Biol Chem *265*, 15788-15795.

Victora, G.D., Schwickert, T.A., Fooksman, D.R., Kamphorst, A.O., Meyer-Hermann, M., Dustin, M.L., and Nussenzweig, M.C. (2010). Germinal center dynamics revealed by multiphoton microscopy with a photoactivatable fluorescent reporter. Cell *143*, 592-605.

Vikstrom, I., Carotta, S., Luthje, K., Peperzak, V., Jost, P.J., Glaser, S., Busslinger, M., Bouillet, P., Strasser, A., Nutt, S.L.*, et al.* (2010). Mcl-1 is essential for germinal center formation and B cell memory. Science *330*, 1095-1099.

Vinuesa, C.G., Tangye, S.G., Moser, B., and Mackay, C.R. (2005). Follicular B helper T cells in antibody responses and autoimmunity. Nat Rev Immunol *5*, 853-865.

Voncken, J.W., Roelen, B.A., Roefs, M., de Vries, S., Verhoeven, E., Marino, S., Deschamps, J., and van Lohuizen, M. (2003). Rnf2 (Ring1b) deficiency causes gastrulation arrest and cell cycle inhibition. Proc Natl Acad Sci U S A *100*, 2468-2473.

Walker, E., Manias, J.L., Chang, W.Y., and Stanford, W.L. (2011). PCL2 modulates gene regulatory networks controlling self-renewal and commitment in embryonic stem cells. Cell Cycle *10*, 45-51.

Wang, J.H., Avitahl, N., Cariappa, A., Friedrich, C., Ikeda, T., Renold, A., Andrikopoulos, K., Liang, L., Pillai, S., Morgan, B.A.*, et al.* (1998). Aiolos regulates B cell activation and maturation to effector state. Immunity *9*, 543-553.

Wang, J.M., Chao, J.R., Chen, W., Kuo, M.L., Yen, J.J., and Yang-Yen, H.F. (1999). The antiapoptotic gene mcl-1 is up-regulated by the phosphatidylinositol 3-kinase/Akt signaling pathway through a transcription factor complex containing CREB. Mol Cell Biol *19*, 6195-6206.

Wang, N.S., McHeyzer-Williams, L.J., Okitsu, S.L., Burris, T.P., Reiner, S.L., and McHeyzer-Williams, M.G. (2012). Divergent transcriptional programming of class-specific B cell memory by T-bet and RORalpha. Nat Immunol *13*, 604-611.

Weill, J.C., Le Gallou, S., Hao, Y., and Reynaud, C.A. (2013). Multiple players in mouse B cell memory. Curr Opin Immunol *25*, 334-338.

Wen, W., Peng, C., Kim, M.O., Ho Jeong, C., Zhu, F., Yao, K., Zykova, T., Ma, W., Carper, A., Langfald, A.*, et al.* (2013). Knockdown of RNF2 induces apoptosis by regulating MDM2 and p53 stability. Oncogene.

Wong, C.W., and Privalsky, M.L. (1998). Components of the SMRT corepressor complex exhibit distinctive interactions with the POZ domain oncoproteins PLZF, PLZF-RARalpha, and BCL-6. The Journal of biological chemistry *273*, 27695-27702.

Woodland, R.T., Fox, C.J., Schmidt, M.R., Hammerman, P.S., Opferman, J.T., Korsmeyer, S.J., Hilbert, D.M., and Thompson, C.B. (2008). Multiple signaling pathways promote B lymphocyte stimulator dependent B-cell growth and survival. Blood *111*, 750-760.

Wu, L., Timmers, C., Maiti, B., Saavedra, H.I., Sang, L., Chong, G.T., Nuckolls, F., Giangrande, P., Wright, F.A., Field, S.J.*, et al.* (2001). The E2F1-3 transcription factors are essential for cellular proliferation. Nature *414*, 457-462.

Wu, X., Johansen, J.V., and Helin, K. (2013). Fbxl10/Kdm2b recruits polycomb repressive complex 1 to CpG islands and regulates H2A ubiquitylation. Mol Cell *49*, 1134-1146.

Wu, Z., Lee, S.T., Qiao, Y., Li, Z., Lee, P.L., Lee, Y.J., Jiang, X., Tan, J., Aau, M., Lim, C.Z.*, et al.* (2011). Polycomb protein EZH2 regulates cancer cell fate decision in response to DNA damage. Cell Death Differ *18*, 1771-1779.

Wu, Z.L., Zheng, S.S., Li, Z.M., Qiao, Y.Y., Aau, M.Y., and Yu, Q. (2010). Polycomb protein EZH2 regulates E2F1-dependent apoptosis through epigenetically modulating Bim expression. Cell Death Differ *17*, 801-810.

Xu, Z., Zan, H., Pone, E.J., Mai, T., and Casali, P. (2012). Immunoglobulin class-switch DNA recombination: induction, targeting and beyond. Nature reviews Immunology *12*, 517-531.

Yamane, A., Resch, W., Kuo, N., Kuchen, S., Li, Z., Sun, H.W., Robbiani, D.F., McBride, K., Nussenzweig, M.C., and Casellas, R. (2011). Deep-sequencing identification of the genomic targets of the cytidine deaminase AID and its cofactor RPA in B lymphocytes. Nature immunology *12*, 62-69.

Yamashita, M., Kuwahara, M., Suzuki, A., Hirahara, K., Shinnaksu, R., Hosokawa, H., Hasegawa, A., Motohashi, S., Iwama, A., and Nakayama, T. (2008). Bmi1 regulates memory CD4 T cell survival via repression of the Noxa gene. J Exp Med *205*, 1109-1120.

Yap, K.L., Li, S., Munoz-Cabello, A.M., Raguz, S., Zeng, L., Mujtaba, S., Gil, J., Walsh, M.J., and Zhou, M.M. (2010). Molecular interplay of the noncoding RNA ANRIL and

methylated histone H3 lysine 27 by polycomb CBX7 in transcriptional silencing of INK4a. Mol Cell *38*, 662-674.

Ye, B.H., Cattoretti, G., Shen, Q., Zhang, J., Hawe, N., de Waard, R., Leung, C., Nouri-Shirazi, M., Orazi, A., Chaganti, R.S.*, et al.* (1997). The BCL-6 proto-oncogene controls germinal-centre formation and Th2-type inflammation. Nat Genet *16*, 161-170.

Yoshida, H., Matsui, T., Yamamoto, A., Okada, T., and Mori, K. (2001). XBP1 mRNA is induced by ATF6 and spliced by IRE1 in response to ER stress to produce a highly active transcription factor. Cell *107*, 881-891.

Yoshida, H., Okada, T., Haze, K., Yanagi, H., Yura, T., Negishi, M., and Mori, K. (2000). ATF6 activated by proteolysis binds in the presence of NF-Y (CBF) directly to the cis-acting element responsible for the mammalian unfolded protein response. Molecular and cellular biology *20*, 6755-6767.

Yoshida, T., Ng, S.Y., Zuniga-Pflucker, J.C., and Georgopoulos, K. (2006). Early hematopoietic lineage restrictions directed by Ikaros. Nature immunology *7*, 382-391.

Yu, M., Mazor, T., Huang, H., Huang, H.T., Kathrein, K.L., Woo, A.J., Chouinard, C.R., Labadorf, A., Akie, T.E., Moran, T.B.*, et al.* (2012). Direct recruitment of polycomb repressive complex 1 to chromatin by core binding transcription factors. Mol Cell *45*, 330-343.

Zhang, B., Kirov, S., and Snoddy, J. (2005). WebGestalt: an integrated system for exploring gene sets in various biological contexts. Nucleic Acids Res *33*, W741-748.

Zhang, Y., Xiong, Y., and Yarbrough, W.G. (1998). ARF promotes MDM2 degradation and stabilizes p53: ARF-INK4a locus deletion impairs both the Rb and p53 tumor suppression pathways. Cell *92*, 725-734.

Zhao, J., Ohsumi, T.K., Kung, J.T., Ogawa, Y., Grau, D.J., Sarma, K., Song, J.J., Kingston, R.E., Borowsky, M., and Lee, J.T. (2010). Genome-wide identification of polycomb-associated RNAs by RIP-seq. Mol Cell *40*, 939-953.